ulm university universität **u**ulm

Universität Ulm | 89069 Ulm | Germany

Fakultät für
Mathematik und
Wirtschaftswissenschaften
Institut für
Numerische Mathematik

Speech Signal Noise Reduction with Wavelets

Diplomarbeit an der Universität Ulm

Vorgelegt von:
Bernhard Wieland
bernhard.wieland@uni-ulm.de
am 9. Oktober 2009

Gutachter:
Prof. Dr. Karsten Urban
Prof. Dr. Stefan Funken

Contents

List of Figures

List of Tables

List of Sound Examples

Chapter 1

Introduction and Motivation: Why Wavelets

1.1 Preliminaries

Degradation of signals by noise is an omnipresent problem. In almost all fields of signal processing the removal of noise is a key problem. For magnetic tapes, analogue audio restoration techniques such as "Type A" Dolby Noise Reduction have been already available and successful in the mid-1960s. Until the beginning of the 1990s, digital audio processing had required expensive high-power computers. Upcoming micro-chip improvements and affordable computers have also led to more research on digital audio processing. Furthermore, the invention of high quality digital audio media such as compact discs increased the general awareness and expectation on sound quality. Later, especially digital speech denoising developed to be a more and more interesting field of study, since digital communication via cell phones has become widely used.

In the past, beginning with the work of Norbert Wiener [35], several digital denoising techniques based on Short Time Fourier Transform (STFT) algorithms have been published (see chapter 4) and some reasonable results have already been achieved. In this work I will introduce some denoising algorithms based on the Fast Wavelet Transform (FWT) and develop some improvements. Let's first take a closer look on certain speech sound features before I provide some arguments why wavelet transformations might be preferable to Fourier transform. In the last part of this chapter, I provide the general outline and the structure of this work.

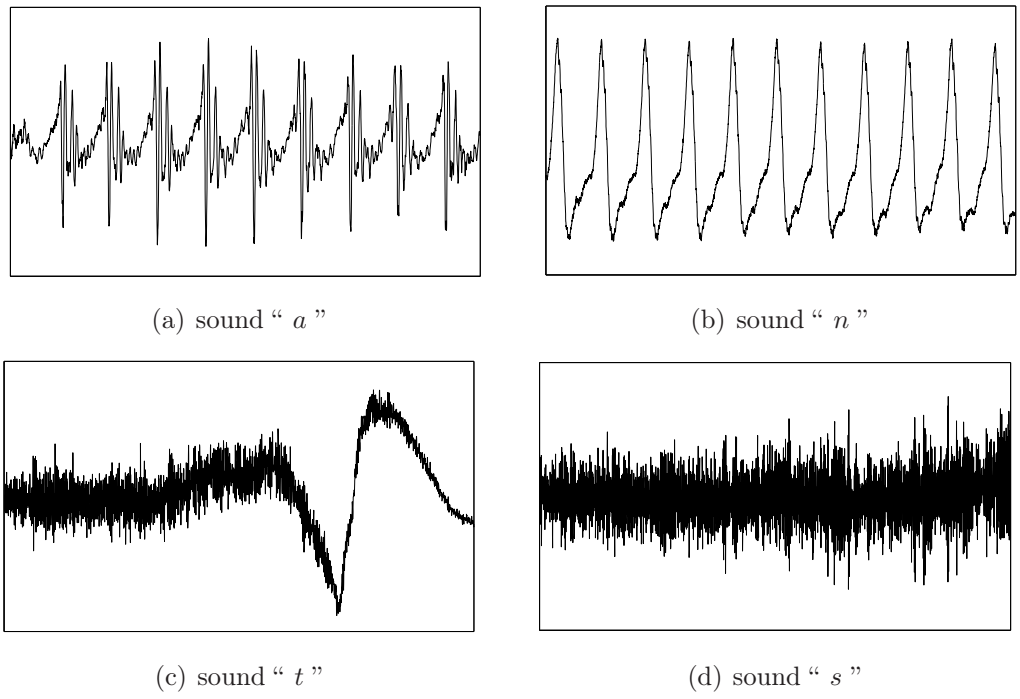

(a) sound " a "

(b) sound " n "

(c) sound " t "

(d) sound " s "

Figure 1.1: 10ms sounds " a ", " n ", " t " and " s "

1.2 Some Notes on Speech Signals

First, I will briefly introduce some characteristics of speech signals, such as auditory quality, characterization of different sounds and problems that might occur. Figure 1.2 shows 10ms of 4 different speech sounds using a sampling rate of 44100 samples per second. We can see that the vowel "a" and the consonant "n" have a relatively regular shape, while "t", pronounced as a single letter (i.e. just "t", not "tee"), and especially the sibilant "s" contain fast oscillating parts that look very similar to noise. Hence, it is clear that denoising will be very sensitive for such speech parts. This is also illustrated by figure 1.2, where the German word "$nichts$" is shown. In black, we see the original signal, the blue graph represents the reconstruction of a noisy version. A Fast Fourier Transform (FFT) based method has been used, namely power spectral filters, see section 4.3. While the "ni"-part seems to be well reconstructed with only minor errors, "ch" vanished completely and "ts" appears only as a small disturbance.

Another problem we have to deal with, is the lack of good measures for sound quality. All methods presented in this work are more or less based on the following quality "measures": Mean Square Error (MSE) or expected MSE, called risk, Signal to Noise Ratio (SNR), and smoothness, see section 3.3. Both, SNR and MSE, evaluate in fact the error of the reconstruction, but SNR puts it in

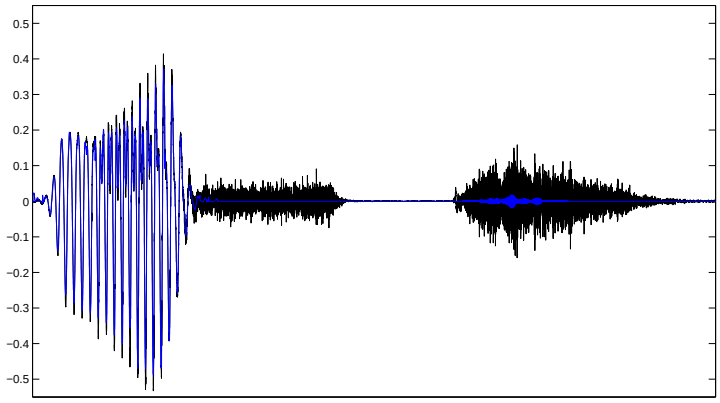

Figure 1.2: Reconstructed (blue) and original (black) German word "*nichts*"

a relation to the signal energy and is measured in decibel (dB). This is more meaningful than simple MSE since for signals with very high energy, small errors are perceived less distracting. However, one can easily illustrate that even SNR is not really appropriate. Suppose that each coefficient of a reconstructed signal is exactly half the original one, then $SNR \approx 3$, which is extremely small. Still, the reconstruction would be of very good sound quality. On the other hand, smoothness does not provide any information about a good approximation of the signal. Smooth reconstructions might be strongly deformed. Furthermore, reconsidering figure 1.1, the original signal might not be smooth at all. Another measure, the Itakura-Saito distance that is supposed to be a better indicator for sound quality, is not appropriate for our models since they is based on Fourier transformed signals and we can therefore not minimize it in wavelet domain. Furthermore, it is not even a metric.

1.3 Motivation

In chapter 2, Fourier and wavelet transformations are introduced and the main differences are described which is the basis for some parts of the following discussion. Hence, if the reader is not familiar with any of these transforms and its differences, I recommend to read chapter 2 first and go on with this section afterwards.

As mentioned, first digital denoising methods were based on Fourier transformations, processing the signal in frequency domain. Even though very good results have been achieved, there are reasons why denoising using wavelet transform algorithms might be preferable to Fourier based methods. Now, I will provide some of these arguments.

A. Auditory Perception: A sound signal that is received by the ear can be described by a function $s : \mathbb{R} \to \mathbb{R}$, where $s(t)$ denotes the local pressure at the corresponding time t. In some way, this one-dimensional signal is transformed into a two-dimensional time-frequency plane, providing information about the occurrence of frequencies at any time, i.e. "when does which frequency occur" [17]. In fact, this is can be seen as a contradiction. Since pure frequencies are represented by complex exponentials $e^{it\omega}$, they can not be associated with a certain time point but last from $-\infty$ to ∞. Vice versa, a certain time point, represented by the Dirac delta function, contains all frequencies and it is not possible to associate a special frequency. Hence, neither the signal itself nor its Fourier transform provide the desired information and the hearing must be based on some compromise between time localization and frequency localization [17]. Even though the STFT provides such a compromise, wavelet transformations seem to come closer to a more intuitive compromise, to rarely "update" low frequencies but to check details, i.e. high frequencies, continuously. This is realized in some way by the wavelet transformation since for high frequencies, the time resolution is much finer than for low frequencies. Furthermore, the FWT treats frequencies in a logarithmic way which is similar to acoustic perception [3].

B. Run-Time / Costs: The wavelet representation of a discretized signal of length N can be obtained in $\mathcal{O}(N)$ whereas the STFT representation requires $\mathcal{O}(N \log M)$ where M denotes the sub-frame length of the used window. Hence, the FWT algorithm might be preferable if the current application is very time sensitive, i.e. for real time applications such as denoising communication transmitted via radio. For example in helicopters, loud background noise is unavoidable and makes communication difficult. Also high quality headphones try to remove background noise to enhance sound quality. However, it is clear that fast and effective denoising techniques are needed.

C. Variety Of Wavelets: The wavelet transform is striking for its great variety of different types and modifications. A whole host of different scaling and wavelet functions (or scaling and wavelet coefficients) provide plenty of possible adjustments and regulating variables. Examples are differentiability properties or the number vanishing moments, symmetry features, complex or real wavelets,... Some well known examples are the set of different Daubechies wavelets, Symmlets and Coiflets. The corresponding scaling and wavelet coefficients can be found in [4] or [34]. The Fourier Transform does not provide such a variety.

D. Musical Noise Problem: Spectral domain denoising, Fourier based, often leads to special residual noise artifacts called musical noise or tonal noise, sometimes regarded even more disturbing than the original Gaussian white noise. An example of typical musical noise is provided by sound example 10. The way musical noise occur can be explained considering a signal of pure noise. In spectral domain, at each frame most of the frequencies will be removed. However, some isolated frequencies will be preserved and perceived as tones. These isolated frequencies randomly change from frame to frame, leading to rapidly time-varying tones [14]. Hence, some post-processing might be necessary [15]. This compares to the wavelet transform, which does not produce such artifacts due to better time resolutions.

E. Image Processing: Wavelet transformation has been widely used for image processing, such as edge or singularity detection [23], image compression (JPEG 2000) and especially image denoising [19], often outperforming existing algorithms based on Fourier Transformations. Some of these algorithms have already been used for the detection of abrupt changes in sound signals [16]. Hence, it is the obvious thing to give wavelet transformations a trial for audio denoising as well. We will try to modify some of the image processing algorithms, in particular the image denoising methods, and test its applicability and performance on noisy speech.

1.4 Outline and Structure

In chapter 2, I provide a brief introduction and comparison of different kinds of wavelet and Fourier transformations. The Continuous Wavelet Transform (CWT) will be only of theoretical interest, though, providing a better understanding of the discrete transform as well as being used for some proofs in chapter 5. Before several kinds of denoising techniques are presented, the general model of noisy speech is given in chapter 3, together with some precise definitions of signal goodness measures such as MSE, risk or SNR. Additionally, some notes on the change of the behavior of transformed noise is provided.

The second part of this work, the presentation of several noise reduction methods, starts in chapter 4 with some well known and commonly used spectral filters, i.e. Fourier transform based denoising filters, based on different noise reduction assumptions. While the Wiener filter is based on risk minimization, spectral subtraction and power subtraction filters are based on rather intuitive approaches, the removal of noise magnitudes. The Ephraim-Malah Filter however uses statisti-

cal assumptions and conditional expectations to estimate the coefficient modulus.

The first wavelet transform based methods, introduced in chapter 5 and 6, try to reconstruct the smoothness of the original signal. The idea of Lipschitz denoising is to remove coefficients such that the produced outcome does not contain negative Lipschitz singularities, i.e. the signal is uniformly Lipschitz positive. Diffusion denoising performs several smoothing steps, each one can be seen as an Euler step to solve a differential equation, modified in a way such that important signal features are less smoothed than noise.

In chapter 7, the general thresholding concept is introduced. Except Visu Shrink, introduced and analyzed in sections 7.3 and 7.4 with the objective to produce smooth signal estimations, all thresholds are based on risk minimization. In chapter 9, I develop some modifications of the soft thresholding function to obtain better results. To reduce the occurrence of disturbing noise artifacts, i.e. find a better compromise between smoothness and risk minimization, I develop the idea of biased risk minimization in chapter 10. Tree structured thresholding, presented in chapter 8, is based on the detection of important coefficients via trees of wavelet detail coefficients, where "important" is in some way defined by the used threshold value.

Finally, in chapter 11, a comprehensive comparison of the different denoising results is provided. Corresponding implementations of all methods and tests for several different speech examples can be found on the attached CD. All speech examples are specified in appendix A. Implementations for wavelet based methods are provided in C++, spectral domain denoising is done in Matlab.

Chapter 2

Wavelet and Fourier Transform

In this chapter, I will briefly introduce different wavelet transform concepts and provide a general comparison with the Fourier transform, supporting the arguments that have been mentioned in section 1.3 for the use of wavelet transforms for denoising purposes instead of Fourier based spectral domain denoising. The introduction will be as short as possible. First, the Continuous Wavelet Transform (CWT) is presented. It is less restrictive than the definitions of the discrete transformations — the Fast Wavelet Transform (FWT) and the Stationary Wavelet Transform (SWT). For these transformations one first needs to introduce Multiresolution Analysis (MRA) to obtain consistent definitions. For more details one may refer to [4], [25] [19] or [27].

2.1 The Continuous Wavelet Transform

For some mother wavelet function $\psi(x)$, one generates a family of dilated and shifted wavelets by

$$\psi^{s,u}(x) = \frac{1}{\sqrt{|s|}}\psi\left(\frac{x-u}{s}\right)$$

with dilation $s \in \mathbb{R}\backslash\{0\}$ and shift $u \in \mathbb{R}$. It holds that $||\psi|| = ||\psi^{s,u}||$ for all s, u. The continuous wavelet transform of a real function $f \in L^2(\mathbb{R})$ is defined as the

inner product of f and $\psi^{s,u}$, i.e.

$$\begin{aligned} Wf(s,u) &:= (f, \psi^{s,u}) \\ &:= \int_{-\infty}^{\infty} f(x)|s|^{-1/2}\psi\left(\frac{x-u}{s}\right)dx \end{aligned} \tag{2.1}$$

for real Wavelets. $Wf(s,u)$ provides information at scale s localized at position u. In theory, all functions ψ can play the role of a wavelet function. For most application one needs a reconstruction formula to recover the function f, though. One can show that for mother wavelets ψ such that

$$C_\psi := 2\pi \int_{-\infty}^{\infty} \frac{|\tilde{\psi}(\omega)|^2}{|\omega|} d\omega < \infty, \tag{2.2}$$

where $\tilde{\psi}$ denotes the Fourier transform of ψ, it holds that

$$f(x) = \frac{1}{C_\psi} \int_{-\infty}^{\infty} \int_{-\infty}^{\infty} Wf(s,u) \frac{1}{s^2} \psi_{s,u}(x) ds\ du. \tag{2.3}$$

Hence, one should restrict on mother wavelets ψ fulfilling (2.2). However, to obtain the reconstruction formula (2.3), it is in most cases enough to require only

$$\tilde{\psi}(0) = \int_{-\infty}^{\infty} \psi(x)\ \mathrm{d}x = 0. \tag{2.4}$$

Such function typically have oscillating properties. Hence the name Wavelets. Some examples are the Morlet wavelet $\psi(x) = e^{i\omega_0 x} e^{-x^2/2\sigma_0^2}$ or the Mexican hat wavelet $\psi(x) = (1-x^2)e^{x^2/2}$. For more details and proofs of above assertions see [4].

2.2 The Discrete Fast Wavelet Transform

Definition 2.2.1. Multiresolution Analysis (MRA)
A sequence of nested, closed subspaces of $V_j \subset L^2(\mathbb{R})$ is called Multiresolution Analysis (MRA) if

(i) $V_j \subset V_{j+1}\ \forall j \in \mathbb{Z}$

(ii) $\overline{\bigcup_{j\in\mathbb{Z}} V_j} = L^2(\mathbb{R})$

(iii) $\overline{\bigcap_{j\in\mathbb{Z}} V_j} = \{0\}$

(iv) $f(\cdot) \in V_j \Leftrightarrow f(2\cdot) \in V_{j+1}\ \forall j \in \mathbb{Z}$

(v) $f(\cdot) \in V_0 \Leftrightarrow f(\cdot + k) \in V_0\ \forall k \in \mathbb{Z}$

(vi) $\exists \varphi \in V_0$ such that $\{\varphi(\cdot - k)\}_{k\in\mathbb{Z}}$ is a stable Riesz basis for V_0

The function φ is sometimes called father or scaling function.

If φ is normalized, then $\{\varphi_{jk}(\cdot) := 2^{j/2}\varphi(2^j \cdot -k)\}_{k\in\mathbb{Z}}$ is a normalized basis of V_j. For a function $f \in L^2(\mathbb{R})$, let f_j denote the projection of f into V_j, i.e. $f_j \in V_j$ such that $f - f_j \in V_j^{\perp}$. Since $V_{j+1} \supset V_j$, projections f_{j+1} into the finer subspace V_{j+1} obtain all information about f that is already provided by f_j plus some additional details . Hence, one can decompose V_{j+1} into

$$V_{j+1} = V_j \oplus W_j, \quad j \in \mathbb{Z}$$

where W_j denotes the so called detail space. We will only discuss the case of orthonormal bases $\{\varphi(\cdot - k)\}_{k\in\mathbb{Z}}$ of V_0. Similar results also hold for biorthognal bases, see e.g. [29]. One can now proof that there is a function ψ such that $\{\psi_{j,k}(\cdot) := 2^{j/2}\psi(2^j \cdot -k)\}_{k\in\mathbb{Z}}$ form an orthonormal basis of the detail space W_j [4]. The function ψ is called mother wavelet.

Since $\varphi \in V_0 \subset V_1$ and, as described above, $\{\sqrt{2}\varphi(2 \cdot -k)\}_{k\in\mathbb{Z}}$ denotes an orthonormal basis of V_1, it and follows that there is a sequence $\{a_k\}_{k\in\mathbb{Z}} \in l^2(\mathbb{Z})$ such that φ can be represented as the linear combination

$$\varphi(x) = \sqrt{2}\sum_{k\in\mathbb{Z}} a_k \varphi(2x - k). \tag{2.5}$$

Since $W_0 \subset V_1$, too, it follows in the same way that there is a sequence $\{b_k\}_{k\in\mathbb{Z}} \in l^2(\mathbb{Z})$ such that ψ can be represented as the linear combination

$$\psi(x) = \sqrt{2}\sum_{k\in\mathbb{Z}} b_k \varphi(2x - k). \tag{2.6}$$

These equations are called dilation equations or two-scale relation, the sequences $\{a_k\}_{k\in\mathbb{Z}}$ and $\{b_k\}_{k\in\mathbb{Z}}$ are called scaling sequence and wavelet sequence, respectively, and characterize the corresponding scaling and wavelet function. With their help we can define the Fast Wavelet Transform (FWT) and its inverse.

Fast Wavelet Transform Let

$$f_{j+1}(x) = \sum_{k\in\mathbb{Z}} c_{j+1,k}\varphi_{j+1,k}(x)$$

be the representation of the projection of a function f into V_{j+1}. One can decompose this into $V_j \oplus W_j$ by

$$f_{j+1}(x) = \sum_{k\in\mathbb{Z}} c_{jk}\varphi_{jk}(x) + \sum_{k\in\mathbb{Z}} d_{jk}\varphi_{jk}(x)$$

with

$$c_{jk} = \sum_{l\in\mathbb{Z}} a_{l-2k}c_{j+1,l}, \tag{2.7}$$

$$d_{jk} = \sum_{l\in\mathbb{Z}} b_{l-2k}c_{j+1,l}. \tag{2.8}$$

This decomposition is called Fast Wavelet Transform (FWT) and we call $c_{j,k}$ approximation coefficients and $d_{j,k}$ detail coefficients. Furthermore, one can reconstruct c_{j+1} from c_j and d_j. This reconstruction is called Inverse Fast Wavelet Transform (IFWT).

$$c_{j+1,k} = \sum_{k\in\mathbb{Z}} a_{l-2k}c_{jk} + \sum_{k\in\mathbb{Z}} b_{l-2k}d_{jk}.$$

The proofs are easy and well known. They can be found e.g. in [19]. There is a strong connection between the CWT and FWT. First, all Wavelet functions obtained from a MRA are good candidates for the CWT, too. Additionally, let $\{c_{J,k}\}_{k=0,..,N-1}$, $N = 2^J$, be some sequence that can be considered as a discretized version of a function f, say $c_{J,k} = (f, \varphi_{J,k})$, then we have

$$c_{j,k} = (\varphi_{j,k}, f) = \int 2^{j/2}\varphi(2^j t - k)f(t)\ \mathrm{d}t \quad \text{and} \tag{2.9}$$

$$d_{j,k} = (\psi_{j,k}, f) = \int 2^{j/2}\psi(2^j t - k)f(t)\ \mathrm{d}t, \tag{2.10}$$

i.e. both coefficients can be seen as a CWT with $s = 2^{-j}$ and $u = k2^{-j}$. Hence, $c_{j,k}$ and $d_{j,k}$ provide information at scale 2^{J-j} localized at position $2^{J-j}k$ with respect to the original sequence c_J that is considered as a representation at scale

one, see [27]. Therefore, a representation of f is provided by

$$\{c_0, d_0, d_1, ..., d_{J-1}\}. \tag{2.11}$$

If only a finite number of coefficients a_k and b_k from (2.5) and (2.6), respectively, are nonzero, the computation of the above representation (2.11) can be done in $\mathcal{O}(N)$. Each coefficient vector d_j and c_j is of length $\mathcal{O}(2^j)$, hence the total length of the representation is $\mathcal{O}(N)$, too.

2.3 The Stationary Wavelet Transform

The Stationary Wavelet Transform (SWT) is a overrepresented form of the FWT. The obtained representation is similar to (2.11), but now each coefficient vector d_j and c_j is of length $\mathcal{O}(N)$, in case of periodic boundary conditions one obtains a length of exactly N and the total number of coefficients is $N \log_2(N) = J2^J$. This is the reason why the SWT is also called non-decimated Wavelet Transform.

Let c_J be a discretized representation of a function f as described above, and let $\{a_k\}_{k\in\mathbb{Z}}$ and $\{b_k\}_{k\in\mathbb{Z}}$ be the coefficients defined by (2.5) and (2.6), respectively. Then, the SWT is defined as

$$\begin{aligned} c_{j,k} &= \sum_{l\in\mathbb{Z}} a_{l-k}^{[J-j]} c_{j+1,l}, \\ d_{j,k} &= \sum_{l\in\mathbb{Z}} b_{l-k}^{[J-j]} c_{j+1,l} \end{aligned}$$

where

$$a_k^{[r]} = \begin{cases} a_n & \text{, if } k = 2^r n \\ 0 & \text{, otherwise .} \end{cases}$$

As for the FWT we have a connection to the CWT, that is

$$c_{j,k} = \int 2^{j/2} \varphi(2^j t - 2^{j-J} k) f(t)\, \mathrm{d}t \quad \text{and} \tag{2.12}$$

$$d_{j,k} = \int 2^{j/2} \psi(2^j t - 2^{j-J} k) f(t)\, \mathrm{d}t. \tag{2.13}$$

Now, $c_{j,k}$ and $d_{j,k}$ provide information of the function f at scale 2^{J-j}, localized at position k, in opposition to FWT coefficients where only localizations at $2^{J-j}k$

are provided. The existence of coefficients at any position $k = 0, ..., N-1$ at each scale often facilitates the detection of correlations between different scales and will be useful for some denoising algorithms (see section 7.9).

Nevertheless, the FWT is embedded in the SWT. Taking at each level j only coefficients $c_{j,k}$ and $d_{j,k}$ such that $k = n2^{J-j}$, $n \in \mathbb{N}$, leads exactly to the corresponding FWT coefficients. To confirm this, replace k in equations (2.12) and (2.13) by $n2^{J-j}$ which leads to (2.9) and (2.10), respectively. In fact, SWT can be seen as a rearrangement of all FWTs with shifted inputs. More precisely, for $shift^m(c_{J,i}) = c_{J,i-m}$, the stationary wavelet transform contains all coefficients of FWTs of $shift^m(c_J)$, $m = 0, ..., N-1$. Actually, this would lead to N^2 coefficients, however, several coefficients appear several times. Removing this redundancy one obtains only $\mathcal{O}(N \log N)$ coefficients and rearranging leads to above representation. This procedure is also called cycle-spinning and further explained and discussed in [2] and [27].

The inverse SWT can be done in several different ways. One possibility is to take only the FWT coefficients and do the inverse FWT as described above. This will be obtained using

$$c_{j+1,l} = \sum_{l \in \mathbb{Z}} a_{l-2k}^{[J-j-1]} c_{j,2k} + \sum_{l \in \mathbb{Z}} b_{l-2k}^{[J-j-1]} d_{j,2k}.$$

In many cases a different approach might be better, though. Since we will process all coefficient due to denoising issues, it might be better to use as well all coefficients to compute the inverse SWT. These considerations lead to

$$\begin{aligned} c_{j+1,l}^{even} &= \sum_{l \in \mathbb{Z}} a_{l-2k}^{[J-j-1]} c_{j,2k} + \sum_{l \in \mathbb{Z}} b_{l-2k}^{[J-j-1]} d_{j,2k} \\ c_{j+1,l}^{odd} &= \sum_{l \in \mathbb{Z}} a_{l-2k}^{[J-j-1]} c_{j,2k+1} + \sum_{l \in \mathbb{Z}} b_{l-2k}^{[J-j-1]} d_{j,2k+1} \\ c_{j+1,l} &= \frac{c_{j+1,l}^{even} + c_{j+1,l}^{odd}}{2} \end{aligned}$$

which is the average of all inverse FWTs of coefficients obtained from FWTs taking at each step either only odd or even coefficients. One can show that this leads to the average of all N inverse FWTs of shifted inputs mentioned above. A complete discussion and proofs are provided in [27].

2.4 The Fourier Transform

Definition 2.4.1. The Continuous Fourier Transform (CFT) is defined as

$$F(\omega) := \int_{-\infty}^{\infty} f(t)e^{-i2\pi t\omega}\ \mathrm{d}t. \tag{2.14}$$

For signal analysis we need to introduce another form, the short-time Fourier transform or windowed Fourier Transform which — for some window or frame function g of compact support — is given by

$$F(\omega,\tau) := \int_{-\infty}^{\infty} f(t)g(t-\tau)e^{-i2\pi t\omega}\ \mathrm{d}t. \tag{2.15}$$

Definition 2.4.2. The Discrete Fourier Transform (DFT) is defined as

$$X_m = \sum_{k=0}^{N-1} x_k e^{-i\frac{2\pi km}{N}} \tag{2.16}$$

where the sequence $\{x_k\}_{k=0,\dots,N-1}$ may represent a discretized function. The discrete Short-Time Fourier Transform (STFT) for some window g is expressed by

$$X_{m,n} = \sum_{k\in\mathbb{Z}} x_k g(k-n)e^{-i\frac{2\pi km}{M}}, \tag{2.17}$$

where $g(k) \neq 0$ only if $k \in \{0,\dots,M-1\}$. M is called sub-frame length. It depends on the application if x_k is assumed to be zero for $k \notin \{0,\dots,N-1\}$ or if x_k is extended periodically.

The windowed Fourier transform provides additional time resolution information. This is essential for speech signal processing since different sounds, e.g. vowels or consonants, lead to completely different frequency ranges, see also chapter 1.2. The length of a typical speech processing window is usually chosen to be between 20 to 40 milliseconds [12]. Furthermore, overlapping windows are necessary for good denoising results. On the other hand it is too expensive to evaluate $X_{m,n}$ at each possible value of n. Hence, to obtain an overlap of 50-75%, the actual time resolution will be at most 5ms, or $N/4$ in the discrete case.

For fixed n, the STFT coefficients $X_{m,n}$, $m = 0,\dots,M-1$, can be computed in $\mathcal{O}(M\log M)$ using the Fast Fourier Transform algorithm (FFT), presented for

example in [14]. Hence, the complete Fourier representation with time resolution as described can be obtained in $\mathcal{O}(N \log M)$, where a full time resolution would require $\mathcal{O}(NM \log M)$.

A widely used class of windows, compactly supported on $[0, 1]$ and with subframe length M, is given by

$$g_\alpha(k) := \alpha - (1 - \alpha) cos\left(\frac{2\pi k}{M}\right).$$

These functions are called generalized Hamming windows, named after Richard Hamming. The frames for the most commonly used values of α are

$\alpha = 1$	rectangular window
$\alpha = 0.5$	Hann or Hanning window, named after Julius von Hann
$\alpha = 0.53836$	Hamming window .

For more Details see [14].

2.5 Comparison

The idea of both, wavelet and Fourier transform, is based on the computations of inner products of some function f and some analyzing functions to obtain a time-frequency representation [3]. To illustrate this, let's define

$$g_{m,n}(k) \;\; := \;\; g(k-n)e^{-i\frac{2\pi km}{M}},$$

the product of a shifted version of some window function g and a complex exponential. Hence, similar to the inner product (2.10), we have

$$X_{m,n} \;\; = \;\; (g_{m,n}, x)_2,$$

even though the inner is now considered to be discrete. I.e., $g_{m,n}$ plays a similar role than the wavelet function $\psi_{j,k}$. The first index of both functions refers to the frequency and the second one to a time shift, as illustrated in figure 2.1.

However, the way the frequency is characterized differs. For large j, one can see that the $\psi_{j,k}$ is a strongly concentrated or shrunken version of itself whereas g is not shrunken but "filled" with oscillations for large m. The support of $\psi_{j,k}$ is proportional to 2^{-j} whereas indices m of $g_{m,n}$ are rather proportional to the number of oscillations of $real(g)$. I.e. the wavelet transform provides a kind of "zoom in " property, for large j coefficients $d_{j,k}$ contain only information about a

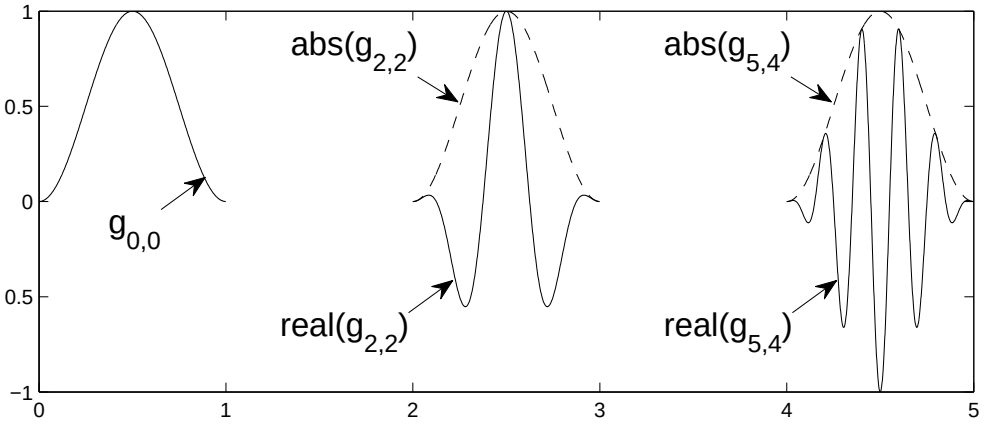

(a) typical window function $g = g_{0,0}$, $g(t) = 0.5\mathbb{1}_{[0,1]}(t)\,(1 - cos\,(2\pi t))$

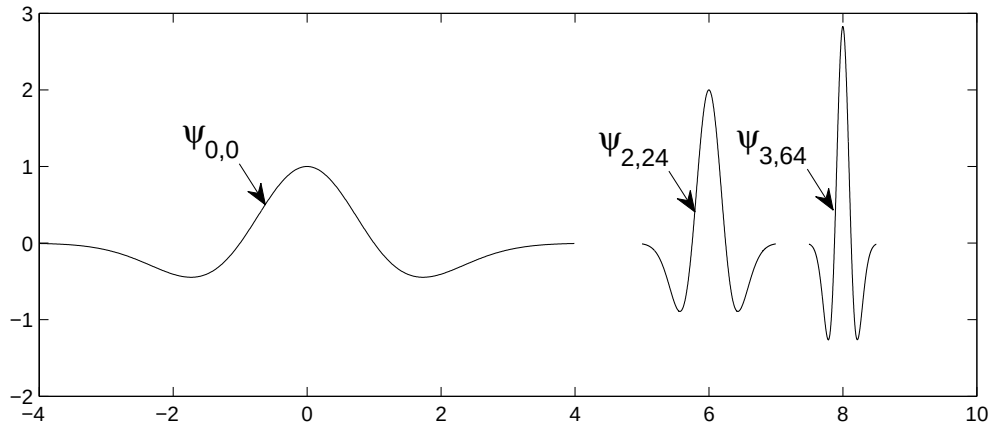

(b) wavelet $\psi = \psi_{0,0}$, $\psi(t) = \mathbb{1}_{[-4,4]}(t)(1 - t^2)e^{-t^2/2}$

Figure 2.1: (a) window function $g_{m,n}$, (b) wavelet function $\psi_{j,k}$.

very short time period in contrast to coefficients $X_{m,n}$. Hence, local effects can be detected much easier using wavelets and might be a better choice whenever good time resolutions at high frequencies are required.

This assumption can be supported by a comparison of the two phase space lattices, provided in figure 2.2. The STFT lattice is illustrated in figure 2.2(a), i.e. the points $(m, n) = \mathbb{Z}^2$, figure 2.2(b) visualizes the FWT lattice. In this case the grid is given by $(2^j, k2^{-j})$. Hence, in both cases the y-axis represents the possible frequencies and the x-axis for each frequency the corresponding time evaluation points.

To clarify the differences, consider a function f, supported on $[0, 1]$, periodically expendable and represented by a discretized version s_i, $i = 0, ..., N-1$, and let's take for example $N = 1024 = 2^{10}$. As shown above by (2.11), one can obtain the wavelet representation of f, $\{c_0, d_0, d_1, ..., d_9\}$, in $\mathcal{O}(N)$, where the vectors

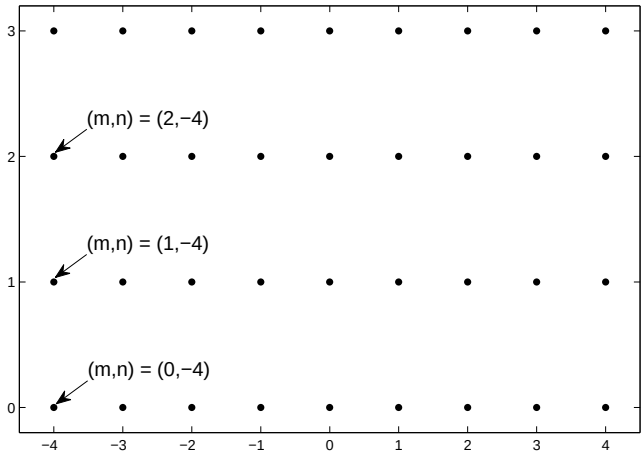

(a) STFT phase space lattice

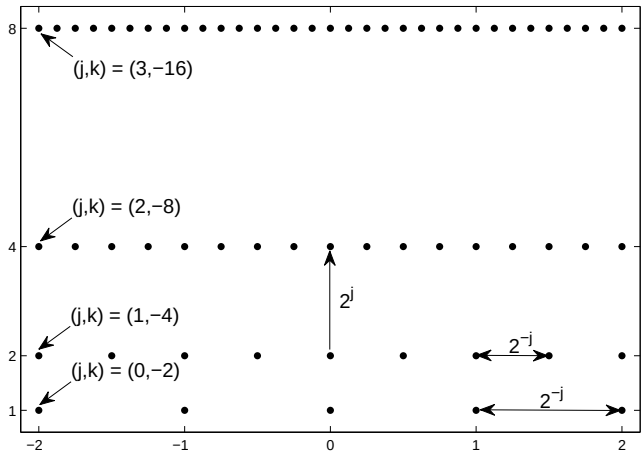

(b) FWT phase space lattice

Figure 2.2: (a) STFT phase-space lattice, (b) FWT phase-space lattice

$d_i \in \mathbb{R}^{2^i}$ denote the details at frequency 2^i and $c_0 \in \mathbb{R}$ the approximation coefficient. Hence, the phase space lattice is given by $\{(j,k)|j = 0,..,9, k = 0,..,2^j\}$, i.e. one obtains evaluations for 9 different frequencies, high frequencies more time evaluations than low ones.

Let's now take a look on the STFT. Suppose the sub-frame length of the used window function g is chosen to be $M = 256$. One then obtains evaluations at 256 frequencies $0,..,255$. As described in section 2.4, one will not evaluate $X_{m,n}$ for all n. Here let's allow only 50% intersection of two shifted windows. In this example, this would lead to 8 time evaluations per frequency and costs of $8 \cdot \mathcal{O}(Mlog(M)) = \mathcal{O}(Nlog(M))$. No intersection would lead to 4 time-evaluations and exactly N Fourier coefficients, but would still require $\mathcal{O}(Nlog(N))$ operations.

In summary, the number of points in the FWT phase-space lattice totals N, distributed on $J-1$ frequencies, $N/2$ points for the highest frequency, just 2 for the lowest one, one detail and one approximation coefficient. The STFT lattice consists of $cMN/M = cN$ points, evenly distributed on M frequencies, i.e. just cN/M points for each frequency. Here, c refers to the overlapping rate of the windows. I.e. for 50%, we have $c = 2$.

Chapter 3

A General Noise and Speech Model

3.1 Noisy Speech Signal Model

Suppose a data vector y of finite length n is given and represents a combination of an unknown speech signal and some as well unknown noise that is added to the signal, i.e.

$$y_i = s_i + e_i, \quad i = 0, ..., n-1 \tag{3.1}$$

where s_i refers to the unknown noise-free signal at time t_i and e_i is considered to be the additional noise. Furthermore, for notational and algorithmic reasons, we assume y to be periodic extensible, i.e. $y_i = y_{i+kn}$ for all $k \in \mathbb{Z}$, and n of the form $n = 2^J$ for some $J \in \mathbb{N}$. The periodicity is legitimated by considering only signals s silent at the beginning and at the end.

From the observed data y we will try to estimate the original signal s. In the following we assume s and e to be independent. For most denoising methods one assumes e to be a vector of independent identically distributed (i.i.d.) normal random numbers with $e_i \sim N(0, \sigma^2)$, i.e. Gaussian white noise with variance σ^2 that is not necessarily known. However, for some methods less restrictive assumptions suffice. In any case we assume the expected noise to be zero, i.e. $\mathbb{E}[e] = 0$.

A second noise model is necessary for transformed coefficients. However, the linearity of both, Fourier and Wavelet transform, leaves the additivity of model (3.1) unchanged. Let's denote the transformations of the data vector y and its components s and e by Y_{pq}, S_{pq} and E_{pq}, respectively, where p refers to the

frequency and q stands for the time parameter, i.e. $(p,q) \mathrel{\widehat{=}} (m,n)$ in the Fourier transform case and $(p,q) \mathrel{\widehat{=}} (j,k)$ in the wavelet transform case as described in section 2.4. As mentioned, the linearity of both transformations leads to a second noise model

$$Y_{pq} = S_{pq} + E_{pq}, \quad (p,q) \in \mathcal{I} \tag{3.2}$$

where $\mathcal{I}$ is the set of all possible indices in time-frequency domain. In the wavelet case, Y, S and E may refer — if necessary — to both, approximation and detail coefficients. However, most denoising algorithms leave approximation coefficients unchanged and we do not consider the remaining approximation coefficients anyway.

Let x be some data in time domain and X its transformation into time-frequency domain. For orthogonal FWT it holds that $||x||_2 = ||X||_2$, i.e. norms in time and time-frequency domain are equal (see [19]). In the biorthogonal case the Riesz basis property of (2.2.1) ensures equivalent norms. In the Fourier case it holds that $||x||_2^2 = \frac{1}{n}||X||_2^2$, also known as Parseval's theorem. Hence, considering norms in time domain is equivalent to restrict on norms in time-frequency domain, especially minimizing in time-frequency domain minimizes (or nearly minimizes in the biorthogonal Wavelet case) in time-domain.

3.2 Noise Transformation

One should pay some additional attention on the noise and its property change after transformation. For $\mathbb{E}[e] = 0$ it is clear that $\mathbb{E}[E] = 0$ holds, too. Further noise properties are given by its covariance matrix Q, i.e.

$$\begin{aligned} Q_{i,j} &= \mathbb{E}\left[e_i e_j\right], \\ Q &= \mathbb{E}\left[ee^T\right]. \end{aligned}$$

Since discrete Fourier and Wavelet transformations are linear, there is a matrix A such that

$$Y = Ay,\ S = As,\ E = Ae$$

and the new covariance matrix Q^W of E is obtained by

$$\begin{aligned} Q^A &= \mathbb{E}\left[EE^T\right] \\ &= \mathbb{E}\left[Aee^TA^T\right] \\ &= AQA^T.. \end{aligned} \tag{3.3}$$

In the Wavelet case it might be useful to derive the form of Q^A for some special noise distributions and normalize the wavelet coefficients

$$Y_{jk}^{new} = \frac{1}{\sqrt{Q^A_{jk,jk}}} Y_{jk} \tag{3.4}$$

to obtain stationary noise [19].

First, for orthogonal Wavelet transformations, A is orthogonal, too. Now, if e represents white noise, i.e. $Q = \sigma^2 I$ where I is the identity matrix and σ^2 the noise variance, then $Q^A = \sigma^2 I$, too. Hence, the noise remains uncorrelated, stationary and the variance does not change either. No normalization is necessary.

Let's now discuss a more general assumption. Suppose the original noise is stationary and the correlation between two noise data points depends only on their distance. Then, Q is a symmetric Toeplitz matrix and one can prove the following lemma.

Lemma 3.2.1. *Let $E_{jk}, (j,k) \in \mathcal{I}$, represent wavelet coefficients obtained by either orthogonal or biorthogonal FWT of stationary noise with symmetric Toeplitz covariance matrix. Then, the variance of each coefficient depends only on the level j, i.e.*

$$\mathbb{E}[E^2_{j,k}] = \sigma_j^2 \tag{3.5}$$

Proof. Since Q is Toeplitz, we have $Q_{u,v} = q_{|u-v|}$. Using equation (2.8) one obtains

$$\begin{aligned} \mathbb{E}[E_{J-1,k}E_{J-1,l}] &= \sum_u \sum_v b_{u-2k} b_{v-2l} \mathbb{E}[e_u e_v] \\ &= \sum_u \sum_v b_{u-2k} b_{v-2l} q_{|u-v|}. \end{aligned}$$

Substituting $m = u - 2k$ and $n = v - 2l$ yields to

$$\begin{aligned}\mathbb{E}[E_{J-1,k}E_{J-1,l}] &= \sum_m \sum_n b_m b_n q_{|2(k-l)+m-n|} \\ &= \mathbb{E}[E_{J-1,k+r}E_{J-1,l+r}].\end{aligned}$$

The same holds for scaling coefficients using equation (2.7). Hence, at level $J-1$ the covariance matrices of detail and approximation coefficients are Toeplitz, too. Thus, we have

$$\mathbb{E}[E^2_{J-1,k+r}] = \mathbb{E}[E^2_{J-1,k}] = \sigma^2_{J-1},$$

a constant variance at level $J-1$. One can repeat this procedure for any other level in exactly the same way. □

In fact, the covariance matrix $Q = \sigma^2 I$ for Gaussian white noise is a special Toeplitz matrix, too. However, even though lemma 3.2.1 holds as well for biorthogonal wavelet coefficients, $E_{j,k}$, $(j,k) \in \mathcal{I}$, might be correlated and not stationary (i.e. $\sigma_{j_1} \neq \sigma_{j_2}$ for $j_1 \neq j_2$) in opposite to the case of orthogonal FWT.

3.3 Some Definitions and Notations

Let us now collect some definitions used later for the analysis of denoising methods and for the evaluation of denoised speech signals. The following "measures" constitute a first set of possible evaluations of the goodness of signal approximations.

Definition 3.3.1. Given a certain denoising method called T, denote estimates of s by $\hat{s}^T$. The following expected values refer to the unknown noise, often assumed to be normally distributed. Let's define

- Mean Square Error (MSE) of s and $\hat{s}^T$

$$\begin{aligned}MSE(s,\hat{s}^T) &= \frac{1}{n}||s-\hat{s}^T||^2 \\ &= \frac{1}{n}\sum_{i=0}^{n-1}|s_i - \hat{s}^T_i|^2 \end{aligned} \tag{3.6}$$

- Bias of s and $\hat{s}^T$

$$bias^2(s,\hat{s}^T) = \frac{1}{n}||s - \mathbb{E}\hat{s}^T||^2 \tag{3.7}$$

- Variance of $\hat{s}^T$

$$var(\hat{s}^T) = \frac{1}{n}\mathbb{E}\left[||\hat{s}^T - \mathbb{E}\hat{s}^T||^2\right] \tag{3.8}$$

- Risk

$$\begin{aligned} risk(s, \hat{s}^T) &= \mathbb{E}\left[MSE(s, \hat{s}^T)\right] && (3.9)\\ &= \frac{1}{n}\sum_{i=0}^{n-1}\mathbb{E}\left[|s_i - \hat{s}_i^T|^2\right] \\ &= bias^2(s, \hat{s}^T) + var(\hat{s}^T). && (3.10) \end{aligned}$$

  the expected MSE for a given Method T. Some easy calculations lead to equation (3.10) and are not specified here.

- Ideal Risk

$$\mathfrak{R}(s, T) = \inf_{\hat{s}^T} risk(s, \hat{s}^T) \tag{3.11}$$

  which is the infimum of all risks that can be achieved using method T.

- Signal to Noise Ratio (SNR)

$$\begin{aligned} SNR(s, \hat{s}^T) &= 10 * \log_{10}\frac{||s||^2}{||s - \hat{s}^T||^2} \text{ or} && (3.12)\\ SNR(s, y) &= 10 * \log_{10}\left(||s||^2/||e||^2\right) && (3.13) \end{aligned}$$

  measured in decibels (dB).

All these definitions can be modified for transformed coefficients Y, S and E, replacing n by the number of transformed coefficients, i.e. $\#(p, q) = |\mathcal{I}|$. For FWT and FFT and under the assumption of periodic functions we have $|\mathcal{I}| = n$, but not for STFT and SWT. All summations need to be done over all possible indices $(p, q) \in \mathcal{I}$. As mentioned above, the l^2-norms in time and time-frequency domain are equivalent, i.e. minimization in time domain is equivalent to minimization in time-frequency domain.

Chapter 4

Spectral Domain Denoising

In this chapter we will briefly discuss some well known and widely used denoising methods based on STFT, as described for example in [12], [13], [14], [31], [35]. Nevertheless, all these filters could be almost directly applied on wavelet detail coefficients instead of STFT coefficients, too. Hence, I used the general notation introduced in chapter 3, referring to the Fourier transform only as much as necessary. A comparison of these filters applied on STFT and FWT coefficients, respectively, can be found in [13]. These experiments has been based only on different SNR measures but not on human perception. However, it turned out that these filters applied on Fourier transform coefficients provide better results than applied on Wavelet detail coefficients. Hence, it will be necessary to create different methods that benefit from special wavelet properties as mentioned in chapter 1, e.g. the finer time resolution.

4.1 Noise Reduction Filter Model

First, I will introduce some further SNR definitions that are especially used for theoretical analysis of spectral domain denoising methods, only defined for coefficients in time-frequency domain. Let X denote the transformation of some sequence x, for variances $R_X(p,q)$ and R_X denoted by

$$\begin{aligned} R_X(p,q) &= \mathbb{E}[|X_{pq}|^2] \\ R_X &= \mathbb{E}[||X||^2] \end{aligned}$$

one defines "a priori SNR"

$$\xi_{pq} = \frac{R_S(p,q)}{R_E(p,q)} \tag{4.1}$$

and "a posteriori SNR"

$$\gamma_{pq} = \frac{R_Y(p,q)}{R_E(p,q)}. \tag{4.2}$$

Due to the independence of S and E and for $\mathbb{E}[E] = 0$, it is clear that $R_Y = R_S + R_E$ and hence

$$\gamma_{pq} = 1 + \xi_{pq}.$$

Some commonly used methods to determine ξ_{pq} are provided in section 4.5.

Considering noise models (3.1) and (3.2), spectral domain denoising can be generalized as shown in figure 4.1. It is based on a so called gain or transfer function $H : \mathbb{R}^+ \to [0,1]$, a function of one parameter, the "a priori SNR" $\xi_{p,q}$. The estimation $\hat{S}_{p,q}$ of $S_{p,q}$ is given by

$$\hat{S}_{p,q} = H_{p,q} \cdot Y_{p,q} \tag{4.3}$$

where $H_{p,q} := H(\xi_{p,q})$. The fact that $H_{p,q} \in [0,1]$ ensures each coefficient is either preserved or shrunken but not enlarged. To obtain $\xi_{p,q}$ one needs to determine the noise variance $R_E(p,q)$ which is constant for all $(p,q) \in \mathcal{I}$ for stationary noise, for Gaussian white noise $R_E(p,q) \equiv \sigma^2$. Otherwise, some normalizations similar to (3.4) might be useful to avoid current and expensive noise variance updating. The actual gain function H depends on the used filter, i.e. the denoising method.

For the following filters, the gain function is chosen to be real even though the transformed coefficients may be complex. Hence, these filters only change the spectral amplitude but not phase. However, Ephraim and Malah show that the optimal phase estimator is given by the phase of the noised transformed coefficients [12]. Hence, real gain functions are sufficient.

4.2 Wiener Filter

One of the most common filters and basis for many others [14],[31],[12] is the Wiener Filter (WF), published already in 1949 by Norbert Wiener [35]. We use the noise model in spectral domain as described in (3.2), that is

$$Y_{pq} = S_{pq} + E_{pq},$$

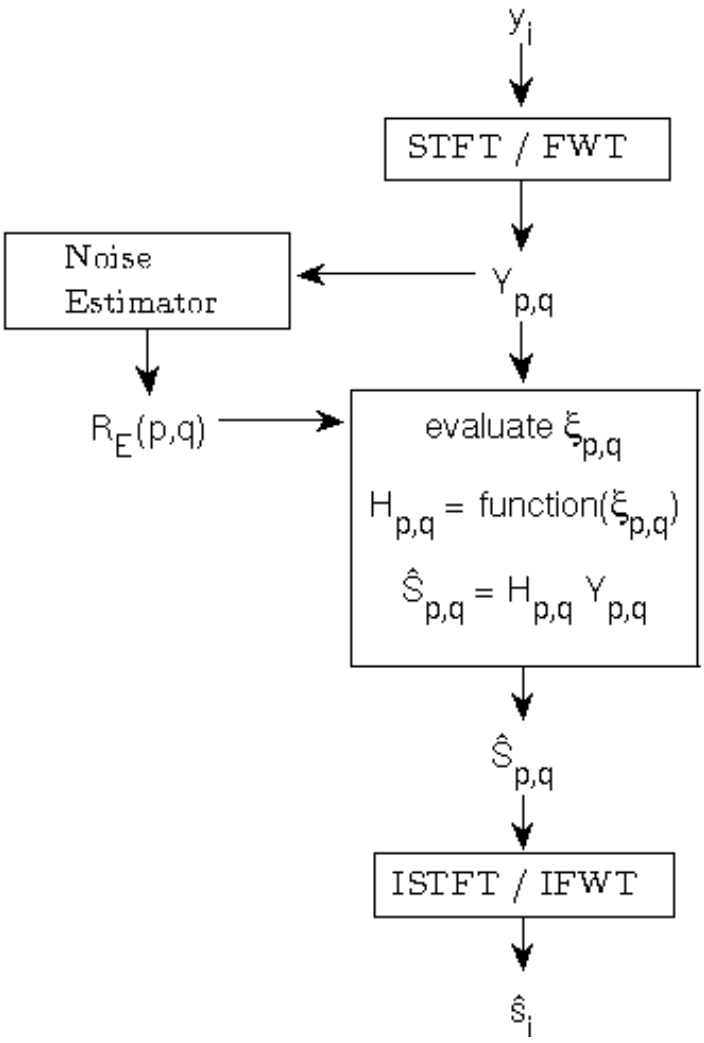

Figure 4.1: General spectral domain denoising algorithm

and try to find an "optimal" gain function H_{pq}. The idea of the Wiener filter is to minimize the Risk function (3.9) in spectral domain, i.e for $n = |\mathcal{I}|$ one minimizes

$$\begin{aligned} Risk(S, \hat{S}) &= \frac{\mathbb{E}\left[||S - \hat{S}||^2\right]}{n} \\ &= \frac{\mathbb{E}\left[||S - HY||^2\right]}{n}. \end{aligned}$$

Norbert Wiener proposed to use the zero of the risk's partial derivative with respect to H, i.e. to find a gain function H such that

$$\begin{aligned} n\,\frac{\partial Risk(S, \hat{S})}{\partial H} &= 2\mathbb{E}\left[(S - HY)\bar{Y}\right] \\ &= 2\left(\mathbb{E}\left[S\bar{Y}\right] - H\mathbb{E}\left[||Y||^2\right]\right) \\ &= 0. \end{aligned}$$

Therefore, with $R_X = \mathbb{E}\left[||X||^2\right]$, one obtains

$$\begin{aligned} H^{Wiener} &= \frac{\mathbb{E}\left[S\bar{Y}\right]}{R_Y} \\ &= \frac{\mathbb{E}\left[(Y - E)\bar{Y}\right]}{R_Y} \\ &= \frac{R_Y - \mathbb{E}\left[E\bar{Y}\right]}{R_Y} \\ &= \frac{R_Y - \mathbb{E}\left[E(\bar{S} + \bar{E})\right]}{R_Y} \\ &= \frac{R_Y - R_E}{R_Y}, \end{aligned}$$

applying the independence of E and S which implies $\mathbb{E}[E\bar{S}] = 0$ for $\mathbb{E}[E] = 0$. Using ξ_{pq} and γ_{pq} as defined by (4.1) and (4.2), respectively, the gain function is given by

$$\begin{aligned} H_{pq}^{Wiener} &= \frac{R_Y(p,q) - R_E(p,q)}{R_Y(p,q)} \\ &= \frac{\gamma_{pq} - 1}{\gamma_{pq}} = \frac{\xi_{pq}}{1 + \xi_{pq}} \end{aligned} \tag{4.4}$$

and leads to estimations of S_{pq} given by

$$\hat{S}_{pq}^{Wiener} = H_{pq}^{Wiener}\, Y_{pq}. \tag{4.5}$$

The fact that ξ_{pq} in (4.5) is positive ensures H_{pq}^{Wiener} to be in $[0,1]$, i.e. Wiener filtering can be considered as shrinking coefficients. Considering above equations, one can see H^{Wiener} as both, a function of a priori SNR and a posteriori SNR. However, in each case we need to find approximations for γ_{pq} or ξ_{pq}, respectively. Some methods are presented in section 4.5. Assuming the knowledge of $R_S(p,q) = S_{pq}^2$ and $E_{pq} \sim N(0,\sigma^2)$, a priori noise ξ_{pq} could be exactly evaluated and the risk function would be given by

$$risk(S, \hat{S}^{Wiener}) = \frac{1}{|\mathcal{I}|} \sum_{(pq)\in\mathcal{I}} \frac{S_{pq}^2 \sigma^2}{S_{pq}^2 + \sigma^2}. \tag{4.6}$$

The proof is straightforward using simple calculations and the definition of MSE.

4.3 Spectral Subtraction and Power Subtraction Filter

Some widely used alternatives are the Spectral Subtraction Filter (SSF) and the Spectral Power Filter (PSF) [13], [14]. In contrast to the Wiener filter which is based on a well-defined optimality criterion, i.e. the minimization of the risk function, SSF and PSF use a rather intuitive approaches. The idea of SSF is to remove the noise magnitude, i.e. simplified we have

$$|\hat{S}_{pq}^{SSF}| = |Y_{pq}| - \sqrt{R_E(p,q)}$$

and

$$\hat{S}_{pq}^{SSF} = \frac{|Y_{pq}| - \sqrt{R_E(p,q)}}{|Y_{pq}|} Y_{pq}$$

This method is especially useful for systems using multiple microphones, one recording noisy speech and another noise only. Assuming $|Y_{pq}| = \sqrt{R_Y(p,q)}$, one can use above notations and with $\gamma_{pq} = 1 + \xi_{pq}$, one obtains

$$\begin{aligned} H_{pq}^{SSF} &= \frac{\sqrt{R_Y(p,q)} - \sqrt{R_E(p,q)}}{\sqrt{R_Y(p,q)}} \\ &= 1 - \sqrt{\frac{1}{1+\xi_{pq}}} \qquad (4.7) \\ \hat{S}_{pq}^{SSF} &= H_{pq}^{SSF}\, Y_{pq}. \qquad (4.8) \end{aligned}$$

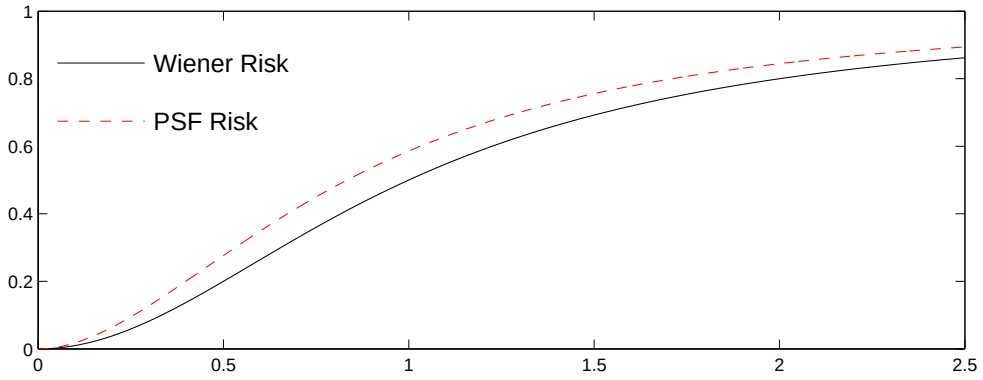

Figure 4.2: Risk function for Wiener and power spectral filter

A similar filter, the PSF, is based on the idea of obtaining gain functions $H \approx S/Y$. Since $\mathbb{E}\left[|S|^2\right] = R_S = R_Y - R_E$, an appropriate choice is given by

$$\begin{aligned} H_{pq}^{PSF} &= \frac{\sqrt{R_Y(p,q) - R_E(p,q)}}{\sqrt{R_Y(p,q)}} \\ &= \sqrt{\frac{\xi_{pq}}{1+\xi_{pq}}} \end{aligned} \tag{4.9}$$

which is in fact just the square root of the Wiener filter. Similar to (4.6), if ξ_{pq} is given exactly, the risk function can be provided,

$$risk(S, \hat{S}^{PSF}) = \frac{1}{|\mathcal{I}|} \sum_{(pq)\in\mathcal{I}} 2S_{pq}^2 \left(1 - \sqrt{\frac{S_{pq}^2}{S_{pq}^2 + \sigma^2}}\right). \tag{4.10}$$

In figure 4.2 the Wiener risk is compared with the PSF risk as a function of one single coefficient S and with $\sigma^2 = 1$. It is clear that the Wiener risk is smaller since it is constructed to minimize the risk function. However, PSF may have other advantages. A hole class of similar filters is given in [31], changing only few parameters, e.g. using other roots but the square root.

4.4 Ephraim-Malah Filter

The following more complex filter has been presented by Ephraim and Malah in [12]. It is based on the following statistical assumptions: the FFT coefficients Y_{pq}, S_{pq} and E_{pq} can be seen as Gaussian random variables with zero mean, i.e. $X_{pq} \sim N(0, R_X(p,q))$, $X \in \{Y, S, E\}$. This is motivated by the central limit theorem, since each coefficient is a weighted sum of some "random"

variables. Sufficiently separated samples of the original signals are almost independent. Appropriate Windows (e.g. Hanning windows) reduces correlations between widely separated coefficients but enlarges correlations between adjacent coefficients. However, correlations between transformed coefficients approach zero for large frame lengths. hence, we assume that the coefficients are pairwise independent (or at least only weakly dependent). For more details see [12].

The Ephraim-Malah Filter (EMF) pursues the estimation of the spectral amplitude using conditional expectations, i.e. for

$$\begin{aligned} S_{pq} &= A_{pq}e^{i\alpha_{pq}} \\ Y_{pq} &= B_{pq}e^{i\beta_{pq}}, \end{aligned}$$

one estimates A_{pq} based on the set of observations $\{Y_{pq}|(p,q) \in \mathcal{I}\}$. The pairwise independence ensures that the estimation $\hat{A}_{pq}$ of A_{pq} depends only on Y_{pq}, i.e. only on coefficients of same time and frequency. More precise, the estimation is given by the conditional expectation

$$\begin{aligned} \hat{A}_{pq} &= \mathbb{E}\left[A_{pq}|Y_{pq}\right] \\ &= \frac{\int_0^\infty \int_0^{2\pi} a_{pq} P(Y_{pq}|a_{pq},\alpha_{pq}) P(a_{pq},\alpha_{pq})\ d\alpha_{pq} da_{pq}}{\int_0^\infty \int_0^{2\pi} P(Y_{pq}|a_{pq},\alpha_{pq}) P(a_{pq},\alpha_{pq})\ d\alpha_{pq} da_{pq}} \end{aligned}$$

where $P(\cdot)$ denotes probability density functions

$$\begin{aligned} P(Y|a,\alpha) &= \frac{1}{\pi R_E} exp\left(-\frac{|Y - ae^{i\alpha}|^2}{R_E}\right) \\ P(a,\alpha) &= \frac{a}{\pi R_S} exp\left(-\frac{a^2}{R_S}\right). \end{aligned}$$

As shown in [12], substituting the above equations into the integral leads to

$$\hat{A}_{pq} = \frac{\sqrt{\pi\xi_{pq}}}{1+\xi_{pq}} exp\left(-\frac{\xi_{pq}}{2}\right)\left((1+\xi_{pq})I_0\left(\frac{\xi_{pq}}{2}\right) + \xi_{pq} I_1\left(\frac{\xi_{pq}}{2}\right)\right) B_{pq} \qquad (4.11)$$

where I_n is the modified Bessel function of order n,

$$I_n(x) = \frac{1}{2\pi}\int_0^{2\pi} cos(\beta n) e^{xcos\beta} d\beta.$$

As mentioned above, the optimal phase estimator $\hat{\alpha}_{pq}$ is given by β_{pq}. For that

reason the EMF gain function and the estimator $\hat{S}_{pq}^{EMF}$ can now be obtained by

$$\begin{aligned} H_{pq}^{EMF} &= \frac{\hat{A}_{pq}}{B_{pq}} && (4.12) \\ \hat{S}_{pq}^{EMF} &= H_{pq}^{EMF}\, Y_{pq} \\ &= H_{pq}^{EMF}\, B_{pq} e^{i\beta_{pq}} \\ &= \hat{A}_{pq} e^{i\beta_{pq}}. && (4.13) \end{aligned}$$

4.5 A priori SNR Estimation

The a priori SNR ξ_{pq} is given by the ration of signal spectral component variance $R_S(p,q)$ and noise spectral component variance $R_E(p,q)$. Let's take first a look at the latter one. Then, I will provide some different methods of estimating ξ_{pq} as shown for example in [12].

Noise Spectral Component Variance In practice this variance is estimated using an interval without speech, hence only affected by noise. Assuming the noise to be stationary, i.e. $R_E(p,q) \equiv const$, it suffices to estimate R_E only one time. For a fixed window indicated by q_0 with pure zero mean noise and n samples, that is the sample variance

$$\hat{R}_E = \frac{1}{n-1} \sum_{p=0}^{n-1} Y_{pq_0}^2.$$

However, it is not always easy to determine pure noise time intervals. Especially for non-stationary noise, one needs to update R_E regularly. Nevertheless it is the most common method, also used in professional software, e.g. the open source audio editor Audacity. For some applications like communication from a helicopter, additional microphones are installed recording only noise, facilitating the estimation of R_E. We will see later that there are wavelet based denoising methods that can be realized without explicit noise variance estimation.

A priori SNR Since $R_Y(p,q) = \mathbb{E}[|Y_{pq}|^2] = |Y_{pq}|^2$ is known, with above estimation of $R_E(p,q)$ one could use $R_S(p,q) = R_Y(p,q) - \hat{R}_E(p,q)$ leading to the approximations

$$\begin{aligned} \hat{\gamma}_{pq} &= |Y_{pq}|^2 / \hat{R}_E(p,q), \\ \hat{\xi}_{pq}^{(1)} &= \hat{\gamma}_{pq} - 1. \end{aligned}$$

However, using just one coefficient of the transformed input to estimate a priori noise is probably too imprecise. Furthermore, as the name says, the variances rather indicate a kind of volatility around (p, q) than an approximation of Y_{pq} or S_{pq}, respectively. Hence, assuming only slowly in time varying variances R_E and R_S, averaging several values Y_{pq} might be preferable [12]. Let's base the estimation on L consecutive observations $Y_{p,q}, Y_{p,q-1}, ..., Y_{p,q-L+1}$ of same frequency but in different time frames. One assumes these values to be independent, which would be reasonable for non-overlapping frames. Now, one uses the sample variance of these values and obtains

$$\hat{R}_S(pq) = \begin{cases} \frac{1}{L}\sum_{l=0}^{L-1} |Y_{p,q-l}|^2 - R_E(p,q) & \text{, if nonnegative} \\ 0 & \text{, otherwise} \end{cases}$$

which leads to

$$\hat{\xi}_{pq}^{(2)} = \begin{cases} \frac{1}{L}\sum_{l=0}^{L-1} \hat{\gamma}_{p,q-l} - 1 & \text{, if nonnegative} \\ 0 & \text{, otherwise.} \end{cases}$$

where as above $\hat{\gamma}_{p,q-l} = \frac{|Y_{p,q-l}|^2}{R_E(p,q-l)}$. In practice, this average is replaced by a recursive averaging,

$$\bar{\gamma}_{pq} = \alpha\bar{\gamma}_{p,q-1} + (1-\alpha)\frac{\gamma_{pq}}{\beta}$$

where $0 \leq \alpha < 1,\ \beta \geq 1$. The choices of α and β depend on the used filter and on auditory perception. Some examples can be found in [12]. Now, the estimator for a priori SNR is given by

$$\hat{\xi}_{pq}^{(3)} = \begin{cases} \bar{\gamma}_{pq} - 1 & \text{, if nonnegative} \\ 0 & \text{, otherwise.} \end{cases}$$

Another similar estimator, especially used in combination with the Wiener filter, is given by

$$\hat{\xi}_{pq}^{(4)} = \alpha\hat{\xi}_{p,q-1}^{(4)} + (1-\alpha)\mathbb{1}_{\{\gamma_{pq}\geq 1\}}(\gamma_{pq} - 1)$$

with initial condition $\hat{\xi}_{p,-1}^{(4)} = 1$ which has been verified to be appropriate [12].

Chapter 5

Lipschitz Denoising

The idea of Lipschitz denoising is based on the detection of Lipschitz regularities using local maxima of the wavelet transform. The same results can be obtained using more general Besov regularities instead (see section 7.4). However, in this case Lipschitz regularity is more illustrative and facilitates the understanding. The presented method is based on the work of Mallat, Hwang and Zhong [22], [23], [24]. It has been successfully applied on edge detection and image enhancement. I will provide some examples of Lipschitz regularities and its detection with the help of wavelets and investigate the usage of the presented methods in Audio signal denoising.

5.1 Lipschitz Regularity

In the first section I will introduce the notion of Lipschitz regularity and its practical meaning as well as a definition of singularity based on Lipschitz regularities. Furthermore I will provide some examples of different Lipschitz regularities for a better understanding.

Definition 5.1.1. (Lipschitz Regularity)

(i) Let $n \in \mathbb{N}$ and $\alpha \in \mathbb{R}$ such that $n \leq \alpha \leq n+1$. A function f is called Lipschitz α at x_0 if there exist constants A and $h_0 > 0$ as well as a polynomial $P_n(h)$ of order n such that the following holds $\forall\ h < h_0$:

$$|f(x_0 - h) - P_n(h)| \leq A|h|^\alpha. \tag{5.1}$$

(ii) The function is said to be uniformly Lipschitz α in the interval (a, b) if there exists a constant A and for each $x_0 \in (a, b)$ there is a polynomial $P_n(h)$ of order n such that (5.1) is satisfied if $x_0 + h \in (a, b)$.

(iii) The Lipschitz regularity of f at x_0 is defined as $\sup\{\alpha | f$ is Lipschitz α at $x_0\}$.

(iv) We say that f is singular at x_0 if it is not Lipschitz 1 at x_0.

Lipschitz regularity gives an indication of differentiability. A function f that is continuously differentiable at x_0 is Lipschitz 1. If the derivative of f is not continuous but bounded at x_0, f is still Lipschitz 1, therefore according to 5.1.1 not singular at x_0. Let $n \in \mathbb{N}$ and $\alpha > n$. A function f that is Lipschitz α at x_0 is n times differentiable at x_0 and $P_n(h)$ is identical to the n-th Taylor polynomial of f at x_0. Lipschitz regularity provides even more information. Suppose the Lipschitz regularity of f at x_0 is α_0 with $n < \alpha_0 < n + 1$, then f is n times differentiable at x_0 but its nth derivative is singular at x_0. Furthermore, α_0 characterizes this singularity.

Remark 5.1.2.

(i) One can prove that if f is Lipschitz α at x_0 then its primitive is Lipschitz $\alpha + 1$ at the same point.

(ii) The opposite is not true: Let a primitive F of a function f be Lipschitz α, then f is not necessarily Lipschitz $\alpha - 1$. This is due to possible oscillations as shown in [23].

However, if f is uniformly Lipschitz α on an interval (a, b) for $\alpha \notin \mathbb{Z}, \alpha > 1$ then its primitive is Lipschitz $\alpha + 1$ on the same interval. By extending this property one can define negative uniform Lipschitz exponents for tempered distributions. A tempered distribution can be characterized as "slow growing", e.g. locally integrable function with at most polynomial growth $f(x) = O(|x|^r)$ for some r which includes all functions $f \in L^p(\mathbb{R})$, $p \geq 1$. A formal definition can be found for example in [37] and many other fundamental books on functional analysis.

Definition 5.1.3. For a tempered distribution f and for $\alpha \in \mathbb{R} \setminus \mathbb{Z}$ a non-integer real number and $(a, b) \subset \mathbb{R}$ a real interval, f is said to be uniformly Lipschitz α on (a, b) if its primitive is uniformly Lipschitz $\alpha + 1$ on (a, b).

Having this definition in mind we can redefine the notion of singularity in a more general way than 5.1.1 (iv).

Definition 5.1.4. We will call a function f isolated singular at x_0 if there is no interval (a, b) with $x_0 \in (a, b)$ such that f is uniformly Lipschitz 1 but there is an interval (a, b), $x_0 \in (a, b)$, such that f is uniformly Lipschitz 1 over any subinterval of (a, b) that does not include x_0.

I already mentioned that continuously differentiable functions and functions with noncontinuous but bounded derivatives are Lipschitz 1 and therefore not singular. I will provide some more examples for a better understanding of Lipschitz regularity. Later I will refer to these examples to demonstrate how to use wavelet transform to detect singularities.

Example 1. (The step function)
The primitive of a step function

$$s(x) = \begin{cases} 0 & \text{, if } x < 0 \\ 1 & \text{, if } x \geq 0 \end{cases}$$

is continuous but not differentiable at $x = 0$. However, since it is piecewise linear the primitive is still Lipschitz 1 in a neighborhood of 0 and therefore uniformly Lipschitz α_0 for $\alpha_0 < 1$. Hence, the step function is uniformly Lipschitz α_1 for $\alpha_1 < 0$. Definition 5.1.3 is only defined for non-integer α, that's why we can not say that s is Lipschitz 0. Nevertheless it has an isolated Lipschitz α_1 singularity at $x = 0$.

Example 2. (The Dirac delta function)
The step function s is the primitive of the Dirac delta function, defined as

$$\delta(x) = \begin{cases} \infty & \text{, if } x = 0 \\ 0 & \text{, if } x \neq 0. \end{cases}$$

Thus we can immediately conclude from definition 5.1.3 and the preceding example that it is uniformly Lipschitz α for $\alpha < -1$ in a neighborhood of $x = 0$, hence singular at $x = 0$.

Example 3. ($\sqrt{|x|}$)
$f(x) = \sqrt{|x|} = |x|^{\frac{1}{2}}$ is continuous and differentiable for all $x \neq 0$, but it is not Lipschitz 1 since the derivative

$$f'(x) = 0.5 * sgn(x) * |x|^{-\frac{1}{2}} = \begin{cases} 0.5 * x^{-\frac{1}{2}} & \text{, if } x > 0 \\ -0.5 * (-x)^{-\frac{1}{2}} & \text{, if } x < 0. \end{cases}$$

is not bounded in any neighborhood of $x = 0$ (see figure 5.1). Thus, f is not Lipschitz 1 and it directly follows from definition 5.1.1 that the function is Lipschitz $\frac{1}{2}$. For $n = 0$ and $P_n(h) \equiv 0$ we get

$$\left| |x_0 + h|^{\frac{1}{2}} - P_n(h) \right| = |h|^{\frac{1}{2}} \leq A|h|^{\alpha}$$

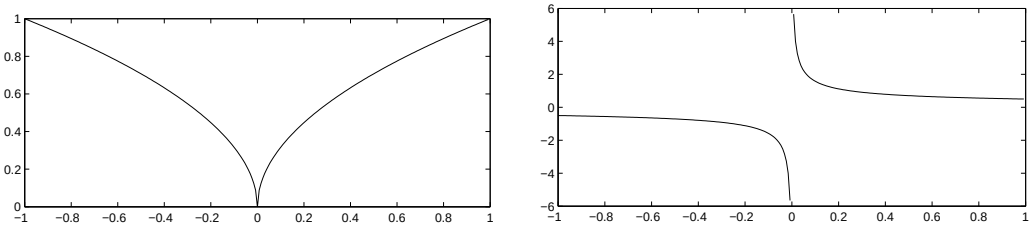

Figure 5.1: Example 3: Graph of $\sqrt{|x|}$ (a) and its derivative (b)

which is obviously true for $\alpha = \frac{1}{2}$ and $A = 1$.

Example 4. (Gaussian white noise)
As mentioned for example in [1] Gaussian white noise is singular almost everywhere and has a uniform Lipschitz regularity of $-\frac{1}{2}$. Later we shall see that common audio speech signals have positive Lipschitz regularities and therefore they can be distinguished from Gaussian white noise.

5.2 Lipschitz Regularity Detection with the Wavelet Transform

Let us now come to the relation of Lipschitz regularity and the continuous wavelet transform. For a wavelet function ψ, define the dilation of ψ as

$$\psi_s(x) = \frac{1}{s}\psi(\frac{x}{s})$$

and the continuous wavelet transform of a function $f \in L^2(\mathbb{R})$ as the convolution of f and ψ_s

$$Wf(s,x) := f * \psi_s := \int_{-\infty}^{\infty} f(u)\frac{1}{s}\psi\left(\frac{x-u}{s}\right)\,\mathrm{d}u. \tag{5.2}$$

Please note that this definition is slightly different from the CWT introduced in section 2.1. Instead of an inner product as in formula (2.1) the wavelet transform is now written as a convolution which will facilitate some proofs. Furthermore, $\frac{1}{\sqrt{s}}$ is replaced by $\frac{1}{s}$. This makes it easier to detect Lipschitz regularities from the wavelet transform. However, the difference between both transforms is just a constant factor depending on the scale and does not change anything of the

general concept. We say that ψ has n vanishing moments if

$$\int_{-\infty}^{\infty} x^k \psi(x)\, \mathrm{d}x = 0 \tag{5.3}$$

for all nonnegative integers $k < n$. Obviously, this definition is the same for both definitions of the CWT. The following theorem provides a way how to detect the Lipschitz regularity of a function f with the help of the decay of the Wavelet transform as a function of the scale s.

Theorem 5.2.1. *Let ψ be a real wavelet function with compact support and n vanishing moments. For $f \in L^2(\mathbb{R})$, $[a, b] \subset \mathbb{R}$ and $0 < \alpha < n$ the following statements are equivalent:*

- *For all $\epsilon > 0$, f is uniformly Lipschitz α on $(a + \epsilon, b - \epsilon)$.*
- *There is a constant A_ϵ such that for $x \in (a + \epsilon, b - \epsilon)$ and $s > 0$*

$$|Wf(s, x)| \leq A_\epsilon s^\alpha. \tag{5.4}$$

Proof. For only continuously differentiable wavelet functions and $n = 1$ a proof of the theorem can be found in [18]. In the case of n vanishing moments, $n > 1$, for any positive integer $p < n$ there exists another wavelet function ψ^1 such that

$$\psi(x) = \frac{d^p \psi^1(x)}{dx^p}$$

and, in the sense of weak derivatives, it holds that

$$\begin{aligned} Wf(s, x) &= f * \psi_s(x) && (5.5)\\ &= \frac{d^p}{dx^p}(f * s^p \psi^1_s)(x) && (5.6)\\ &= s^p \left(\frac{d^p f}{dx^p} * \psi^1_s \right)(x). && (5.7) \end{aligned}$$

Let p be an integer such that $0 < \alpha - p < 1$. The function f is uniformly Lipschitz α if and only if $d^p f / dx^p$ is uniformly Lipschitz $\alpha - p$ which is according to the already proven case $n = 1$ equivalent to

$$\left| \frac{d^p f}{dx^p} * \psi^1_s(x) \right| \leq A_\epsilon s^{\alpha - p} \tag{5.8}$$

Eventually, using equation (5.7), this is equivalent to equation (5.4). □

There is a similar result based on the Fourier transform, considering the scale s "equivalent" to $1/\omega$ for frequencies ω. A function f is uniformly Lipschitz α on $\mathbb{R}$ if

$$\int_{-\infty}^{\infty} |\hat{f}(\omega)|(1+|\omega|^{\alpha})d\omega < \infty,$$

where $\hat{f}(\omega)$ denotes the Fourier transform of f. This sufficient condition implies that $|\hat{f}(\omega)|$ has a decay "faster" than $1/\omega^{\alpha}$ for large frequencies ω. In opposition to the Fourier transform condition, (5.4) is sufficient and necessary as well as localized on finite intervals.

Remark 5.2.2.

- If ψ has exactly n vanishing moments, the decay of $|Wf(s,x)|$ does not tell us anything about Lipschitz regularities $\alpha > n$. For example $sin(x)$ has regularity $+\infty$, but the decay of $|Wf(s,x)|$ would be of order s^n.
- For $\alpha < 0, \alpha \notin \mathbb{Z}$ equation (5.4) remains valid to characterize uniform Lipschitz exponents. This follows directly from definition 5.1.3 of negative Lipschitz regularities.

However, to detect the Lipschitz regularity at a point x_0 theorem 5.2.1 imposes to measure the decay of $Wf(s,x)$ in a whole two-dimensional neighborhood of x_0, which is useless for numerical computations. The next section will provide numerically more efficient methods.

5.3 Wavelet Transform Modulus Maxima

In the following we suppose f and ψ to be real. Now, I will provide the exact definition of the meaning of modulus maxima and maxima lines.

Definition 5.3.1.

- A modulus maxima is defined as a point (s_0, x_0) such that for any x in a neighborhood of x_0 we have $|Wf(s_0,x)| < |Wf(s_0,x_0)|$. We still call (s_0, x_0) a modulus maxima if the inequality is strict for only the right or only the left side of the neighborhood of x_0, i.e. if (s_0, x_0) is a strict extrema on either the left or the right side of x_0.
- A maxima line is defined as a connected curve in the scale space (s, x) along all points are modulus maxima.

The next theorem shows that if there are no modulus maxima in a neighborhood of x_0 at fine scales, then the function is uniformly Lipschitz α in this neighborhood for $\alpha <$ n.

Theorem 5.3.2. *Let ψ be a n-times continuously differentiable wavelet function with compact support and n vanishing moments and let $f \in L^1([a,b])$.*

- *If there is a scale $s_0 > 0$ such that $|Wf(s,x)|$ has no local maxima for all scales $s < s_0$ and $x \in (a,b)$, then $\forall \epsilon > 0$ and $\alpha < n$ f is uniformly Lipschitz α in $(a+\epsilon, b-\epsilon)$.*
- *If ψ is additionally the n-th derivative of a smoothing function θ, i.e. $\theta = \mathcal{O}(\frac{1}{1+x^2})$ and $\int \theta(x)\ \mathrm{d}x \neq 0$, then f is uniformly Lipschitz n on such an interval.*

Proof. The exact proof is very technical and can be found in [23]. In short, for the first part one proves by induction that if $|Wf(s,x)|$ has no maxima, for any n and any $\epsilon > 0$ there is a constant $A_{\epsilon,n}$ such that

$$|Wf(s,x)| \leq A_{\epsilon,n} s^n \tag{5.9}$$

holds for $x \in (a+\epsilon, b-\epsilon)$ and $s < s_0$. Then one can apply theorem 5.2.1. For the second part of the proof, we write $\psi = d^n\theta/dx^n$ and get, in the weak sense of derivatives,

$$|Wf(x,s)| = s^n \frac{d^n f}{dx^n} * \theta_s(x).$$

The first part of the theorem and equation (5.9) now implies that for any $\epsilon > 0$ and $x \in (a+\epsilon, b-\epsilon)$

$$\left| \frac{d^n f}{dx^n} * \theta_s(x) \right| \leq A_{\epsilon,n}.$$

Since the integral of $\theta(x)$ is not vanishing, this equation implies that $d^n f/dx^n$ is bounded by $A_{\epsilon,n}$ and from definition 5.1.1 we get that f is uniformly Lipschitz n on $(a+\epsilon, b-\epsilon)$. □

In other words the theorem states that in any neighborhood where the wavelet transform of f has no modulus maxima at fine scales, f can not be singular and the closure of the set of points where f is not Lipschitz n is included in the closure of the wavelet transform maxima of f. Hence, all singularities of f can be detected by following the maxima lines when the scale goes to zero.

In the following we suppose that the function f has no fast oscillations. We say a function f has fast oscillations if it is not Lipschitz α although its primitive is Lipschitz $\alpha+1$. One example of a fast oscillating function could be $sin(1/x)$ in

the neighborhood of $x = 0$. However, such "fast oscillations" are not important for our denoising models. The following theorem characterizes singularities from the behavior of modulus maxima.

Theorem 5.3.3. *Let ψ be of compact support, n times continuously differentiable and the n-th derivative of a smoothing function. Furthermore let f be a tempered distribution and $x_0 \in (a, b)$. We assume that $\exists s_0 > 0$ and a constant C such that for $x \in (a, b)$ and $s < s_0$, all modulus maxima belong to a cone defined by*

$$|x - x_0| \leq Cs. \tag{5.10}$$

Then the following statements hold:

- *For any $x_1 \in (a, b), x_1 \neq x_0$, f is uniformly Lipschitz n in a neighborhood of x_1.*
- *Let $\alpha < n, \alpha \notin \mathbb{Z}$, then f is Lipschitz α at x_0 if and only if there exists a constant A such that at each modulus maxima (s, x) in the cone (5.10) it holds that*

$$|Wf(s, x)| \leq As^{\alpha}. \tag{5.11}$$

Proof. One can prove the first part with the help of theorem 5.3.2. It follows directly that f is Lipschitz n at all points $x_1 \neq x_0$. For any $\epsilon > 0$ such that $a + 2\epsilon < x_0 - 2\epsilon$ there exits s_ϵ such that for $s < s_\epsilon$ and $x \in (a + \epsilon, x_0 - \epsilon)$ the wavelet transform $|Wf(s, x)|$ has no maxima (i.e. (s, x) is not in the cone (5.10)). Hence, with theorem 5.3.2 one concludes that f is uniformly Lipschitz n in a neighborhood of $x_1 \in (a, x_0)$. Obviously, the same proof can be done for $x_1 \in (x_0, b)$.

The main difference between the second part of this theorem and theorem 5.2.1 is that we consider only points in the cone (5.10) and look only on modulus maxima. However, the truth of equation (5.11) can be followed directly from theorem 5.2.1. So it remains to prove that the Lipschitz regularity at x_0 depends only on the modulus maxima in the cone (5.10). Let $x_1 \in (a, x_0)$ and $x_2 \in (x_0, b)$. Since f is Lipschitz n in the neighborhood of x_1 and x_2 one obtains from theorem 5.2.1 that there exists $s_0 > 0$ such that for $s < s_0$,

$$|Wf(s, x_1)| \leq A_1 s^n \text{ and} \tag{5.12}$$

$$|Wf(s, x_2)| \leq A_2 s^n. \tag{5.13}$$

For $x \in (x_1, x_2)$ and $s < s_0$, $|Wf(s, x)|$ is smaller or equal to $|Wf(s, x_1)|$, $|Wf(s, x_2)|$ and all modulus maxima in the cone (5.10) for $s < s_0$. Further-

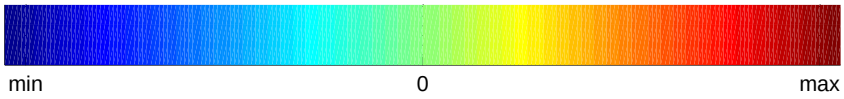

Figure 5.2: Colorbar: blue indicates smallest, red biggest values

more, all the modulus maxima are smaller or equal to As^α. From (5.12) and (5.13) and since $\alpha < n$ (which implies that f is also Lipschitz α at x_1, and x_2), one derives that there exists a constant B such that for $x \in (x_1, x_2)$ and $s < s_0$

$$|Wf(s,x)| \leq Bs^\alpha.$$

Now, one can apply again theorem 5.2.1 since $x_0 \in (x_1, x_2)$ and one obtains that f is Lipschitz α at x_0. □

For the detection of Lipschitz regularity, it is useful to rewrite equation (5.11) in the following form:

$$log|Wf(x,s)| \leq log(A) + \alpha log(s). \tag{5.14}$$

Thus, theorem 5.3.3 says that the Lipschitz regularity at a point x_0 is given by the maximum slope of straight lines that remain above $log|Wf(x,s)|$ for (s,x) in the cone defined by (5.10) and on a logarithmic scale.

Usually we deal with discretized functions, let's assume the resolution is 1. Hence, the smallest possible scale is 1. In fact it doesn't even make sense to talk about singularities or discontinuities as well as Lipschitz regularities for the discrete case. However, we will see that evaluating the decay of $|Wf(s,x)|$ up to the finest scale $s = 1$ already provides good results. Let us again take a look at the examples introduced in section 5.1. Instead of determine α by finding the slope of the line that is above all modulus maxima as proposed by (5.14) we use the line best approximating (in mean square error sense) a function "through" the modulus maxima since we can not evaluate $Wf(s,x)$ at any scale.

For the following computations, I evaluated the functions at 256 equidistant points in the interval $[-1, 1)$. An algorithm similar to the stationary wavelet transform is used, taking into account that we used a slightly different definition of the continuous wavelet transform. The wavelet function $\psi(x)$ is chosen to be a quadratic spline of support $[-1, 1]$ and with one vanishing moment, as suggested by Mallat and Hwang in [23]. The algorithm has also been described by Mallat and Zhong in [24].

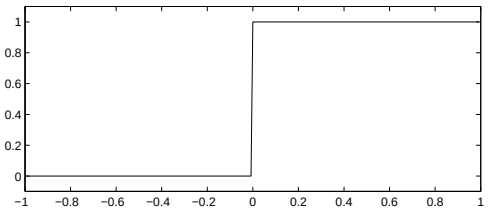

(a) graph of a step function

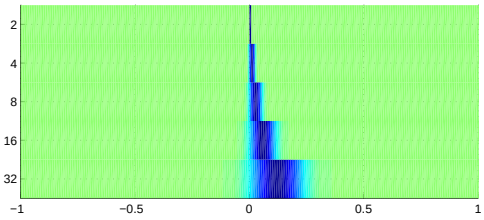

(b) stationary wavelet transform $Wf(s,x)$ at scales $s = 2^n, n = 1, ..., 5$

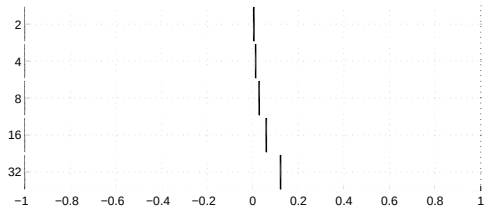

(c) modulus maxima of $Wf(s,x)$

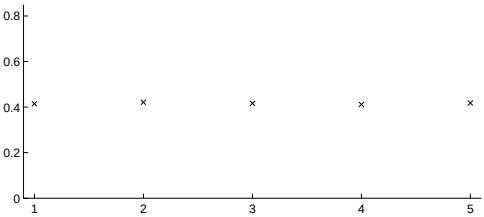

(d) $log_2(Wf(s,x))$ as a function of $log_2(s)$ for all modulus maxima

Figure 5.3: Example 1: The step function

In example 1 we analyzed a step function, plotted in figure 5.3(a). In figure 5.3(b) one can see its wavelet transform $Wf(s,x)$ at scales $s = 2^n, n = 1, ..., 5$. Here and in the following, the colors indicate the values of $Wf(s,x)$ as described by the colorbar in figure 5.2. Here, only in a neighborhood of $x = 0$, the wavelet transform coefficients are nonzero (and negative), all other coefficients vanish. The fact that there are only non-positive values is due to the fact that the used wavelet function ψ satisfies $\psi(x) \geq 0$ for $x \leq 0$ and $\psi(x) \leq 0$ for $x > 0$. In figure 5.3(c) the modulus maxima are plotted. One can see that we have only one modulus maxima at each scale $s = 2^n, n = 1, ..., 5$ and one cold imagine that there would be a maxima line connecting all modulus maxima and converging to $x = 0$ if we would not be restricted on discretized signals and therefore on just a handful scales. However, figure 5.3(c) indicates a Lipschitz regularity of less than 1 at $x = 0$. At the same time, using the first part of theorem 5.3.3, we know that at any $x \neq 0$ we have a Lipschitz regularity of at least 1. To obtain the Lipschitz regularity at x_0 we can use figure 5.3(d). One can see that $log_2(Wf(s,x))$ as a function of $log_2(s)$ is almost constant. According to the second part of theorem 5.3.3 it is now clear that the function is Lipschitz 0 at $x = 0$ since there is a constant A (the value of the modulus maxima) such that $log_2(W(s,x)) \leq log_2(A) + 0 * log_2(s)$. Hence, we verified the result obtained in example 1.

In figure 5.4 the graph of an approximation to the Dirac delta function, introduced in example 2, is shown as well as its wavelet transform and modulus

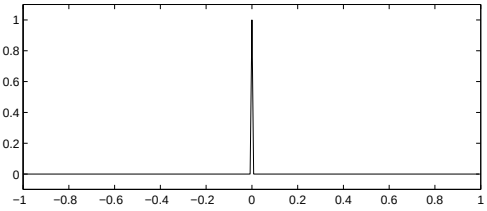

(a) graph of $\delta(x) = 1$ for $x = 0$ and $\delta(x) = 0$ otherwise as an approximation of the Dirac delta function

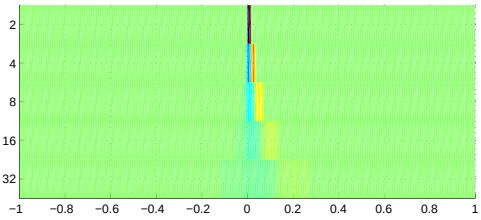

(b) stationary wavelet transform $W\delta(s, x)$ at scales $s = 2^n, n = 1, ..., 5$

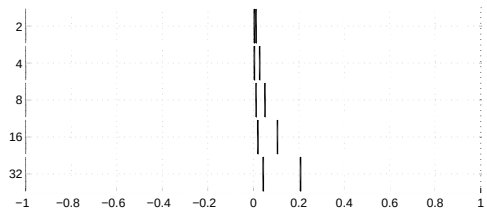

(c) modulus maxima of $W\delta(s, x)$

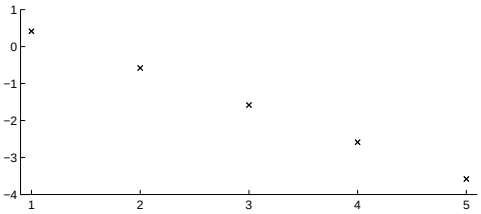

(d) $log_2(W\delta(s, x))$ as a function of $log_2(s)$ for all modulus maxima

Figure 5.4: Example 2: Dirac delta function

maxima. In this case we have two modulus maxima lines, both converging to $x = 0$. The reason why figure 5.4(d) plots only one point per scale is that the two modulus maxima in each scale have the same amplitude, respectively. However, one can see that a straight line through these points has a slope of about -0.8. This does not coincide exactly with the result provided in example 2 where we have proved that the Dirac delta function is Lipschitz -1. This is due to the approximation of the Dirac delta function and the discretization. In this case one could obtain better results using for example Haar wavelets where the slope would be almost exactly -1.

Figure 5.5 shows the plots of example 3. I proved that the Lipschitz regularity is $\alpha = 0.5$. Indeed one can see in figure 5.5(d) that the line that approximates best (in the sense of mean square error) a line through the points has a slope of about 0.4. So again, we obtain a rough approximation for α. For many applications this is already good enough, though. Furthermore, the steps from $log(s) = 3$ to $log(s) = 4$ and from $log(s) = 4$ to $log(s) = 5$ are almost 0.5. The other modulus maxima that occur on scale $s = 2$ don't affect these results since they are out of the cone of influence. Furthermore, their appearance is neither a contradiction to theorem 5.3.2 nor the regularity at these parts since regularity is only a necessary condition.

The last example is Gaussian white noise with standard deviation $\sigma = 0.2$ where I claimed Lipschitz regularity to be $\alpha = -0.5$. A random sample can be

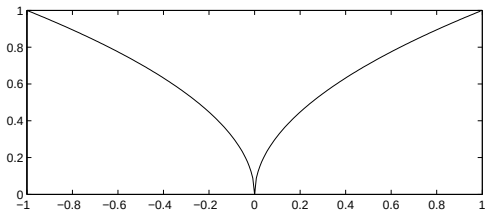

(a) graph of $f(x) = \sqrt{|x|}$

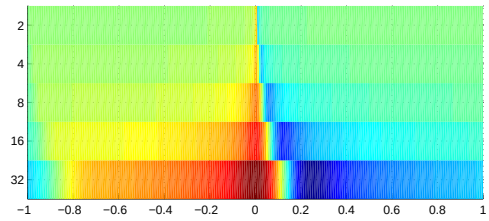

(b) stationary wavelet transform $Wf(s,x)$ at scales $s = 2^n, n = 1, ..., 5$

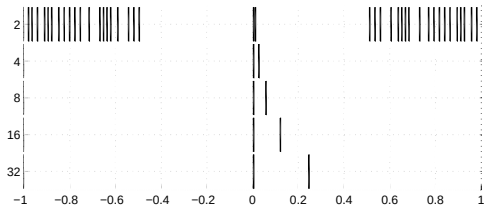

(c) modulus maxima of $Wf(s,x)$

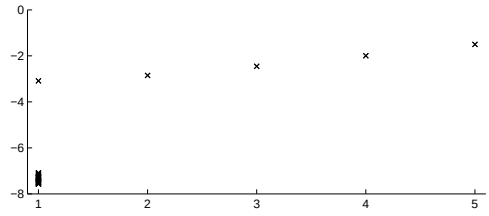

(d) $log_2(Wf(s,x))$ as a function of $log_2(s)$ for all modulus maxima

Figure 5.5: Example 3: $\sqrt{|x|}$

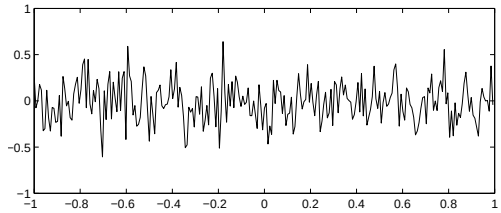

(a) graph of Gaussian white noise with $\sigma = 0.2$

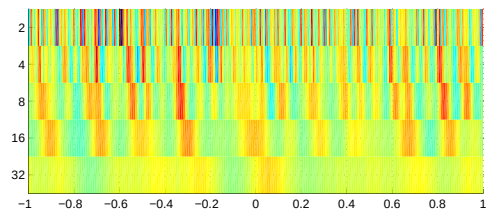

(b) stationary wavelet transform $Wf(s,x)$ at scales $s = 2^n, n = 1, ..., 5$

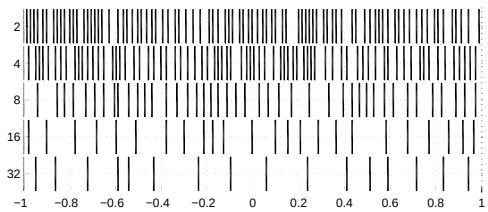

(c) modulus maxima of $Wf(s,x)$

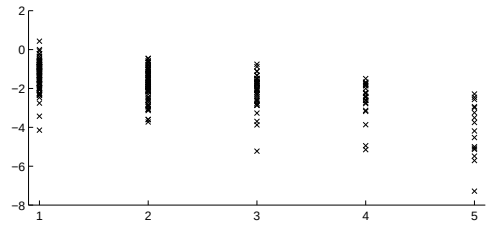

(d) $log_2(Wf(s,x))$ as a function of $log_2(s)$ for all modulus maxima

Figure 5.6: Example 4: Gaussian white noise

seen in figure 5.6. With the help of the plot of $log(Wf(x,s)$ in a $log(s)$ scale one can verify this claim. In figure 5.6(d) all modulus maxima are plotted. One can see that the overall average decrease is about -0.5. However, one can not expect the slope to be $-0,5$ at each cone of influence since the randomness also leads to smoother and less smooth parts. Anyway, in the next section it is described that one can still use the properties described by above theorems for the reconstruction of noisy signals.

5.4 Denoising Based on Wavelet Maxima

In general, Lipschitz denoising can be seen as a 5-step procedure. First, one applies the modified SWT algorithm on the noisy input signal. This algorithm slightly differs from the algorithm introduced in section 2.3: each coefficient of the wavelet representation is multiplied by a level dependent factor that turns the wavelet maxima slopes in a way such that they directly indicate the Lipschitz regularity. In the second step one determines the modulus maxima of the detail coefficients. We leave the approximation coefficients untouched, therefore no modulus maxima need to be detected here. Thirdly, one needs to decide which maxima are mostly influenced by noise and therefore need to be removed. Afterwards, using the remaining maxima, one needs to reconstruct/determine the wavelet coefficients that should be used for the last step, the inverse modified SWT.

It is clear that the crucial question is how to implement the third and forth step. We analyzed before that common signal features are of Lipschitz regularity not less than 0. Even the step functions, for images one of the most important signal features, is of Lipschitz regularity $\alpha = 0$. Noise however creates singularities of negative Lipschitz regularity. It can be seen in figure 5.6 that white noise produces singularities of regularity $\alpha \approx -\frac{1}{2}$. Furthermore, isolated "clicks" which are common noise artifacts in audio signals can be represented as delta functions of singularity $\alpha \approx -1$, see figure 5.4. Hence, we try to remove all modulus maxima on maxima lines with negative slope. It is however very difficult to exactly determine modulus maxima lines since, by contrast with above examples, singularities are not well isolated from each other and it is not clear to which singularity a modulus maxima may belong. I therefore propose a much simpler and faster method, providing already relatively good results as shown below in figure 5.7.

For the wavelet modulus maxima selection, I propose to consider each cone of influence as defined by (5.10) separately. A wavelet modulus maxima should be

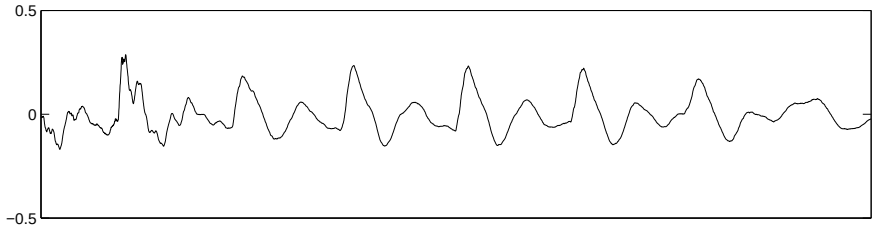

(a) Original speech signal

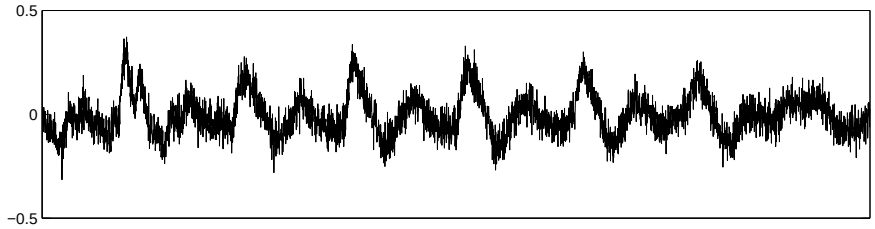

(b) Noisy speech signal, $\sigma = 0.05$

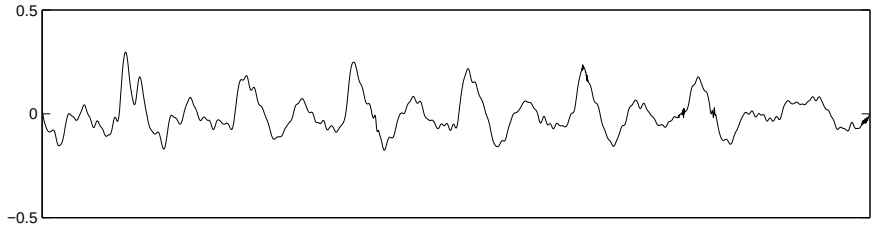

(c) Denoised speech signal

Figure 5.7: Lipschitz denoising: 100ms speech, $\sigma = 0.05$

removed if there is a larger modulus maxima in the same cone at the next smaller scale, i.e. a direct line between these maxima would have negative slope. Only at the finest scale, one needs to consider the slope of whole maxima lines. At each scale we use the largest (if there is any) modulus maxima in the actual cone and determine if the slope of a straight line approximating the curve through these maxima (as a function of $log(s)$) is rather negative or positive. In the latter case one keeps the modulus maxima, otherwise it has to be removed.

Mallat and Hwang use a special reconstruction algorithm using only the remaining modulus maxima [23]. It is based on several projections, similar to repetitive wavelet and inverse wavelet transformations. However, to many details disappear using this algorithm. Hence, I propose again a different way. If a modulus maxima is not affected by noise but contains only important signal features, it is likely that the surrounding coefficients are important, too, and should be used for the reconstruction of the signal, whereas coefficients next to removed maxima are likely to be mainly affected by noise as well and don't need to be kept. The reconstruction algorithm works now in the following way: suppose we are given two subsequent modulus maxima at some level j, at position k and l,

then one distinguishes the following cases:

(i) both maxima are supposed to be removed, then
$\hat{S}_{jk}, ..., \hat{S}_{jl} = 0$

(ii) both maxima are supposed to be kept, then
$\hat{S}_{jk} = Y_{jk}, ..., \hat{S}_{jl} = Y_{jl}$

(iii) only the maxima at position k is supposed to be kept, then
$\hat{S}_{ji} = Y_{ji}$ for $k \leq i \leq \frac{k+l}{2}$, $\hat{S}_{ji} = 0$ for $\frac{k+l}{2} < i \leq l$

(iv) only the maxima at position l is supposed to be kept, then
$\hat{S}_{ji} = 0$ for $k \leq i \leq \frac{k+l}{2}$, $\hat{S}_{ji} = Y_{ji}$ for $\frac{k+l}{2} < i \leq l$

In fact, this selection algorithm denotes a "keep or kill" method. To obtain additional smoothing, one may change cases (iii) and (iv). E.g. for a "smooth" filter function $f : \{k, ..., l\} \to [0, 1]$ one can use

$$\hat{S}_{ji} = f(i) \cdot Y_{ji}.$$

The function f should be chosen to be zero at the modulus maxima that is to be removed and one for the the other maxima, strictly increasing or decreasing in between. However, I tested several different filters, obtaining only minor changes and no audible improvements.

Figure 5.7 provides a section of 100ms of speech example 4, Gaussian white noise with $\sigma = 0.05$ has been added and denoised using Lipschitz denoising. Experiments led to an optimal choice of $J = 4$, i.e. processing only 4 scales, and orthogonal Daubechies wavelets with 7 vanishing moments. Furthermore, the constant C of equation (5.10) has been chosen to be 10. Smaller values lead to less noise reduction while larger values produce too much signal deformation. One can see that a huge amount of noise has been reduced. Indeed, SNR has been improved from 8.696dB to 16.149dB, MSE has been reduced from $\sigma^2 = 2.5e-3$ to $4.493e-4$. More examples and comparisons can be found in chapter 11.

However, some problems occur using Lipschitz denoising. First, since only 4 scales are used for the denoising algorithm, the remaining approximation coefficients still contain some noise, a constant background low frequency noise, like the noise of a far away highway. Lipschitz denoising turned out to be incapable of removing this noise artifact without strong signal deformation. Hence, an additional post-processing might be necessary, using one of the denoising algorithms presented in the following chapters, applied only on the remaining approximation coefficients. A second problem, similar though, is that signals with only small

amount of noise influence are too much deformed, see table 11.2. E.g. for the same speech signal, but now adding Gaussian white noise of much smaller standard deviation $\sigma = 0.01$, the SNR even decreases from 22.672dB to 19.380dB. Nevertheless, the sound quality has been improved a lot. This is in fact one of the main problems in denoising, that SNR and other measures do not provide enough information about auditory quality. A third problem is the denoising of sibilants like “s”, “sh”, “z” and others. Lipschitz denoising treats some of them like noise and strongly deforms, sometimes almost removes such sounds. However, on balance, it already provides a very good denoising technique.

Chapter 6

Diffusion Denoising

6.1 Introduction

For the signal $y(t)$ the Partial Differential Equation (PDE)

$$\begin{aligned} v_u(t,u) &= \frac{\partial}{\partial t}\left(g(v_t^2(t,u))v_t(t,u)\right) && (6.1)\\ v(t,0) &= y(t) && (6.2)\\ (t,u) &\in \mathbb{R}\times[0,+\infty) && (6.3) \end{aligned}$$

describes a diffusion process v, embedding the signal $y(\cdot)$ into a family of functions $v(\cdot,u)$. For constant diffusivity function $g \equiv c$ this PDE is identical to the heat equation $v_u = cv_{tt}$ that can be interpreted as temperature at location t in some body at time u. Eventually, (as $u \to \infty$), the temperature of the body will equalize. Hence, one can see $v(t,u)$ as smoothed version of $y(t)$ with smoothing parameter u. In our case we consider t to be the signal time while u is called diffusion time or smoothing parameter. The idea behind diffusion denoising is to smooth noisy data y up to a certain level, i.e. up to a diffusion stopping time U. Ones uses $v(\cdot,U)$ as an approximation of the original signal s. In their work about edge detection using diffusion [28], Perona and Malik propose a diffusivity function of the form

$$g(x^2) = \frac{1}{1+\frac{x^2}{\lambda^2}} \tag{6.4}$$

where λ denotes a threshold parameter. Suppose λ is in some way related to the "derivative" of Gaussian noise, or discretized, to the difference between two coefficients. Then, for derivatives much larger than λ, which is an indication for important edges, g becomes small and less smoothing is done. Otherwise, one

expects the derivative to be influenced mainly by noise, hence g should be large and strong smoothing is performed.

A discretized version of 6.1 based on Euler's method is given by

$$v_i(u+\tau) \;=\; v_i(u) + \frac{\tau}{h}\left[g\left(\dot{v}_i^2(u)\right)\dot{v}_i(u) - g\left(\dot{v}_{i-1}^2(u)\right)\dot{v}_{i-1}(u)\right], \qquad (6.5)$$

where $v_i(u) = v(t_i, u)$ with $t_{i+1} - t_i = h$ and τ the step sizes in signal time and diffusion, respectively. The derivative $\dot{v}_i(u) = \frac{\delta}{\delta t}v(t_i, u)$ can be obtained by numerical differentiation, e.g.

$$\dot{v}_i(u) \;=\; \frac{1}{h}\left(v_{i+1}(u) - v_i(u)\right).$$

Since we are not interested in precise solutions of PDE (6.1) but only in a smoothed version of y, here, this simple one-step-method — namely Euler's method — is sufficient.

An example of smoothing by diffusion is shown in figure 6.1. Gaussian white noise has been added to a sine function and denoised using the method described above with constant diffusivity function $g \equiv 1$, diffusion time step size $\tau = 0.1$ and signal time resolution $h = 1$:

$$v_i^{neu} \;=\; v_i + 0.1\left(v_{i+1} - 2v_i + v_{i-1}\right).$$

One can see in figures 6.1(a) and 6.1(b) that a view iterations are already sufficient to achieve strong smoothing while differences between further iterations seem to be rather small. Although the denoised version of figure 6.1(d) is very close to the original sine function, as k approaches infinity the signal would converge to constant 0, i.e. the integral or average value of the signal. Hence, a crucial question will be when to stop the iteration or how to change the diffusivity function g in a way such that $v(t, u)$ leads to a good approximation of $s(t)$.

6.2 Diffusion of Wavelet Coefficients

Even though it seems the results of the example provided above and illustrated in figure 6.1 are close to the actual sine function, it is not enough to use such simple smoothing algorithms. Small oscillatory details are usually smoothed first by such smoothing filters. However, these details are one of the most important features of audio signals [32]. To distinguish important audio signal features from noise we apply (6.4) and (6.1) to the detail coefficients of a wavelet representation of the signal. Hence, large derivatives lead to small changes of the new coefficient

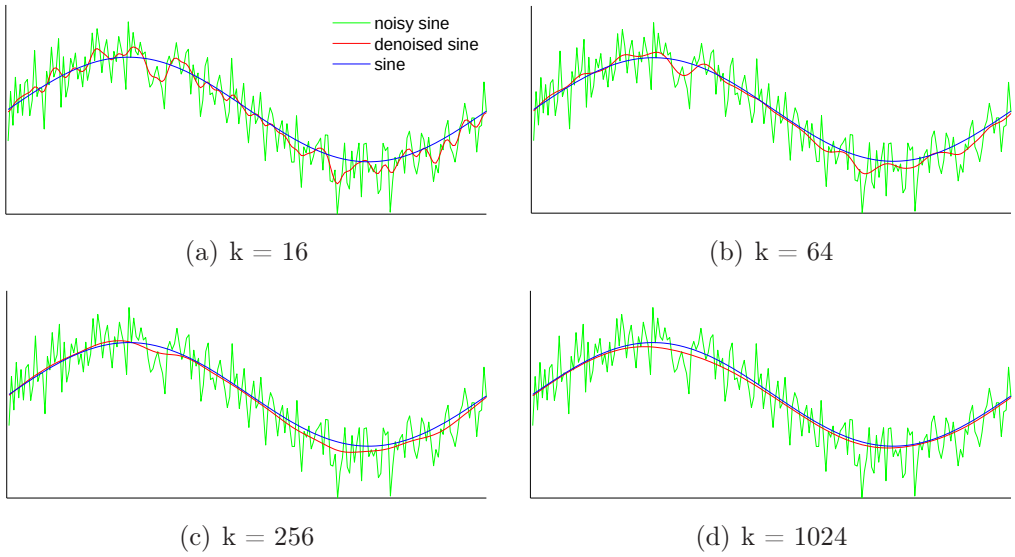

(a) k = 16 (b) k = 64

(c) k = 256 (d) k = 1024

Figure 6.1: Diffusion of noisy sine function

which is deduced from the idea that large differences between neighboring wavelet coefficients indicate important acoustic events and should not be smoothed [32]. Such an event is usually well localized in time but appears at several different levels. Hence, smoothing should be suppressed or enhanced equally throughout all levels and the diffusivity function used to update some coefficient Y_{jk} should not just depend on coefficients at level j but on coefficients at all levels and same location as Y_{jk}. Hence, for each time step k, $k = 0, ..., n-1$, one computes a diffusivity value g_k that is used at all levels and particular time. This procedure has to be done once at the beginning of each iteration. A crucial question is which differences should enter a particular diffusivity. In the following some realizations of this method are provided.

FWT Based Diffusion Denoising

Welk, Bergmeister and Weickert [32] propose a simple method based on the idea to use the wavelet coefficients of all levels at a fixed time k given by

$$\left(Y_{0,\lfloor \frac{k}{2^J} \rfloor}, Y_{1,\lfloor \frac{k}{2^{J-1}} \rfloor}, ..., Y_{J-1,\lfloor \frac{k}{2} \rfloor}\right).$$

Since g_k should represent the difference between coefficients at time k and $k-1$ the direct approach would be to use

$$\begin{aligned} g_k &:= g\left(\sum_{j=0}^{J-1}\left(Y_{j,\lfloor\frac{k}{2^{J-j}}\rfloor} - Y_{j,\lfloor\frac{k-1}{2^{J-j}}\rfloor}\right)^2\right) \\ &= g\left(\sum_{j=0}^{J-1}\left(Y_{j,\lfloor 2^j k/2^J\rfloor} - Y_{j,\lfloor 2^j(k-1)/2^J\rfloor}\right)^2\right). \end{aligned} \tag{6.6}$$

Vice versa, the associated time of some wavelet coefficient Y_{jk} is supposed to be $2^{J-j}k$ and therefore (6.5) can be modified to

$$\begin{aligned} Y_{jk}^{neu} &= Y_{jk} + \frac{\tau}{2^{J-j}}\left(g_{2^{J-j}(k+1)}\frac{Y_{j,k+1}-Y_{jk}}{2^{J-j}} - g_{2^{J-j}(k)}\frac{Y_{jk}-Y_{j,k-1}}{2^{J-j}}\right) \\ &= Y_{jk} + \frac{\tau}{2^{2(J-j)}}\left(g_{2^{J-j}(k+1)}[Y_{j,k+1}-Y_{jk}] - g_{2^{J-j}(k)}[Y_{jk}-d_{j,k-1}]\right) \end{aligned} \tag{6.7}$$

where 2^{J-j} is the signal time step size at level j which holds under the assumption of a signal time resolution $h=1$. In fact, since $2^{J-j}k$ is always even, it is only necessary to compute g_k for even values of k.

However, a point of criticism is that diffusivity at different locations depend on different numbers of coefficients.The number of levels j where $\lfloor\frac{k}{2^{J-j}}\rfloor = \lfloor\frac{k-1}{2^{J-j}}\rfloor$ depends on k and therefore the number of terms on the sum of (6.6) that are unequal zero depends on k, too. I therefore propose a slightly different diffusivity function that ensures each summand to be nonzero, precisely

$$g_k := g\left(\sum_{j=0}^{J-1}\left(\frac{Y_{j,\lfloor\frac{k}{2^{J-j}}\rfloor+1} - Y_{j,\lfloor\frac{k}{2^{J-j}}\rfloor}}{2^{J-j}}\right)^2\right). \tag{6.8}$$

The two coefficients $Y_{j,\lfloor\frac{k}{2^{J-j}}\rfloor+1}$ and $Y_{j,\lfloor\frac{k}{2^{J-j}}\rfloor}$ are chosen such that their corresponding times enclose k, i.e.

$$2^{J-j}\left(\left\lfloor\frac{k}{2^{J-j}}\right\rfloor + 1\right) \geq k \geq 2^{J-j}\left(\left\lfloor\frac{k}{2^{J-j}}\right\rfloor\right).$$

Furthermore, to normalize the differences, we need to divide by time step size 2^{J-j} of the corresponding level j.

SWT Based Diffusion Denoising

An easier formula can be obtained using stationary wavelet transform coefficients.

The time resolution is level-independent and the diffusivity can be obtained by

$$g_k := g\left(\sum_{j=0}^{J-1}\left(Y_{j,k}-Y_{j,k-1}\right)^2\right). \tag{6.9}$$

However, the results are not much better than using above methods though the complexity of updating the wavelet coefficients is increasing by a factor of $\log n$. Hence, in the following we concentrate on the diffusivity function defined by (6.8).

6.3 Choice of Parameters

There are three parameters we need to adjust, the threshold value λ for the computation of the diffusivity function g in equation (6.4), the diffusion step size τ in equation (6.5) and finally the number of diffusion steps, i.e. the number of iterations of formula (6.7).

Choice of diffusion step size τ: Since we are not interested in a precise solution of a differential equation but just in smoothing of the input leading ideally to good auditory properties, it is not necessary to choose very small τ. Furthermore, due to the fact that each iteration is of complexity $\mathcal{O}(n)$, we will rather use some larger τ to save some iterations, at the expense of a denoised signal of a little less quality. However, I performed several tests using different values, inferring that $\tau = 1$ is already sufficient and provides no worse results than much smaller step sizes. For example, the difference to a method using $\tau = 0.1$ and 10 times more iterations is almost imperceptible.

Choice of threshold λ: First, the notion "threshold" might be misleading, since we do not treat coefficients above and below λ differently. It is rather a wight of the diffusivity function. However, for large λ, the smoothing step (6.7) is much stronger than for small values, since $g(x^2) \approx 1$ for $\lambda^2 >> x^2$ whereas for small λ, the diffusivity g approaches zero and only little smoothing is done. For image edge detection, Perona and Malik took λ as 90% of the integral value of the histogram of absolute values of of all gradients throughout an image [28]. This value needed to be evaluated at each iteration. In fact, it can be considered as a weighted average of noise gradients. It is "expensive" to evaluate this value, though. Welk, Bergmeister and Weickert [32] use constant thresholds, fixed by hand, for audio denoising, although, as mentioned before, the threshold should be related in some way to the expected difference of two random noise coefficients. Since noise should reduce at each iteration, I propose to reduce the threshold at

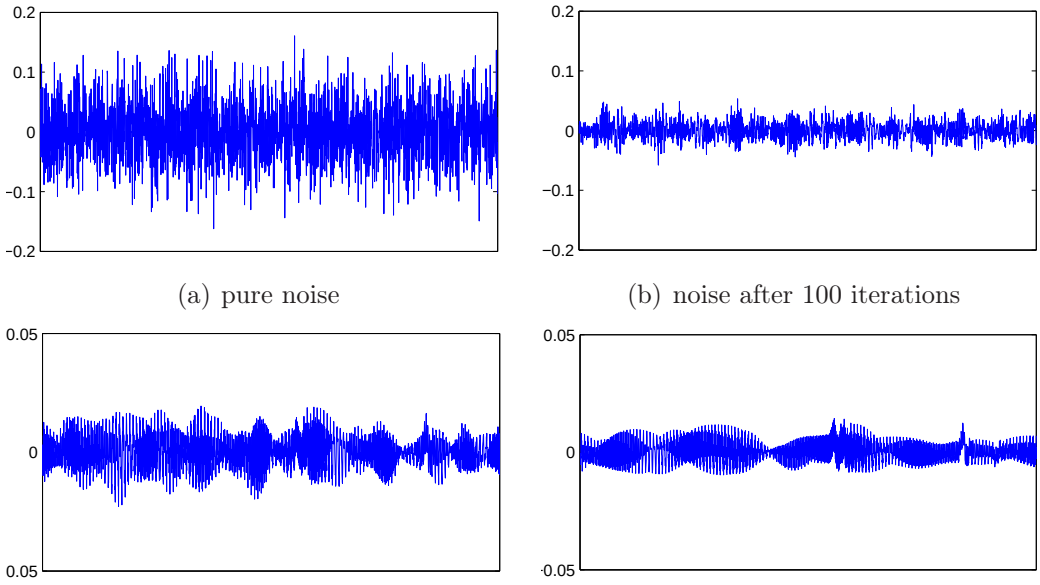

(a) pure noise

(b) noise after 100 iterations

(c) noise after 1000 iterations

(d) noise after 5000 iterations

Figure 6.2: Diffusion denoising of 50ms pure noise

each step, too. The variance of the difference of two independent and identically distributed Gaussian random variables is given by two times the variance of the original random variable, hence standard deviation is obtained by $\sqrt{2}\sigma$. Hence, I propose to start with the universal threshold $\lambda^{diff} = \sqrt{2}\sigma\sqrt{2\log n} = 2\sigma\sqrt{\log n}$, introduced in chapter 7 and section 7.3. This value denotes, with high probability, an upper bound for Gaussian random variables of variance $2\sigma^2$. We will use this value although the difference of two Gaussian random variables is not Gaussian anymore. However, I tested different thresholds, too, and λ^{diff} seemed to be an appropriate choice. Furthermore, several experiments leaded to a shrinking factor of $\delta = 99\%$ at each iteration to obtain relatively good results. Of course, for diffusion step sizes $\tau \neq 1$, one needs to adjust the shrinking factor.

NUMBER OF ITERATIONS: The choice of the shrinking factor solves in some way the problem of the stopping time. Knowing δ and σ, it is clear that after some iterations, the threshold will be too small to cause any significant signal change. For the examples provided in chapter 11, I stopped after 80 iterations.

Diffusion denoising holds some problems, though. First, all assumptions and choices of parameters are based on rather intuitive considerations and some experiments. There is no guarantee that diffusion denoising indeed leads to good results. Furthermore, as shown in figure 6.2, one can see that even pure noise is not removed completely, even though for this plot no threshold shrinking has

been done. Instead, diffusion denoising produces signals containing a characteristic constant background "noisy beeping", an example is provided by sound example 11.

However, the denoising results are similar to Lipschitz denoising, referred to SNR and MSE measures. Only for signals with only little noise, diffusion denoising outperforms Lipschitz denoising significantly, see table 11.2 and 11.3. For noisy speech with larger noise variance, using just SNR and MSE, no preference can be recognized.

Chapter 7

Thresholding Methods

This chapter deals with different thresholding methods. Section 7.1 introduces the most commonly used thresholding methods, hard and soft thresholding. Sections 7.3 to 7.9 are basically about the detection of "optimal" thresholds, where the notion of optimality might differ at each section.

In the following we assume the noise e_i of model (3.1) to be independent Gaussian white noise with variance σ^2, i.e.

$$e_i \sim N(0, \sigma^2), \quad i = 0, ..., n-1.$$

Using orthogonal FWT, it holds that

$$E_{jk} \sim N(0, \sigma^2), \quad (j,k) \in \mathcal{I},$$

as shown in section 3.1. Furthermore, we assume $|\mathcal{I}| = n$ to simplify notations.

7.1 Hard and Soft Thresholding

Hard thresholding is a typical "keep or kill" method, where all coefficients with modulus less than threshold λ are set to be zero, the other coefficients remain unchanged, i.e.

$$\begin{aligned} hard_\lambda(x) &= \mathbb{1}_{\{|x|>\lambda\}} \cdot x \\ &= \begin{cases} x & \text{, if } |x| > \lambda \\ 0 & \text{, otherwise.} \end{cases} \end{aligned} \tag{7.1}$$

The function $hard_\lambda(x)$ is plotted in figure 7.1(a), using the threshold value $\lambda = 1$. Soft thresholding, shown in figure 7.1(b), is a little different since no coefficient

remains unchanged. Any modulus larger than the threshold is shrunken by λ, i.e. soft thresholding is given by

$$\begin{aligned} soft_\lambda(x) &= sgn(x)(|x| - \lambda)_+ \\ &= (x - sgn(x)\lambda)_+ \\ &= \begin{cases} x - \lambda & , \text{if } x > \lambda \\ x + \lambda & , \text{if } x < -\lambda \\ 0 & , \text{if } x \in [-\lambda, \lambda] \end{cases} \end{aligned} \tag{7.2}$$

There is a connection of soft thresholding and the spectral subtraction method introduced in section 4.3. Considering the first part of equation (4.7) and assuming $\sqrt{R_Y(p,q)} = |Y_{pq}|$ and $\lambda = \sigma$, both filters are equivalent, i.e. $soft_\lambda(Y_{pq}) = H_{pq}^{SSF} Y_{pq}$, since $H_{pq}^{SSF} \geq 0$ as shown in section 4.5. However, we will not take the standard deviation as threshold value.

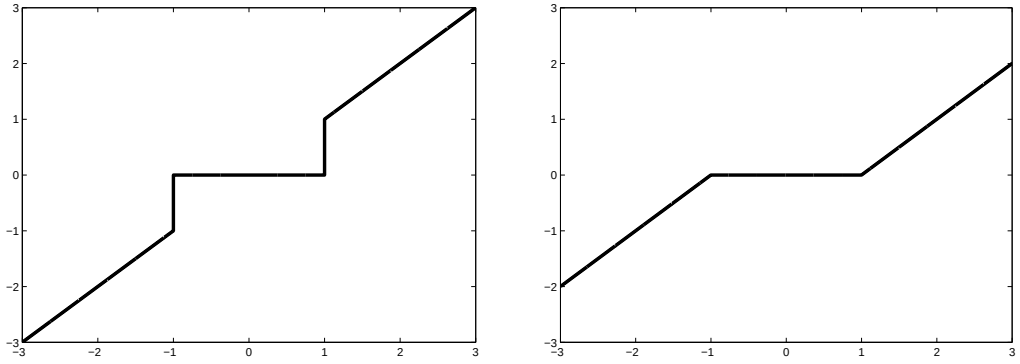

(a) hard (b) soft

Figure 7.1: Hard and Soft Thresholding, threshold $\lambda = 1$

7.2 Selective Wavelet Reconstruction

In this section we will discuss a method related to hard thresholding but more general, called Selective Wavelet Reconstruction (SWR). It provides a lower bound for the risk of hard thresholding and we will also use the following results for comparisons with soft thresholding methods. However, SWR is not a thresholding method and only of theoretical use. In fact, it is just a general "keep or kill" method, more precise

$$\hat{S}_{jk}^{SWR} = \delta_{jk} Y_{jk}, \quad \delta_{jk} \in \{0, 1\}, \quad (j,k) \in \mathcal{I}.$$

Given the knowledge of the original signal coefficients S_{jk} one could derive the optimal values of δ, in the sense of minimizing the risk function.

Theorem 7.2.1. *The optimal SWR estimator is obtained using*

$$\delta_{jk}^{opt} = \mathbb{1}_{\{|S_{jk}|>\sigma\}}$$

and the expected MSE of S and $\hat{S}^{SWR}$ is given by the ideal risk

$$\mathfrak{R}(S, SWR) = \frac{1}{n} \sum_{(jk)\in\mathcal{I}} min(|S_{jk}|^2, \sigma^2)$$

Proof. Leaving a coefficient untouched, i.e. $\hat{S}_{jk} = Y_{jk}$, one obtains a risk contribution of

$$\mathbb{E}[(S_{jk} - \hat{S}_{jk})^2] = \mathbb{E}[(S_{jk} - Y_{jk})^2] = \mathbb{E}[E_{jk}^2] = \sigma^2.$$

Suppose $|S_{jk}| > \sigma$, then "killing", i.e. $\hat{S}_{jk} = 0$, would lead to the risk contribution

$$\mathbb{E}[(S_{jk} - \hat{S}_{jk})^2] = \mathbb{E}[(S_{jk})^2] > \sigma^2$$

which would be worse than "keeping" the coefficient. In the same way, if $|S_{jk}| \leq \sigma$, it is better to remove the coefficient since

$$\mathbb{E}[(S_{jk} - \hat{S}_{jk})^2] = \mathbb{E}[(S_{jk})^2] \leq \sigma^2$$

is at least as good as leaving the coefficient untouched. Hence, at each coefficient the above definition of δ leads to an expected MSE of $min(|S_{jk}|^2, \sigma^2)$. □

7.3 VisuShrink

The first and easiest thresholding method, called VisuShrink, is based on soft thresholding using the so called universal threshold [8]

$$\lambda^{VS} = \sigma\sqrt{2\log n}. \tag{7.3}$$

The estimation $\hat{S}_{jk}^{VS}$ is therefore given by

$$\hat{S}_{jk}^{VS} = soft_{\lambda^{VS}}(Y_{jk}). \tag{7.4}$$

Although the threshold does not depend on the input data (therefore "universal"), it provides already good results as illustrated by the following theorem. Indeed, we can mimic SWR — which would require total knowledge of signal S — essentially within a factor $2\log n$.

Theorem 7.3.1. *Using the universal threshold and soft thresholding as defined above one obtains*

$$risk(S, \hat{S}^{VS}) \leq (2\log n + 1)\left(\frac{\sigma^2}{n} + \mathfrak{R}\left(Y, SWR\right)\right)$$

Proof. I will provide only an outline of the proof. For more details see [8]. One shows for $X \sim N(\mu, 1)$ and $\lambda = \sqrt{2\log n}$ with $n \geq 2$ that

$$\mathbb{E}\left[(soft_\lambda(X) - \mu)^2\right] \leq (2\log n + 1)(1/n + min(\mu^2, 1))$$

holds. Summation leads to the deserved result. With

$$\begin{aligned} \mathbb{E}\left[(soft_\lambda(X) - \mu)^2\right] &= 1 - 2P\left(|X| < \lambda\right) + \mathbb{E}\left[min\left(X^2, \lambda^2\right)\right] \\ &\leq 1 + \lambda^2 \\ &\leq (1 + 2\log n)(1/n + 1) \end{aligned} \tag{7.5}$$

using $min\left(X^2, \lambda^2\right) \leq \lambda^2$ and

$$\begin{aligned} \mathbb{E}\left[(soft_\lambda(X) - \mu)^2\right] &\leq 2 - 2P\left(|X| < \lambda\right) \\ &\leq 2P\left(|X| \geq \lambda\right) + \mu^2 \end{aligned}$$

using $min\left(X^2, \lambda^2\right) \leq X^2$ it is enough to show that

$$2P\left(|X| \geq \lambda\right) + \mu^2 \leq (2\log n + 1)(1/n + \mu^2)$$

which can be done with the help of some simple statistical calculus [8]. □

It might be surprising that the threshold depends on the number of input data such that joining two signals would change its value. However, the philosophy behind the dependence on the signal length is rather taking more samples on a given interval. Hence, adding more samples enhances redundancy and there is less information in the additional data. Therefore, important coefficients are concentrated in a very slowly growing data set while at the same time the signal energy is the same in time and wavelet domain. For that reason one expects the magnitude of these important coefficients to grow. Additionally, the dependence

of λ^{VS} on n is weak as illustrated by table 7.1. Doubling λ^{VS}, i.e. $\lambda^{VS} \to 2\lambda^{VS}$, requires n to be raised to the power of 4, $n \to n^4$, as seen in table 7.1 from first to last row, $n = 64$ to $n = 16777216$. Another reason for the dependence on

J	$n = 2^J$	λ^{VS}
6	64	2.884053773201766
8	256	3.330218444630791
10	1024	3.723297411059034
12	4096	4.078667960675236
16	65536	4.709640090061899
20	1048576	5.265537695468319
24	16777216	5.768107546403532

Table 7.1: Universal Threshold as a function of the number of samples

n is discussed in the next section. For an increasing number of coefficients the probability to have very large values E_{jk} increases, in other words the expected maximum noise coefficient value becomes larger. To completely remove noise, we need to adjust the threshold value. However, for most applications one does not compute the full wavelet representation up to level $j = 0$. Suppose a signal of length $n = 2^J$ is given and a wavelet representation up to level $j_0 > 0$ is evaluated, then the universal threshold needs to adjusted to

$$\lambda^{VS} = \sigma\sqrt{2\log\left(2^{J-j_0}\right)}.$$

and therefore, increasing n does not change the threshold value.

7.4 Adapting to unknown smoothness

For smoothness analysis it is useful to consider more appropriate function spaces than Lebesgue spaces $L_p[0,1]$ since its norm

$$||f||_{L_p[0,1]} = \left(\int_0^1 |f(t)|^p dt\right)^{\frac{1}{p}}, \ 1 \le p < \infty$$

provides little smoothness information. Sobolev spaces $W_p^k[0,1]$ can be seen as complete extensions of $C^k[0,1]$ in $L_p[0,1]$ with Sobolev norm

$$\begin{aligned} ||f||_{W_p^k} &= \left(\sum_{n=0}^{k} ||f^{(n)}||_{L_p[0,1]}\right)^p, \ 1 \le p < \infty \\ ||f||_{W_\infty^k} &= \max_{0\le n\le k} ||f^{(n)}||_{L_\infty[0,1]} \end{aligned}$$

where all derivatives are considered in weak sense [37]. Finally, there are even more general spaces called Besov spaces [6], [9], [19]. For the r-th difference of a $L_p[0,1]$-function given by

$$\Delta_h^r f = \sum_{k=0}^{r} \binom{r}{k} (-1)^k f(t+kh)$$

one defines the r-th modulus of smoothness of f

$$w_{r,p}(f;t) = \sup_{h \le t} ||\Delta_h^r f||_{L_p[0,1-rh]}$$

and for $r > \alpha$ the Besov semi-norm

$$\begin{aligned} |f|_{B_{pq}^{\alpha}} &= \left(\int_0^1 \left(\frac{w_{r,p}(f;u)}{u^{\alpha}} \right)^q \frac{du}{u} \right)^{\frac{1}{q}}, \ 1 \le q < \infty \\ |f|_{B_{p\infty}^{\alpha}} &= \sup_{0<t<1} \frac{w_{r,p}(f;h)}{t^{\alpha}}. \end{aligned}$$

Eventually, the Besov norm is defined as

$$||f||_{B_{pq}^{\alpha}} = ||f||_{L_p[0,1]} + |f|_{B_{pq}^{\alpha}}. \tag{7.6}$$

In this definition, α can be seen as an indication of smoothness. Functions of Besov spaces are typically piecewise smooth. For a wavelet expansion

$$f(t) = \sum_{k=0}^{2^J-1} c_{Jk}\varphi_{Jk}(t) + \sum_{j=J}^{\infty} \sum_{k=0}^{2^j-1} d_{jk}\psi_{jk}(t)$$

one defines the so called Besov sequence space [9], [6] given by the norm

$$\begin{aligned} ||d||_{b_{pq}^{\alpha}} &= \left(\sum_{j=J}^{\infty} 2^{j\beta q} \left(\sum_{k=0}^{2^j-1} |d_{jk}|^p \right)^{\frac{q}{p}} \right)^{\frac{1}{q}}, \ 1 \le q < \infty \\ ||d||_{b_{p\infty}^{\alpha}} &= \sup_{j \ge J} \left(2^{j\beta} \left(\sum_{k=0}^{2^j-1} |d_{jk}|^p \right)^{\frac{1}{p}} \right). \end{aligned}$$

where $\beta = \alpha + 1/2 - 1/p$. There are two constants $c_0(\alpha, p, q)$ and $c_1(\alpha, p, q)$ independent of f such that

$$c_0||f||_{B^\alpha_{pq}} \leq ||d||_{b^\alpha_{pq}} \leq c_1||f||_{B^\alpha_{pq}}. \tag{7.7}$$

This norm equivalence provides methods of measuring smoothness in wavelet domain.

We will now show that VisuShrink produces reconstructed signals $\hat{s}^{VS}$ that are with high probability at least as smooth as the original signal s in the following sense [6]:

Theorem 7.4.1. *Let $(s_i = s(t_i))_{i=0}^{n-1}$ represent a function in Besov space $B^\alpha_{pq}[0,1]$ and $(\hat{s}_i^{VS})_{i=0}^{n-1}$ its estimation using VisuShrink and an orthonormal wavelet basis. There is a sequence π_n independent of s and B^α_{pq} with $\pi_n \to 1$ as $n \to \infty$ and a constant $C(B^\alpha_{pq})$ such that*

$$P\left(||\hat{s}^{VS}||_{B^\alpha_{pq}} \leq C \cdot ||s||_{B^\alpha_{pq}}\right) \geq \pi_n. \tag{7.8}$$

For the proof of this theorem we first prove the following lemmas where π_n is determined. Furthermore, we show that with probability π_n the estimated signal wavelet coefficients are smaller (in absolute value) than the actual signal wavelet coefficients.

Lemma 7.4.2. *Let $(z_i)_{i\in\mathbb{N}}$ be i.i.d Gaussian random variables with $z_0 \sim N(0, \sigma^2)$. For*

$$\pi_n := P\left(\max_{0\leq i<n}(z_i) \leq \sigma\sqrt{2\log n}\right) \tag{7.9}$$

it holds that $\lim_{n\to\infty} \pi_n = 1$.

Proof. We use the fact that

$$\lim_{n\to\infty} P\left(\max_{0\leq i<n}(z_i) \leq x\right) = e^{-a} \quad \Leftrightarrow \quad \lim_{n\to\infty} n(1-\Phi(x)) = a$$

where $\Phi(x)$ is the distribution of z_i. Furthermore, it holds that $1-\Phi(x) \sim \sigma^2\frac{\phi(x)}{x}$

as $x \to \infty$. Hence, for $x = \sigma\sqrt{2\log n}$ we get

$$\begin{aligned} & \lim_{n\to\infty} \pi_n = 1 \\ \Leftrightarrow \quad & \lim_{n\to\infty} n\sigma^2 \frac{\phi(\sigma\sqrt{2\log n})}{\sigma\sqrt{2\log n}} = 0 \\ \Leftrightarrow \quad & \lim_{n\to\infty} n\sigma^2 \frac{1}{\sqrt{2\pi}\sigma} \frac{1}{n\sigma\sqrt{2\log n}} = 0 \end{aligned}$$

which is obviously true. □

Lemma 7.4.2 also ensures that for observed data containing only noise and no signal information, i.e. $s_i = 0,\ i = 0, ..., n-1$, noise is removed completely with probability π_n. Indeed, no noise can be heard listening to denoised signals using VisuShrink. However, it is clear that signal information will be deformed, too. The next lemma makes this even more clear.

Lemma 7.4.3. *With π_n as defined by (7.9)*

$$P\left(|\hat{S}_{jk}^{VS}| \le |S_{jk}| \ \ \forall\ (j,k) \in \mathcal{I}\right) \ge \pi_n \tag{7.10}$$

for all $S \in \mathbb{R}^n$.

Proof. Let A_n denote the event $\left\{\max_{0\le i<n}(z_i) \le \sigma\sqrt{2\log n}\right\}$. We show that

$$A_n \Rightarrow |\hat{S}_{jk}^{VS}| \le |S_{jk}| \ \ \forall\ (j,k) \in \mathcal{I}.$$

Since $P(A_n) \ge \pi_n$, this will prove the lemma. If $\hat{S}_{jk}^{VS} = 0$ it is clear that the right side holds. For each coordinate where $\hat{S}_{jk}^{VS} \neq 0$ we have

$$|\hat{S}_{jk}^{VS}| = |Y_{jk}| - \sigma\sqrt{2\log n}$$

and since A_n holds, $|Y_{jk} - S_{jk}| \le \sigma\sqrt{2\log n}$ which leads to

$$|S_{jk}| \ge |Y_{jk}| - \sigma\sqrt{2\log n} = |\hat{S}_{jk}^{VS}|.$$

□

Proof of theorem 7.4.1. From (7.7) we get

$$\begin{aligned} c_0||s||_{B_{pq}^\alpha} \le \quad & ||S||_{b_{pq}^\alpha} \quad \le c_1||s||_{B_{pq}^\alpha} \text{ and} \\ c_0||\hat{s}^{VS}||_{B_{pq}^\alpha} \le \quad & ||\hat{S}^{VS}||_{b_{pq}^\alpha} \quad \le c_1||\hat{s}^{VS}||_{B_{pq}^\alpha} \end{aligned}$$

since c_0 and c_1 are independent of the used signal. Using Lemma 7.4.3 we get with a probability greater or equal to π_n.

$$\begin{aligned} ||\hat{s}^{VS}||_{B^{\alpha}_{pq}} &\leq \frac{1}{c_0}||\hat{S}^{VS}||_{b^{\alpha}_{pq}} \\ &\leq \frac{1}{c_0}||S||_{b^{\alpha}_{pq}} \\ &\leq \frac{c_1}{c_0}||s||_{B^{\alpha}_{pq}}. \end{aligned}$$

So theorem 7.4.1 holds for π_n of lemma 7.4.2 and $C = c_1/c_2$. □

7.5 Minimax Threshold

In the above section an easy threshold has been introduced that already provides good visual and auditory results. However, it is based on the idea of removing all noise without regarding possible signal destruction. In fact, those denoised signals often sound dully since most of the high frequencies are removed, too. In the following sections we will derive thresholds that minimize the risk function, i.e. the expected mean square error. As already seen in (3.9) and (3.10), the risk function can be seen as a sum of bias squared and variance. The best threshold to minimize the variance is far away of being a good choice to make the bias smaller, though. More precisely,

$$\lim_{\lambda\to\infty} var(\hat{S}^{\lambda}) = \lim_{\lambda\to\infty} \frac{1}{n}\mathbb{E}||\hat{S}^{\lambda} - \mathbb{E}\hat{S}^{\lambda}||^2 = 0, \tag{7.11}$$

$$\lim_{\lambda\to\infty} bias^2(S, \hat{S}^{\lambda}) = \lim_{\lambda\to\infty} \frac{1}{n}||S - \mathbb{E}\hat{S}^{\lambda}||^2 = \frac{1}{n}||S||^2. \tag{7.12}$$

Hence, thresholds minimizing the risk function are best compromises between variance and bias.

In this section we are interested in a minimax risk threshold, i.e. a threshold λ^* such that

$$\sup_S risk(S, \hat{S}^{\lambda})$$

becomes minimal, i.e.

$$\sup_S risk(S, \hat{S}^{\lambda^*}) = \inf_{\hat{S}^{\lambda}} \sup_S risk(S, \hat{S}^{\lambda}). \tag{7.13}$$

In words, we are looking for a threshold that minimizes the risk assuming the worst possible signal. Hence, it is not data adaptive. Let us first consider the

risk contribution of a single coefficient defined by

$$\rho(\lambda, S) = \mathbb{E}\left[(soft_\lambda(Y) - S)^2\right]. \tag{7.14}$$

Risk is then obtained by $risk(\lambda) = \frac{1}{n}\sum \rho(\lambda, S_{jk})$. In the following we always assume noise to be Gaussian with density ϕ and distribution Φ,

$$\begin{aligned} \phi(x) &= \frac{1}{\sigma\sqrt{2\pi}} e^{\frac{-x^2}{2\sigma^2}} \\ \Phi(x) &= \int_{-\infty}^{x} \phi(x)dx. \end{aligned}$$

So far, we don't know the value of $\rho(\lambda, S)$ neither how to minimize it. The following lemmas provide a form of $\rho(\lambda, S)$ that requires only the evaluation of ϕ and Φ. First, we introduce the expected error after soft thresholding and come then to the computation of $\rho(\lambda, S)$.

Lemma 7.5.1. *Let $Y = S+E \sim N(S, \sigma^2)$ and $\hat{S}^\lambda = soft_\lambda(Y)$. Call $E^\lambda = \hat{S}^\lambda - S$ the bias of the thresholding method. It holds that*

$$\begin{aligned} \mathbb{E}E^\lambda = S &+ \Phi(\lambda - S)(\lambda - S) \\ &+ \Phi(\lambda + S)(-\lambda - S) \\ &+ \phi(\lambda - S)(\sigma^2) \\ &+ \phi(\lambda + S)(-\sigma^2) \end{aligned} \tag{7.15}$$

Proof.

$$\begin{aligned}
\mathbb{E}\hat{S}^{\lambda} &= \int_{-\infty}^{\infty} soft_{\lambda}(x)\phi(x-S)dx \\
&= \int_{\lambda}^{\infty}(x-\lambda)\phi(x-S)dx + \int_{-\infty}^{-\lambda}(x+\lambda)\phi(x-S)dx \\
&= \int_{\lambda-S}^{\infty}(x+S-\lambda)\phi(x)dx + \int_{-\infty}^{-\lambda-S}(x+S+\lambda)\phi(x)dx \\
&= (S-\lambda)\left[1-\Phi(\lambda-S)\right] + \int_{\lambda-S}^{\infty} x\phi(x)dx \\
&\quad + (S+\lambda)\left[\Phi(-\lambda-S)\right] + \int_{-\infty}^{-\lambda-S} x\phi(x)dx
\end{aligned}$$

Using $x\phi(x) = -\sigma^2\phi'(x)$ and $\Phi(-x) = 1-\Phi(x)$ one obtains

$$\begin{aligned}
\mathbb{E}\hat{S}^{\lambda} = 2S &+ \Phi(\lambda-S)(\lambda-S) \\
&+ \Phi(\lambda+S)(-\lambda-S) \\
&+ \phi(\lambda-S)(\sigma^2) \\
&+ \phi(\lambda+S)(-\sigma^2)
\end{aligned} \tag{7.16}$$

Since $\mathbb{E}E^{\lambda} = \mathbb{E}\hat{S}^{\lambda} - S$ the proof is done. □

Lemma 7.5.2. *Using the assumptions of lemma 7.5.1 we have*

$$\begin{aligned}
\rho(\lambda, S) &= \mathbb{E}\left[(\hat{S}^{\lambda}-S)^2\right] \\
&= 2\sigma^2 + 2\lambda^2 - S^2 \\
&\quad + \Phi(\lambda-S)(-\sigma^2-\lambda^2+S^2) \\
&\quad + \Phi(\lambda+S)(-\sigma^2-\lambda^2+S^2) \\
&\quad + \phi(\lambda-S)(-\sigma^2(\lambda+S)) \\
&\quad + \phi(\lambda+S)(-\sigma^2(\lambda-S))
\end{aligned} \tag{7.17}$$

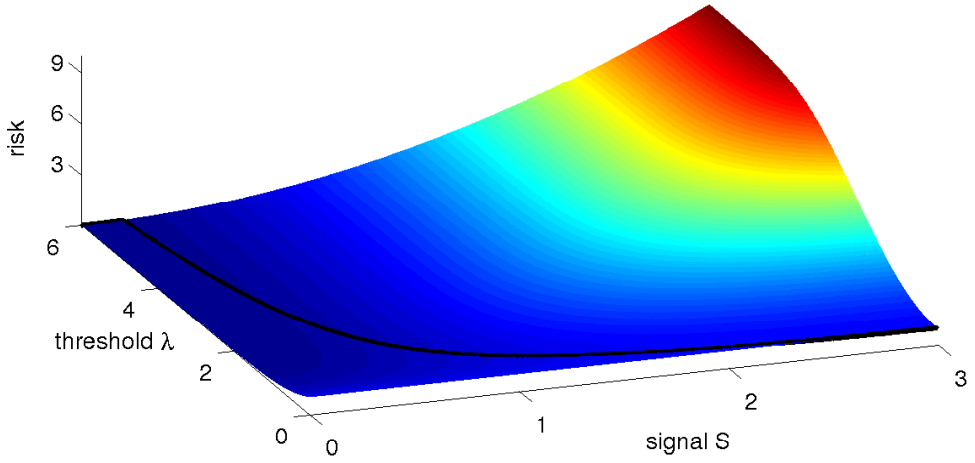

Figure 7.2: Risk $\rho(\lambda, S)$ for uncorrupted coefficient S and, in black, $\rho(\lambda^{opt}(S), S)$

Proof.

$$\begin{aligned}\mathbb{E}\left[(\hat{S}^{\lambda} - S)^2\right] &= \int_{-\infty}^{\infty} \left[soft_{\lambda}^2(x) - 2S soft_{\lambda}(x) + S^2\right] \phi(x - S)dx \\ &= \int_{-\infty}^{\infty} soft_{\lambda}^2(x)\phi(x - S)dx \; - 2S\mathbb{E}[\hat{S}^{\lambda}] + S^2\end{aligned}$$

The second term is already known from lemma 7.5.1. One can calculate the first term in the following way:

$$\int_{-\infty}^{\infty} soft_{\lambda}^2(x)\phi(x - S)dx = \int_{\lambda - S}^{\infty} (x + S - \lambda)^2\phi(x)dx + \int_{-\infty}^{-\lambda - S} (x + S + \lambda)^2\phi(x)dx$$

After expanding the parenthesized terms in the integrals, one uses

$$\int_a^b x^2\phi(x)dx = -x\sigma^2\phi(x)|_a^b + \sigma^2 \int_b^b \phi(x)dx$$

and as in the previous lemma $x\phi(x) = -\sigma^2\phi'(x)$. After some calculations, putting everything together leads to equation (7.17). □

Figure 7.2 illustrates the risk development as a function of thresholds λ and uncorrupted coefficients S. In this example, the noise variance σ^2 is chosen to be 1. Apparently, large coefficients require small threshold values. For large S and λ, bias is growing very fast and although some large λ would reduce most

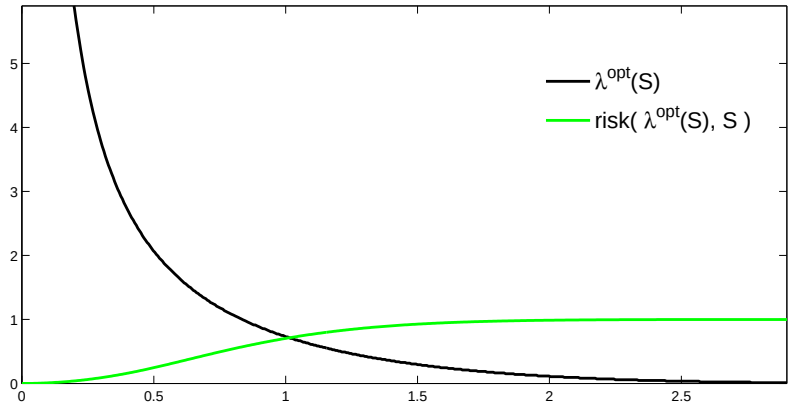

Figure 7.3: Optimal threshold value λ with corresponding risk

of the variance, risk is in this case dominated by a large bias. The contrary is true for small coefficients S. Risk is dominated by variance and requires therefore large thresholds. The development of the risk minimizing threshold $\lambda^{opt}(S)$ and the corresponding risk is illustrated by the black line in figure 7.2. For better visualization, $\lambda^{opt}(S)$ and $\rho(\lambda^{opt}(S), S)$ are plotted as functions of S in figure 7.3. One can see that for large coefficients the optimal threshold tends to zero and risk remains σ^2. Hence, the minimax threshold λ^* of (7.13) that assumes the worst possible value S would be zero and no thresholding would be done.

Donoho and Johnstone [8] propose a different kind of minimax threshold, based on the ideal risk of Selective Wavelet Reconstruction and the risk approximation given in theorem 7.3.1. For VisuShrink we had

$$risk(\lambda^{VS}) \leq \Lambda \left(\frac{\sigma^2}{n} + \frac{1}{n} \sum_{(j,k)\in\mathcal{I}} min(S_{jk}^2, \sigma^2) \right)$$

where Λ was given by $2log(n) + 1$. The objective of their work presented in [8] is to find a threshold λ^* such that the factor Λ becomes minimal assuming the worst possible values S_{jk}. To obtain this, consider again the risk contribution of a single coefficient S, in fact the worst possible one. It is clear that the best factor we can obtain under uncertainty of S is given by

$$\Lambda^* = \inf_{\lambda} \sup_{S} \frac{\rho(\lambda, S)}{\sigma^2/n + min(S^2, \sigma^2)} \tag{7.18}$$

and the desired threshold λ^* is given by

$$\lambda^* = \text{ largest } \lambda \text{ attaining } \Lambda^*. \tag{7.19}$$

Donoho and Johnstone prove that it is enough to take the maximum over $S \in \{0, \infty\}$ instead of taking the supremum over all possible values of S. Using lemma 7.5.2 one obtains risk contributions

$$\begin{aligned} \rho(\lambda, \infty) &= \sigma^2 + \lambda^2 \\ \rho(\lambda, 0) &= 2(\sigma^2 + \lambda^2)(1 - \Phi(\lambda)) - 2\sigma^2\lambda\phi(\lambda). \end{aligned}$$

Thus, minimizing Λ for a fixed n requires at each step one evaluation of Φ and ϕ. In table 7.2 we can see some threshold values for VisuShrink and Minimax. Additionally, the factor Λ^* is provided. Computations were done for noise variance $\sigma^2 = 1$. However, while λ^* is growing linear with σ for both, VisuShrink and Minimax, the factor Λ^* is not dependent on σ. Therefore, and since Minimax is

k	$n = 2^k$	λ^*	λ^{VS}	Λ^*	$2logn + 1$
6	64	1.4741	2.8841	3.1244	9.3178
8	256	1.8591	3.3302	4.4389	12.0904
10	1024	2.2262	3.7233	5.9502	14.8629
12	4096	2.5751	4.0787	7.6291	17.6355
16	65536	3.2213	4.7096	11.3763	23.1807
20	1048576	3.8079	5.2655	15.5002	28.7259
24	16777216	4.3456	5.7681	19.8846	34.2711

Table 7.2: Minimax vs VisuShrink for $\sigma = 1$

not data adaptive, minimizing has to be done only one time for each value of n and a specific value of σ, e.g. $\sigma = 1$. The results can be stored and used without any more computational effort. Since λ^* is growing very slowly in n, it might be sufficient to store only $\lambda^*(n)$ for $n = 2^k$, $k \in \mathbb{N}$, and use rough approximations for other values of n.

Some further minimax methods are discussed by Donoho and Johnstone in [10] and [11]. It is assumed that the unknown signal s belongs to a known class of smooth functions $\mathcal{F}$, where $\mathcal{F}$ is a ball in a Besov spaces, to achieve more realistic minimax MSE. I.e. the supremum $sup\, risk(s, \hat{s})$ is taken over all $s \in \mathcal{F}$. However, further threshold finders, presented in the following sections, will concentrate on direct MSE or risk minimization instead of minimizing some upper bound.

7.6 Stein Unbiased Risk Estimate

So far, the introduced thresholds and thresholding methods were independent of the given data. Wasting the information contained in the input data is careless, though. Especially assuming the worst possible uncorrupted signal could be

considered as far too pessimistic. Knowing the input Y, it is rather unrealistic to assume S to be either infinity or zero. In the following sections we will see different approaches for data adaptive thresholding methods with the aim of risk minimization and based on soft thresholding. In the subsequent chapter, I will suggest a different kind of thresholding that is based on the idea not to use the same threshold for all coefficients.

Let's now denote the estimator of S using soft thresholding with threshold λ by

$$\begin{aligned} \hat{S}^{\lambda} &= \hat{S}^{soft_{\lambda}} \\ &= soft_{\lambda}(Y) \end{aligned} \tag{7.20}$$

and the MSE and risk of S and $\hat{S}^{\lambda}$ by

$$\begin{aligned} MSE(\lambda) &= MSE(S, \hat{S}^{\lambda}) \\ &= \frac{1}{n}||\hat{S}^{\lambda} - S||^2, \\ risk(\lambda) &= \mathbb{E}[MSE(\lambda)] \end{aligned}$$

Furthermore, for the measurement of the effect of thresholding, define

$$F(\lambda) = \frac{1}{n}||\hat{S}_{\lambda} - Y||^2. \tag{7.21}$$

The first MSE estimator we will discuss is called Stein Unbiased Risk Estimate (SURE) and introduced by Donoho and Johnstone in [9]. Some additional analysis can be found in [19]. It is based on more general work of Charles Stein [30]. Although for a given threshold λ, both, Y and $\hat{S}_{\lambda}$ and therefore also F are known, it is necessary to consider the expectation of this function to find approximations of the expected MSE. I.e. one uses

$$\begin{aligned} \mathbb{E}[F(\lambda)] &= \frac{1}{n}\mathbb{E}\left[||Y - S||^2 + ||S - S_{\lambda}||^2 + 2(Y - S, S - \hat{S}^{\lambda})\right] \\ &= \sigma^2 + risk(\lambda) - \frac{2}{n}\mathbb{E}[(E, E^{\lambda})] \end{aligned} \tag{7.22}$$

where $E^{\lambda} = \hat{S}^{\lambda} - S$ denotes the remaining noise after thresholding. Lemmas 7.6.1 and 7.6.2 will lead to a more useful notation of the third term of equation (7.22).

Lemma 7.6.1. *The derivative of E^{λ}_{jk}, seen as a function of E_{jk}, is given by*

$$\frac{\partial E^{\lambda}_{jk}}{\partial E_{jk}} = \begin{cases} 1 & , \text{ if } |Y_{jk}| > \lambda \\ 0 & , \text{ otherwise} \end{cases}$$

Proof. With the help of equation (7.2) we rewrite E^{λ} as

$$\begin{aligned} E^{\lambda} &= soft_{\lambda}(Y) - S \\ &= \begin{cases} (Y-\lambda) - S & , \text{if } Y > \lambda \\ (Y+\lambda) - S & , \text{if } Y < -\lambda \\ -S & , \text{otherwise} \end{cases} \\ &= \begin{cases} E - \lambda & , \text{if } Y > \lambda \\ E + \lambda & , \text{if } Y < -\lambda \\ -S & , \text{otherwise.} \end{cases} \end{aligned}$$

It is now easy to see that above claim holds. □

Lemma 7.6.2. *Let ϕ be the Gaussian density function with $\mu = 0$. Then*

$$\mathbb{E}\left[E_{jk}E^{\lambda}_{jk}\right] = \sigma^2 P(|Y_{jk}| > \lambda)$$

Proof. Since $x\phi(x) = -\sigma^2\phi'(x)$, we have

$$\begin{aligned} \mathbb{E}\left[E_{jk}E^{\lambda}_{jk}\right] &= \int_{-\infty}^{\infty} E^{\lambda}_{jk}E_{jk}\phi(E_{jk})dE_{jk} \\ &= -\sigma^2 \int_{-\infty}^{\infty} E^{\lambda}_{jk}\phi'(E_{jk})dE_{jk} \\ &= -\sigma^2 \left[E^{\lambda}_{jk}\phi(E_{jk})\right]_{-\infty}^{\infty} + \sigma^2 \int_{-\infty}^{\infty} \frac{\partial E^{\lambda}_{jk}}{\partial E_{jk}}\phi(E_{jk})dE_{jk} \end{aligned}$$

and with lemma 7.6.1 we get

$$\mathbb{E}\left[E_{jk}E^{\lambda}_{jk}\right] = \sigma^2 P\left(|Y_{jk}| > \lambda\right)$$

□

Now we need to find the probability $P(|Y_{jk}| > \lambda)$. Therefore we first define n_0 as the number of wavelet coefficients that are shrunken to zero, i.e. the number

of wavelet coefficients whose modulus is less than or equal to the threshold,

$$\begin{aligned} n_0 &= |\{(j,k) \in \mathcal{I} | Y_{jk}^{\lambda} = 0\}| \\ &= |\{(j,k) \in \mathcal{I} | Y_{jk} \leq \lambda\}|. \end{aligned} \tag{7.23}$$

As shown in [19], it is the obvious choice to use $P(|Y_{jk}| > \lambda) = \frac{n-n_0}{n}$ and one obtains

$$\begin{aligned} \mathbb{E}[(E, E^{\lambda})] &= \sigma^2 \sum_{(j,k)\in\mathcal{I}} P(|Y_{jk}| > \lambda) \\ &= \sigma^2 \sum_{(j,k)\in\mathcal{I}} \frac{n-n_0}{n} \\ &= \sigma^2 (n - n_0) \end{aligned} \tag{7.24}$$

Using equations (7.22) and (7.24) we construct the MSE approximation

$$SURE(\lambda) = F(\lambda) - \sigma^2 + 2\sigma^2 \frac{n-n_0}{n}, \tag{7.25}$$

where $SURE = risk = \mathbb{E}MSE$. Let's mention again that, unlike Minimax, SURE is adaptive, although it is as well derived from MSE expectation.

7.7 Cross Validation

In this section I will introduce Ordinary Cross Validation (OCV) and Generalized Cross Validation (GCV) [26], [21], [20]. Like SURE, both of them can be seen as a function of a threshold parameter λ and are estimates of the MSE function. However, GCV evaluation only requires input data, no additional knowledge is necessary. Estimations of noise variance is not needed either.

In short, the concept of cross validation is given by the construction of several estimates, never using the whole data set. Using these estimates one predicts what the expelled data could have been. Finally one compares the prediction with the actual values of the expelled data.

7.7.1 Ordinary Cross Validation

Ordinary Cross Validation (OCV) is based on the assumption of in some way smooth original data s_i. Hence, each value s_i can be approximated by linear combinations of its neighbors. Let's now define $\tilde{y}_i$ as a weighted average of the observed data $\{y_0, ..., y_{i-1}, y_{i+1}, ..., y_{n-1}\}$. Noise in this component is smoothed,

and therefore it is considered to be relatively noise independent. Let's denote

$$\tilde{s}^{\lambda,i} := IFWT(soft_\lambda(FWT(\{y_0, ..., y_{i-1}, \tilde{y}_i, y_{i+1}, ..., y_{n-1}\})))$$

the reproduced signal after soft thresholding using $\tilde{y}_i$ instead of y_i. One considers $\tilde{s}_i^{\lambda,i}$ as a "prediction" of the coefficient y_i and takes the distance $|\tilde{s}_i^{\lambda,i} - y_i|$ as a measure of optimality of the threshold choice. The distance is dominated by noise for small threshold values while large ones induce too much signal distortion. One repeats the same procedure for each component, i.e. n transformations, threshold procedures and inverse transformations are necessary. Then, one computes

$$OCV(\lambda) = \frac{1}{n}\sum_{i=0}^{n-1}(y_i - \tilde{s}_i^{\lambda,i})^2 \tag{7.26}$$

which is called "Ordinary Cross Validation" or "Leaving Out One - Ordinary Cross Validation". Now one could try to minimize $OCV(\lambda)$ to obtain a near optimal threshold. However, in this version each OCV evaluation in the minimization procedure would contribute costs of $\mathcal{O}(n^2)$. Hence, we need to find more advantageous algorithms. To do so, let's first discuss the choice of $\tilde{y}_i$. A possible value could be $\frac{1}{2}(y_{i-1} + y_{i+1})$ [26], however, to simplify the computation it is useful to take $\tilde{y}_i$ in way such that

$$\tilde{y}_i = \tilde{s}_i^{\lambda,i}. \tag{7.27}$$

Thresholding has a leveling effect and it holds that ([19])

$$\begin{aligned} \tilde{y}_i = \max_i y_i \quad &\Rightarrow \quad \tilde{s}_i^{\lambda,i} \leq \tilde{y}_i \\ \tilde{y}_i = \min_i y_i \quad &\Rightarrow \quad \tilde{s}_i^{\lambda,i} \geq \tilde{y}_i. \end{aligned}$$

which proves the existence of this value. As before $\hat{s}^\lambda$ denotes the reconstructed signal after soft thresholding, i.e.

$$\hat{s}^\lambda \;:=\; IFWT(soft_\lambda(FWT(y))).$$

Using the above choice of $\tilde{y}_i$ one has

$$y_i - \tilde{s}_i^{\lambda,i} \;=\; \frac{y_i - \hat{s}_i^\lambda}{1 - a_i} \tag{7.28}$$

where a_i is given by

$$\begin{aligned} a_i &= \frac{\hat{s}_i^\lambda - \tilde{s}_i^{\lambda,i}}{y_i - \tilde{s}_i^{\lambda,i}} \\ &= \frac{\hat{s}_i^\lambda - \tilde{s}_i^{\lambda,i}}{y_i - \tilde{y}_i} \\ &\approx \frac{\partial \hat{s}_i^\lambda}{\partial y_i}. \end{aligned} \tag{7.29}$$

Assuming the knowledge of a_i, one can approximate $OCV(\lambda)$ in $\mathcal{O}(n)$, leading to

$$OCV(\lambda) = \frac{1}{n}\sum_{i=0}^{n-1} \frac{1}{(1-a_i)^2}(y_i - \hat{s}_i^\lambda)^2 \tag{7.30}$$

Hence, one needs to find a fast evaluable approximation of a_i. As already indicated by formula (7.29), the derivative $\partial \hat{s}_i^\lambda / \partial y_i$ might be a good basis for such an approximation. However, let's introduce first

$$\begin{aligned} D_{(j_1k_1),(j_2k_2)} &:= \frac{\partial Y_{j_1k_1}^\lambda}{\partial Y_{j_2k_2}} \\ &= \frac{\partial}{\partial Y_{j_2k_2}} soft_\lambda(Y_{j_1k_1}). \end{aligned}$$

Using (7.2) one immediately sees that $D_{(j_1k_1),(j_2k_2)} = 0$ for $(j_1, k_1) \neq (j_2, k_2)$ and

$$D_{(jk),(jk)} = \begin{cases} 0 & \text{, if } |Y_{jk}| \leq \lambda \\ 1 & \text{, otherwise} \end{cases}$$

Furthermore, let W denote a wavelet transform matrix and define $A = W^{-1}DW$. Now, one can see that

$$\frac{\partial \hat{s}_i^\lambda}{\partial y_i} = A_{ii}$$

and the evaluation requires only one forward and inverse wavelet transform. Hence, one indeed obtains an approximation of the OCV function that can be obtained in $\mathcal{O}(n)$, replacing a_i in formula (7.30) by A_{ii}.

7.7.2 Generalized Cross Validation

As discussed above, for each OCV evaluation in a minimization procedure, two forward and inverse wavelet transforms are required. Additionally, for small

threshold values, most of the A_{ii} are close to one and the algorithm could become unstable. In this section we will see a similar function that can be minimized in wavelet domain and that avoids the mentioned problems. The idea is to approximate a_i of formula (7.26) using a constant value, say $a_i \equiv \alpha$ for all $i = 0, .., n-1$. In fact one uses the average of all values A_{ii} [33], [21],

$$\begin{aligned} \alpha &= \frac{1}{n}\sum_{i=0}^{n-1} A_{ii} \\ &= \frac{1}{n} \cdot tr(A), \end{aligned}$$

where $tr(A)$ is the trace of A. Since W is regular and $A = W^{-1}DW$, recalling the definition of D, one obtains

$$\alpha = \frac{tr(D)}{n} = \frac{n - n_0}{n}$$

where n_0 is defined by (7.23). Applied to equation (7.26), one obtains the so called generalized cross validation

$$\begin{aligned} GCV(\lambda) &= \frac{1}{n}\frac{1}{(1-\alpha)^2}\sum_{i=0}^{n-1}(y_i - \hat{s}_i^{\lambda})^2 \\ &= \frac{\frac{1}{n}||y - \hat{s}^{\lambda}||^2}{\left(\frac{n_0}{n}\right)^2} \end{aligned} \tag{7.31}$$

If the transform is orthogonal, this is equivalent to

$$\begin{aligned} GCV(\lambda) &= \frac{\frac{1}{n}||Y - \hat{S}^{\lambda}||^2}{\left(\frac{n_0}{n}\right)^2} \\ &= \frac{F(\lambda)}{\left(\frac{n_0}{n}\right)^2} \end{aligned} \tag{7.32}$$

Hence, it is now possible to minimize in wavelet domain and therefore, the computation of $GCV(\lambda)$ is much easier and faster than the evaluation of $OCV(\lambda)$. A special treatment needs to be implemented in the case of $n_0 = 0$, although this case is extremely unlikely for $\lambda > 0$. Especially in the presence of Gaussian white noise we expect to shrink many coefficients to zero. However, one chooses in this case $GCV(\lambda)$ to be $2 * \sigma^2$. A justification is provided in the next section where a more rigorous analysis of the GCV procedure is done.

7.7.3 GCV Analysis

So far, we have no guarantee that GCV really approximates the MSE or $risk$ function. The assumptions for cross validations were rather rough and seem to be very unsound. This section provides a relation of GCV and $SURE$ that indeed ensures the quality of the GCV function. Additionally, a result of asymptotic behavior is provided. Let's call $n_1 = n - n_0$ the number of wavelet coefficients that have not been shrunken to zero. Note that n_1/n should be rather small for most applications since relatively smooth functions can be represented by just a little number of coefficients. Hence, we omit terms of the order $(n_1/n)^2$ and rewrite

$$\begin{aligned} GCV(\lambda) &= \frac{F(\lambda)}{\left(1-\frac{n_1}{n}\right)^2} \\ &= \frac{F(\lambda)}{1-\frac{2n_1}{n}+\left(\frac{n_1}{n}\right)^2} \\ &\approx \frac{F(\lambda)}{1-\frac{2n_1}{n}} \\ &\approx F(\lambda)\left(1+\frac{2n_1}{n}\right) \end{aligned} \tag{7.33}$$

Using formulas (7.22) and (7.24) together with lemma 7.6.2 and assuming the difference $F(\lambda) - \mathbb{E}[F(\lambda)]$ to be very small we have

$$\begin{aligned} F(\lambda) &= \mathbb{E}[F(\lambda)] + (F(\lambda) - \mathbb{E}[F(\lambda)]) \\ &\approx \sigma^2 + risk(\lambda) - \sigma^2\frac{2\mathbb{E}[n_1]}{n} \end{aligned} \tag{7.34}$$

and therefore, neglecting again terms of the order $(n_1/n)^2$, we obtain

$$\begin{aligned} GCV(\lambda) &\approx F(\lambda)\left(1+\frac{2n_1}{n}\right) \\ &\approx F(\lambda) + \frac{2n_1}{n}\sigma^2 + \frac{2n_1}{n}risk(\lambda). \end{aligned}$$

For threshold values near the minimum risk threshold, $risk(\lambda)$ is much smaller than $\sigma^2 = risk(0)$. So we omit the last term of the above equation, too. Now,

one can see the connection to the $SURE$ formula (7.25):

$$\begin{aligned} GCV(\lambda) &\approx F(\lambda) + \frac{2n_1}{n}\sigma^2 && (7.35)\\ &= SURE(\lambda) + \sigma^2 && (7.36)\\ &\approx MSE(\lambda) + \sigma^2 && (7.37) \end{aligned}$$

However, for GCV evaluation there is no need to know the value of σ^2, so no additional noise variance approximation is necessary. This is useful especially for signals with no "silent" parts that are only influenced by noise and would easily provide noise variance approximations. For many applications, such silent parts are hard to determine, anyway. Furthermore, for mean square error minimization the constant term σ^2 does not change anything and GCV should provide good results (see also section 7.8). Formula (7.37) also justifies the choice of $GCV(\lambda)$ for $n_0 = 0$. This case is only likely for very small threshold values and therefore we choose GCV to be equal to $GCV(0) \approx MSE(0) + \sigma^2 = 2\sigma^2$.

Another interesting result is the asymptotic behavior of GCV. Let's therefore denote first λ^{opt} as the optimal threshold, i.e. the threshold that minimizes the expected MSE function, $\lambda^{opt} = argmin\ risk(\lambda)$ and λ^{gcv} the threshold that minimizes the expected GCV function, $\lambda^{gcv} = argmin\ \mathbb{E}GCV(\lambda)$. The next theorem states that $risk(\lambda^{opt})$ and $risk(\lambda^{gcv})$ have the same asymptotic behavior, i.e. for large n both thresholds lead to almost the same risk. An outline of the proof is provided.

Theorem 7.7.1. *With λ^{opt} and λ^{gcv} as given above and for piecewise smooth signals, it holds that*

$$\lim_{n\to\infty} \frac{risk(\lambda^{gcv})}{risk(\lambda^{opt})} = 1 \tag{7.38}$$

Proof. In the first part of the proof, an upper bound of $risk(\lambda^{gcv})/risk(\lambda^{opt})$ is derived. In the second part, I provide a less restrictive explanation why we can expect this upper bound to converge to 1 for piecewise smooth signals. For a detailed proof see [19].

In the following we call $\mu_0 = \mathbb{E}(n_0/n)$ and $\mu_1 = \mathbb{E}(n_1/n) = 1-\mu_0$. Furthermore we have, using (7.34),

$$\begin{aligned} \mathbb{E}GCV(\lambda) &= \mathbb{E}\left[\frac{F(\lambda)}{(n_0/n)^2}\right]\\ &= \left(risk(\lambda) + \sigma^2 - 2\sigma^2\mu_1\right)/\mu_0^2 \end{aligned}$$

Now, we get

$$\begin{aligned}
\left|\frac{risk(\lambda) - (\mathbb{E}GCV(\lambda) - \sigma^2)}{risk(\lambda)}\right| &= \left|1 - \frac{\mathbb{E}GCV(\lambda)}{risk(\lambda)} + \frac{\sigma^2}{risk(\lambda)}\right| \\
&= \left|1 - \frac{risk(\lambda) + \sigma^2 - 2\sigma^2\mu_1}{\mu_0^2 \cdot risk(\lambda)} + \frac{\sigma^2}{risk(\lambda)}\right| \\
&= \left|1 - \frac{1}{\mu_0^2} + \frac{\sigma^2}{risk(\lambda)} \cdot \left(\frac{-1 + 2\mu_1}{\mu_0^2} + 1\right)\right| \\
&= \frac{1}{\mu_0^2}\left|\left(\mu_0^2 - 1 + \frac{\sigma^2}{risk(\lambda)}\mu_1^2\right)\right| \\
&\leq \frac{1}{\mu_0^2}\left(\left|\mu_0^2 - 1\right| + \left|\frac{\sigma^2\mu_1^2}{risk(\lambda)}\right|\right) \\
&= \frac{1}{\mu_0^2}\left((1 - \mu_0^2) + \frac{\sigma^2\mu_1^2}{risk(\lambda)}\right) \\
&=: h(\lambda)
\end{aligned}$$

The function $h(\lambda)$ leads directly to the upper bound of $risk(\lambda^{gcv})/risk(\lambda^{opt})$:

$$\begin{aligned}
risk(\lambda^{gcv})(1 - h(\lambda^{gcv})) &\leq \mathbb{E}GCV(\lambda^{gcv}) - \sigma^2 \\
&\leq \mathbb{E}GCV(\lambda^{opt}) - \sigma^2 \\
&\leq risk(\lambda^{opt})(1 + h(\lambda^{opt}))
\end{aligned}$$

and hence

$$1 \leq \frac{risk(\lambda^{gcv})}{risk(\lambda^{opt})} \leq \frac{1 + h(\lambda^{opt})}{1 - h(\lambda^{gcv})} \tag{7.39}$$

If we can show that $\lim_{n\to\infty} h(\lambda) = 0$ for both thresholds, the proof is done. To obtain this, we have to show that $\mu_1 \to 0$ (which infers $\mu_0 \to 1$) and that $\mu_1^2/risk \to 0$. Let's discuss the behavior of the risk first. In figure 7.2 the risk contribution of a single coefficients with respect to λ is shown and total risk is obtained by $1/n \sum \rho(\lambda, S_{jk})$. Since for large coefficients even optimal thresholds produce a risk contribution of about σ^2, we can assume for non-silent speech signals that at least one signal wavelet coefficient S is large enough such that $\rho(\lambda, S) \geq \sigma^2$. Hence, risk would be at least σ^2/n. Therefore, it is now sufficient to show that $n\mu_1^2 \to 0$.

Let's denote the set of indices where the original signal wavelet coefficients is zero by

$$\mathcal{I}_0 = \{(j,k) \in \mathcal{I} | S_{jk} = 0\}$$

and in the same way $\mathcal{I}_1 = \mathcal{I} - \mathcal{I}_0$ the indices of original signal wavelet coefficients unequal to zero. Suppose the original signal is piecewise polynomial, then the number of nonzero coefficients is proportional to the number of levels, i.e. one can say $|\mathcal{I}_1| = \mathcal{O}(\log n)$, [19]. Then one obtains

$$\begin{aligned} \mu_1(\lambda) &= \frac{1}{n} \sum_{(j,k)\in\mathcal{I}} P(|Y_{jk}| \geq \lambda) \\ &\leq \frac{1}{n} \left(\sum_{(j,k)\in\mathcal{I}_1} 1 + \sum_{(j,k)\in\mathcal{I}_0} P(|E_{jk}| \geq \lambda) \right) \\ &= \frac{|\mathcal{I}_1|}{n} + \frac{|\mathcal{I}_0|}{n} P(|E_{jk}| \geq \lambda). \end{aligned}$$

As n approaches infinity, we have $\lambda^{opt} = \mathcal{O}(\sqrt{\log n})$ for the optimal threshold λ^{opt}, [19]. Since

$$1 - \Phi(x) \approx \sigma^2 \frac{\phi(x)}{x} \text{ as } x \to \infty,$$

it holds that $P(|E_{jk}| \geq \lambda) = \mathcal{O}(1/(n\sqrt{\log n}))$ for threshold values in the neighborhood of λ^{opt}. In summary, we have in the piecewise polynomial case

$$\mu_1 = \mathcal{O}\left(\frac{\log n}{n} + \frac{1}{n\sqrt{\log n}} \right) = \mathcal{O}\left(\frac{\log n}{n} \right)$$

and $n\mu_1^2 = \mathcal{O}(\log^2(n)/n) \to 0$ for threshold values in the neighborhood of λ^{opt}.

Similar arguments hold for general piecewise smooth signals, where one can not assume that most coefficients are exactly zero. However, using $I_0^\varepsilon = \{(j,k) \in \mathcal{I} || S_{jk}| \leq \varepsilon\lambda^{opt}\}$ instead of $\mathcal{I}_0$, similar arguments hold since one can show that there is a level j_0, such that all coefficients in higher levels that are not affected by singularities are of modulus smaller than $\varepsilon\lambda^*$, see [19]. □

7.8 SURE & GCV Minimization

Maarten Jansen assumes *SURE* and *GCV* to be convex functions in λ [19]. I will now provide arguments based on the risk contribution function that support this assumption. Nevertheless, one can show at the same time that there are cases where the risk is not convex and so *SURE* and *GCV* cannot assumed to be convex, either. These cases are very unlikely for speech signals, though.

A function is convex if and only if its second derivative is nonnegative. Simple calculations, using again the fact that $x\phi(x) = -\sigma^2\phi(x)$, lead to the first and

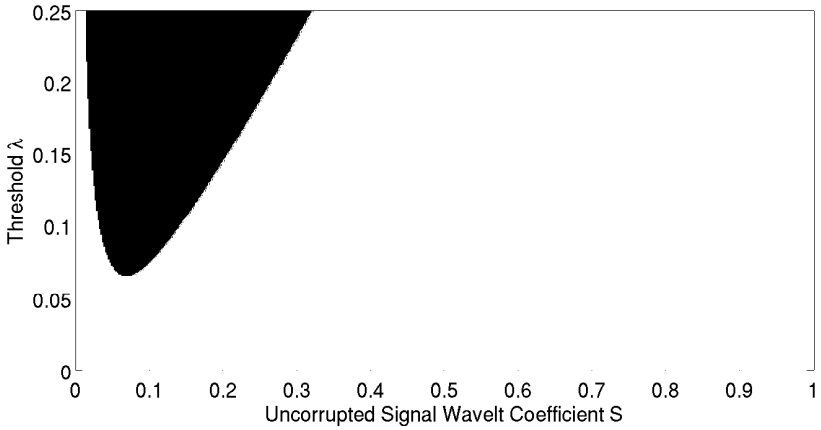

Figure 7.4: Sign of $\partial/\partial\lambda^2(\rho(\lambda, S))$ for $\sigma = 0.05$, black indicates negative and white positive values

second derivative of the risk contribution function $\rho(\lambda, S)$,

$$\begin{aligned}\frac{\partial}{\partial\lambda}\rho(\lambda,S) &= 4\lambda - 2\lambda(\Phi(\lambda+S)+\Phi(\lambda-S)) - 2\sigma^2(\phi(\lambda+S)+\phi(\lambda-S))\\ \frac{\partial^2}{\partial\lambda^2}\rho(\lambda,S) &= 4 - 2(\Phi(\lambda+S)+\Phi(\lambda-S)) - 2S(\phi(\lambda+S)+\phi(\lambda-S)).\end{aligned}$$

Figure 7.4 shows the sign of the second derivative of the risk contribution for $\sigma = 0.05$. The black area indicates pairs (λ, S) such that the sign is negative. Hence, for these pairs the risk contribution is not convex. The total risk is however a sum of all these risk contribution. For S close to zero, we have $\rho(\lambda, S) > 0$ for all λ. Figure 7.4 provides the sign of ρ for threshold values $\lambda \leq 0.25 \approx \sigma\sqrt{2\log 2^{18}}$ which is approximately the universal threshold for $n = 2^{18}$. However, the actual denoising algorithms will usually not evaluate the wavelet representation for more than 12 levels. Hence, 0.25 be seen as an upper bound for λ in this case. Since most of the uncorrupted signal wavelet coefficients S are expected to be zero or very close to zero, $risk(\lambda)$ is strongly influenced by the risk contribution for small S. The black part is supposed to have minor influence on the risk. Furthermore, $\rho(\lambda, S)$ is definitely convex for smaller λ. As a conclusion one can assume the total risk to be convex. For $SURE$ and GCV we have

$$\begin{aligned}risk(\lambda) &= \mathbb{E}SURE(\lambda) \text{ and}\\ SURE(\lambda) &\approx GCV(\lambda) - \sigma^2\end{aligned}$$

which confirms above assumption that $SURE$ and GCV can be expected to convex, too.

Figure 7.5(a) compares the actual mean square error with $SURE$ and GCV

for speech example 9 where Gaussian white noise ($\sigma = 0.05$) has been added. For the computation of $SURE$, σ^2 is obtained by computing the sample variance using about 50 milliseconds of the beginning of the signal where it is assumed to carry only noise. One can see that one obtains a good MSE approximation.

GCV however seems to be "unstable" near zero. Discontinuities occur and furthermore $GCV(\lambda) \neq MSE(\lambda)+\sigma^2$ for small thresholds. Since most coefficients Y_{jk} are close to zero, for small thresholds, even little changes of λ lead to strong changes of n_0 and of the denominator of

$$GCV(\lambda) = \frac{F(\lambda)}{\left(\frac{n_0}{n}\right)^2}. \tag{7.40}$$

At the same time, we showed that GCV can be obtained using $SURE$ and neglecting terms of the order $(n_1/n)^2$. For small thresholds this value might not be as small as expected and cause some errors. Additionally we omitted the term $(n_1/n)risk(\lambda)$ assuming the risk to be much smaller than σ^2 near the optimal threshold. For small thresholds n_1 is still large and we are not close to the optimal λ, though. For larger threshold values, GCV becomes much smoother since most pure noise coefficients are already shrunken to zero and changes of the denominator occur less often and are smaller.

For the minimization we use a special algorithm for convex functions, the so called golden search since the golden value $g = (\sqrt{5} - 1)/2$ is used to divide the search interval into different parts. One starts with four threshold values, the left and right bound of the interval I and two in the middle of the interval such that the distance to the bounds is for both exactly $(1 - g)|I|$. In the next step one determines which of the two thresholds in the middle is the better one. The other one is chosen to be a new bound and one neglects the corresponding old bound, i.e. one shrinks the length of the interval by the factor g in the "direction" of the better value. The new interval is divided into three parts in the same way as above. The choice of the golden value ensures that the better threshold value is again one of the new values in the middle of the interval. Hence, only one new MSE approximation via $SURE$ or GCV has to be performed in each step. Furthermore, the relative distance between two thresholds remains constant. This procedure is repeated until the length of the interval is smaller than a certain bound. This part is performed by the inner while loop of algorithm 7.1.

Now, it remains to choose the initial threshold interval. Of course, on could use $[0, \lambda^{VS}]$ since the universal threshold can be seen as some kind of upper bound

for optimal thresholds. However, first of all it would require the knowledge of σ, which is not necessary for the evaluation of GCV and would eliminate one of its advantages. Furthermore, the discontinuities of the GCV function near zero could cause trouble. Therefore, one starts with rather too large values, i.e. an interval shifted to the right. After the execution of above algorithm one checks if it has changed the left bound of the interval. If so, the minimum of the convex function is definitely in the interval produced by the algorithm. If not, the left bound was too large and one starts again with a new interval until either the left bound changes at some time or the right bound becomes too small. This part is performed by the outer while loop of algorithm 7.1.

Algorithm 7.1 Golden Search Algorithm

$g = \frac{\sqrt{5}-1}{2}$
$\lambda_4 = max\{|S_{jk}|\}$
while $\lambda_4 > \epsilon_1$ and λ_1 unchanged **do**
  $\lambda_1 = \lambda_4/50$
  $\lambda_2 = \lambda_1 + (1-g)(\lambda_4 - \lambda_1)$
  $\lambda_3 = \lambda_4 - (1-g)(\lambda_4 - \lambda_1)$
  compute $mse(\lambda_2)$; compute $mse(\lambda_3)$;
  while $\{\lambda_4 - \lambda_1 > \epsilon_2\}$ **do**
    if $mse(\lambda_2) > mse(\lambda_3)$ **then**
      $\lambda_1 = \lambda_2$; $\lambda_2 = \lambda_3$; $\lambda_3 = \lambda_4 - (\lambda_2 - \lambda_1)$;
      $mse(\lambda_2) = mse(\lambda_3)$; compute $mse(\lambda_3)$;
    else
      $\lambda_4 = \lambda_3$; $\lambda_3 = \lambda_2$; $\lambda_2 = \lambda_1 + (\lambda_4 - \lambda_3)$;
      $mse(\lambda_3) = mse(\lambda_2)$; compute $mse(\lambda_2)$;
    end if
  end while
end while

It might be interesting what happens to signals that are not influenced by noise. It would be desirable to have no or at least only very few changes of the signal, i.e. a threshold as close to zero as possible. For $\sigma^2 = 0$, $SURE$ is given by

$$SURE(\lambda) \quad = \quad F(\lambda) + \sigma^2 - 2\sigma^2 \frac{n_0}{n}$$

and clearly leads to an optimal threshold $\lambda = 0$. Only the first term does not vanish. It is increasing in λ, though, and therefore the optimal threshold is obtained. For GCV this is less clear. However, it also works surprisingly well. The neglected terms are small even for small threshold values since $\sigma^2 = 0$ and most coefficients are already very close to zero, even before thresholding, and

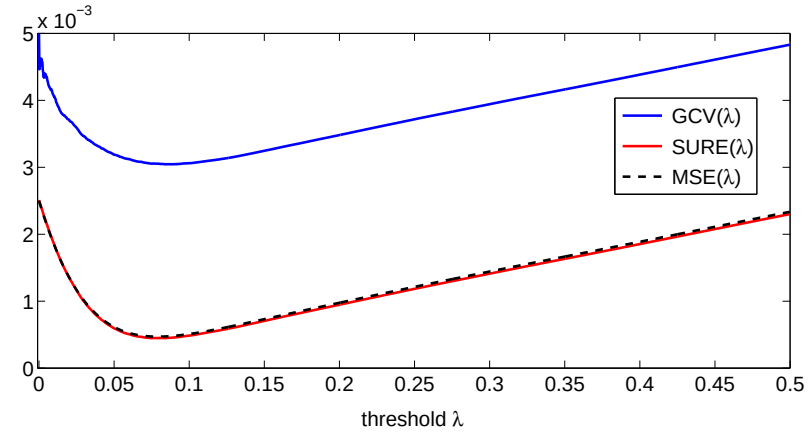

(a) Speech example 9 with Gaussian white noise, $\sigma = 0.05$

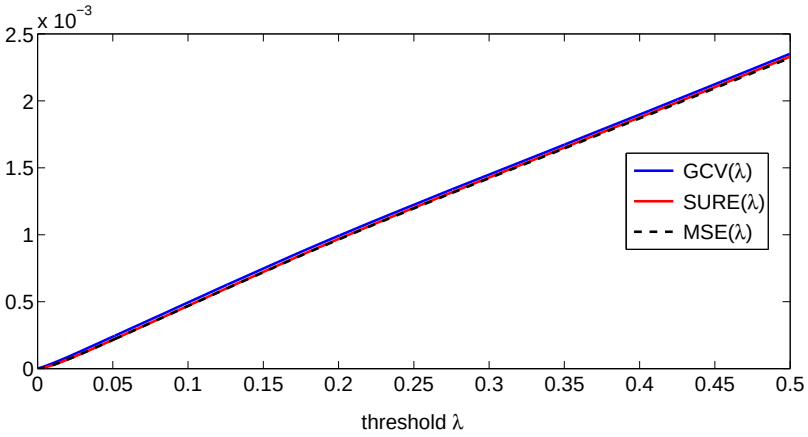

(b) Speech example 9 without noise

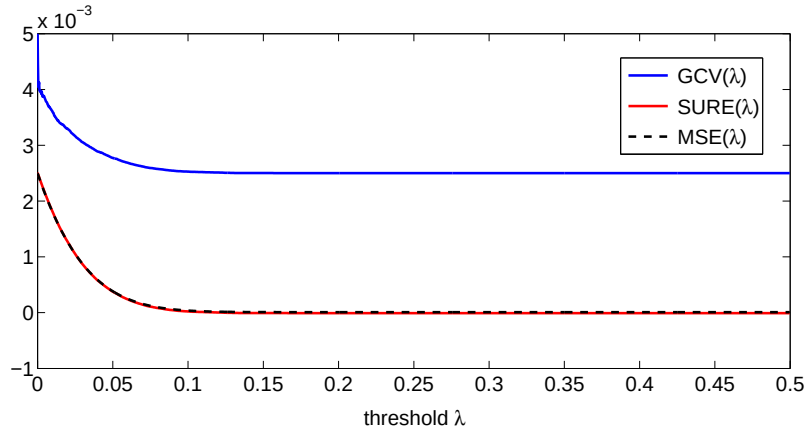

(c) Pure Gaussian white noise, $\sigma = 0.05$

Figure 7.5: MSE, $SURE$ and GCV

for increasing thresholds, the denominator of equation 7.40 changes very slowly. MSE, $SURE$ and GCV in case of pure speech are plotted in figure 7.5(b), again for speech example 9.

A second special case is pure noise, i.e. $S = 0$ for all coefficients. Corresponding MSE, $SURE$ and GCV are shown in figure 7.5(c). Large thresholds should be preferred. Indeed, as λ approaches infinity, both, $SURE$ and GCV, converge to the minimum achievable risk value since $n_0 \to n$ and $F(\lambda) \to \sigma^2$.

7.9 Level Dependent Thresholding

Until now, the introduced thresholding methods made no use of the multiscale representation of the signal. Different levels represent different frequencies and coefficients show different characteristics at different level, as shown in the previous chapter. In this and the following section we will see some suggestions how to use dependencies between different levels [20].

So far we assumed noise to be Gaussian and white, i.e. stationary and uncorrelated noise coefficients. Otherwise, with the knowledge of the covariance matrix Q, one could use formula (3.3) to normalize the wavelet coefficients

$$Y_{jk}^{new} = \frac{1}{\sqrt{Q_{jk,jk}^{A}}} Y_{jk}.$$

But for all that, Q is generally unknown and hard to determine. Suppose noise is stationary Gaussian but correlated in a way such that the correlation between two points depend only on the distance of the points, one obtains a symmetric Toeplitz covariance Matrix Q and in lemma 3.2.1 we have learned that the variance of the transformed noise depends only on the level, i.e.

$$\mathbb{E}[E_{jk}^2] = \sigma_j^2 \quad \forall k \in \mathcal{I}_j$$

where $\mathcal{I}_j$ denotes the set of indices of coefficients at level j. The wavelet transform of stationary correlated noise is only stationery within a given level. Hence, a single threshold for all levels makes no more sense. As mentioned above one could normalize the wavelet coefficients to obtain stationary noise in wavelet domain, too. However, even for this case it is not easy to find good approximations for all values of σ_j. Uncorrelated noise variance can easily be estimated using either very fine scales where little signal information is stored but still noise appears in the same way as in all other scales, or one could use the original data y and try to determine a "silent" part with no signal but corrupted by noise. Instead of the

determination of each σ_j, level dependent thresholding might be useful.

Level dependent thresholding can be applied very easily. One just performs a GCV minimizing procedure at each level separately and obtains for each level a different threshold value. GCV properties are not corrupted by correlated noise. Correlations just lead to a different "sorting" of the coefficients which does not change anything in the GCV computation since at a certain level the noise variance is constant. In statistics this property is called homogeneity of variance.

ADVANTAGES: Level dependent thresholding is not only useful for the processing of correlated noise. Using non-orthogonal wavelet transforms, wavelet noise coefficients will be correlated and non-stationary as mentioned in section 3.1. Although in this case the knowledge of the variance of the original noise coefficients leads to the knowledge of the covariance matrix Q and one could apply (3.3), level dependent thresholding might be easier.

Optimal thresholds do not only depend on the on the noise variance. Signal characteristics play an important role as well. As mentioned earlier, these characteristics might change at different levels. As shown in chapter 5, important coefficients do not necessarily show up at different levels with the same magnitude. In low levels, i.e. at coarse scales, many coefficients contain much information and are therefore large while at levels with finer resolution, large coefficients are rare and most coefficients are influenced only by noise. Hence, fine resolutions require rather large thresholds while at the same time for coarse parts with much signal information, small thresholds are preferable. So even for orthogonal wavelet transformation and stationary uncorrelated white noise, level dependent thresholding might lead to better results. Hence, a single threshold is already a compromise between coarse and fine levels.

DISADVANTAGES: Level dependent thresholding leads to one important disadvantage. At coarse levels, one might not have enough coefficients to obtain good MSE approximations via GCV since for $n = 2^J$, level j consists of only about 2^{J-j} coefficients. The solution could be the use of the stationary wavelet transform (SWT) as described in section 2.3. For SWT, the homogeneity of variance property holds, too. At each level one has n coefficients. Therefore, good MSE approximations can be obtained at each level. Memory and time complexity is now $\mathcal{O}(n \log n)$, though. At each level, the proportion of noise free coefficients remains the same as for FWT. Hence, at coarse scales most coefficients provide signal information, the representation is not sparse there. Hence, it is not useful to process too coarse levels. On the other side, finer levels are still sparse and

contain very few signal information. Additionally, inverse SWT provides an additional smoothing as described in section 2.3 which might improve the output signal quality in the sense of less noisy structures.

7.10 Inter & Intra Scale Thresholding

Xu, Weaver, Healy and Lu [36] describe a denoising method that - with slight modification - can be seen as a thresholding method using inter scale dependencies. It is based on the idea that important signal features show up not only at a single scale but at a hole set of coefficients at the same location but subsequent levels. This assumption has already been justified in chapter 5. To measure if a coefficient should be kept or not, they propose not to use the coefficient magnitude, but a inter scale correlation factor $Corr_l$ defined as the product of l coefficient values at same location but subsequent coarser levels given by

$$corr_{jk}(l) = \prod_{i=0}^{l} Y_{j-i,k} \tag{7.41}$$

To simplify notation, a notion of stationary wavelet transform has been used here, but it works in the same way using FWT coefficients instead. One just needs to find the right coefficients at the same location. Xu et al propose to select at each level the coefficients with largest correlation factors until the sum of the squares of the selected coefficients exceeds a certain threshold value. This threshold value can however be considered to be an upper bound of the signal information and should be selected in a way such that the threshold represents the expected amount of signal information provided at the given scale for the uncorrupted signal.

Jansen modified this algorithm and created a kind of soft thresholding [19]. Now, the correlation factor is not only the measure if a coefficient should be shrunken to zero or not, but it also influences the shrinking value:

$$\hat{S}^{\lambda}_{jk} = \left(1 - \frac{\lambda}{|corr_{jk}(l)|}\right)_{+} Y_{jk}. \tag{7.42}$$

For $l = 0$ this is exactly soft thresholding. Jansen states that already for $l = 1$, this method outperforms the previous ones. Besides, GCV can be evaluated and minimized in exactly the same way as mentioned in earlier sections. Comparisons can be found in chapter 11. Modifications of inter level dependencies are however possible. One could try using a sum of coefficients instead of the product in for-

mula (7.42), or selecting not only coefficients of coarser levels for the computation of the correlation factor.

A method very similar to inter scale thresholding is called intra scale or block thresholding. It is based on the idea that for an important signal coefficient, the neighboring ones should be rather large and important, too, since except for Haar wavelets, neighboring basis functions don't have disjoint support. Block thresholding, as the name indicates, keeps, shrinks or kills not only single coefficients but complete blocks, based on the values of a superset of coefficients. I.e., let I_0 be a set of indices of adjacent wavelet coefficients at a fixed level. Furthermore, let $I_1 \supset I_0$ another set of indices of adjacent coefficients including I_0. Let's denote μ_{I_1} by

$$\mu_{I_1} = \frac{1}{|I_1|} \sum_{(j,k)\in I_1} Y_{jk}^2. \tag{7.43}$$

Similar to (7.42) we use a kind of soft thresholding defined by

$$\hat{S}_{jk} = \left(1 - \frac{\lambda^2}{\mu_{I_1}}\right)_+ Y_{jk} \quad \forall (j,k) \in I_0 \tag{7.44}$$

for a given threshold λ. For $|I_0| = 1$ each coefficient is processed separately. However, the decision if it is better to keep or kill it is still based on information provided by surrounding coefficients. A GCV procedure is again possible.

Block thresholding removes some additional spurious "blips" but inter scale thresholding is still better. However, a variety of modifications and combinations with other methods is possible.

Chapter 8

Tree Structured Thresholding

The method presented in this chapter uses again dependencies between coefficients of different levels. It is based on so called trees of wavelet coefficients and introduced in the following definition:

Definition 8.0.1. For some wavelet coefficient $S_{j,k}$, a coefficient at level $j+1$ is called son of $S_{j,k}$ if it is positioned at the same location. Accordingly, $S_{j,k}$ is called parent of this coefficient. A wavelet tree is a set T of wavelet coefficients such that

(i) there is exactly one coefficient $S_{j_0,k_0} \in T$ with no parent in T, i.e.

(ii) $S_{j_1,k_1} \in T$, where $(j_1,k_1) \neq (j_0,k_0)$, implies the existence of a parent in T

The coefficient S_{j_0,k_0} is called root of the wavelet tree.

For $n = 2^J$ and for some discrete wavelet transform with periodic boundary conditions, each wavelet coefficient S_{jk}, $j < J-1$, has exactly two sons, given by $S_{j+1,2k}$ and $S_{j+1,2k+1}$ and we obtain a full binary tree.

We assume that inter-scale dependencies can be detected in such trees and subtrees in the following way: If a coefficient S_{jk} is large since it contains signal information, we expect coefficients at the same location but level greater than j to be large as well. This fact has already been mentioned and used in chapter 5. At the same time, noise leads to rather local effects and a noise singularities do not appear throughout many different levels. These assumptions are used for tree structured thresholding [19]. One requires approximations $\hat{S}_{jk}$ of the original signal wavelet coefficients to comply two conditions:

(i) $\hat{S}_{jk}^{tree} \in \{Y_{jk}, 0\}$

(ii) $\hat{S}_{jk}^{tree} = 0$ implies each son to be zeros as well

The first condition indicates that we perform some kind of hard thresholding or rather a "keep or kill" method. The second constraint requires each coefficient of the subtree of a "killed" coefficient to be zero, too. Hence, a "killed" coefficient produces a complete zero-subtree.

Similar to risk minimization methods like $SURE$ or GCV, one tries to find the best approximation of the signal as a compromise between closeness of fit and sparseness, or in other words bias and variance. For a given threshold λ, we try to find an approximation that minimizes

$$CPRESS(\hat{S}^{tree}) = ||\hat{S}^{tree} - Y||^2 + \lambda^2 n_1$$

under above constraints. As before, n_0 denotes the number of "killed" coefficients and n_1 the number of kept coefficients. The minimization problem can also be considered in the following way: Find a coefficient selection vector $x \in \{0,1\}^n$ such that

$$CPRESS(x) = \sum_{(j,k)\in\mathcal{I}} (1 - x_{jk})Y_{jk}^2 - x_{jk}\lambda^2 \to min \tag{8.1}$$

under the constraint that $T = \{x_{jk} | x_{jk} = 1\}$ is a wavelet tree. Hence, for each index (j,k) either λ^2 or Y_{jk}^2 is added to the $CPRESS$ value. David L. Donoho describes a connection of tree structured thresholding and the best-ortho basis algorithm [34]. It is shown that using Haar wavelets, both algorithms are equivalent [5], [7]. However, in his work he also provides an algorithm called CART (classification and regression trees), based on dynamic programming, that has been modified and used for the $CPRESS$ minimization.

Algorithm 8.1 provides a minimization method for $CPRESS(x)$ that can be done in $\mathcal{O}(n)$. Values $CPRESS_{jk}[0]$ denote the minimal $CPRESS$ value of a subtree with root Y_{jk} under constraint $\hat{S}_{jk}^{tree} = 0$, while $CPRESS_{jk}[1]$ denotes the minimal subtree value for $\hat{S}_{jk}^{tree} = Y_{jk}$. I.e. the number in brackets denotes the used value of x_{jk}. Furthermore, $\mathcal{I}_j$ denotes the set of the indices of all wavelet coefficients at level j. The algorithm can be subdivided into 4 parts, described in the following paragraphs.

PART I: In the first part of the algorithm, the best $CPRESS$ values of subtrees consisting of only the root element are determined. Optimal x_{jk} is given by $argmin(CPRESS_{J-1,k}(x))$, i.e. for $Y_{J-1,k}^2 > \lambda^2$ it is better to keep the coefficient

Algorithm 8.1 CART Algorithm

PART I. init bottom

for $k \in \mathcal{I}_{J-1}$ **do**
  $CPRESS_{J-1,k}[0] = Y^2_{J-1,k}$
  $CPRESS_{J-1,k}[1] = \lambda^2$
  $x_{J-1,k} = (CPRESS_{J-1,k}[1] < CPRESS_{J-1,k}[0])$
end for

PART II. bottom up algorithm

for $j = J-2$ to J_0 **do**
  for $k \in \mathcal{I}_j$ **do**
    $CPRESS_{jk}[0] = CPRESS_{son1}[0] + CPRESS_{son2}[0] + Y^2_{jk}$
    $CPRESS_{jk}[1] = CPRESS_{son1}[x_{son1}] + CPRESS_{son2}[x_{son2}] + \lambda^2$
    $x_{jk} = (CPRESS_{jk}[1] < CPRESS_{jk}[0])$
  end for
end for

PART III. top down correction

for $j = J_0$ to $J-2$ **do**
  for $k \in \mathcal{I}_j$ **do**
    $x_{son1} = x_{son1} \cdot x_{jk}$
    $x_{son2} = x_{son2} \cdot x_{jk}$
  end for
end for

PART IV. thresholding

for $(j,k) \in \mathcal{I}$ **do**
  $\hat{S}_{jk} = Y_{jk} \cdot x_{jk}$
end for

to obtain a $CPRESS$ contribution of equation (8.1) of only λ^2. Hence, $x_{J-1,k} = 1$.

PART II: The second part is a bottom up algorithm that computes the minimal $CPRESS$ value for all subtrees and the optimal value of the coefficient selection value x_{jk}. $CPRESS$ values can be obtained by the sum of the appropriate $CPRESS$ values of both sons. adding either λ^2 or Y_{jk}^2, depending on x_{jk}. For $x_{jk} = 0$, due to condition (ii) above, $x_{j_1,k_1} = 0$ for all Y_{j_1,k_1} in the subtree with root Y_{jk}. Hence, one has to add $CPRESS[0]$ for both sons and Y_{jk}^2 for the root. In the other case, $x_{jk} = 1$, one can decide for each son either to take $CPRESS[0]$ or $CPRESS[1]$. Obviously, we take the smaller ones, given by $CPRESS[x_{son1}]$ and $CPRESS[x_{son2}]$, respectively, where $son1$ and $son2$ denote the index of the two sons. The root contributes λ^2 to the sum.

PART III: So far, we got for each coefficient Y_{jk} the optimal coefficient selection value x_{jk} under the assumption that Y_{jk} is the root of the tree. Furthermore, we obtained the optimal $CPRESS$ value for the complete tree (or in fact, if $J_0 \neq 0$, for several trees). However, if the coefficient selection value of the parent of any Y_{jk} is zero, we need to adjust the coefficient selection values in the subtree. This is done in the third part of the algorithm, starting at the lowest level, i.e. the top of the tree.

PART IV: Finally, in the last part, the actual thresholding is done and one obtains the approximation $\hat{S}^{tree}$.

For a given threshold λ, algorithm 8.1 provides an efficient way to find the optimal tree. Nevertheless, the problem of finding an optimal threshold value is still unsolved. $CPRESS$ minimization procedures in terms of λ, e.g. golden search introduced for $SURE$ and GCV in 7.8, do not work here. In fact, the minimum would be achieved for $\lambda = 0$ or $\lambda = \infty$. For both thresholds, one obtains $CPRESS(x) = 0$. In the first case, the algorithm would lead to the "optimal" coefficient selection values $x_{jk} = 0$ for all $(j,k) \in \mathcal{I}$ which leads to $CPRESS(x) = 0$. In the second case, $\lambda = \infty$, the algorithm leads to $x_{jk} = 1$ for all $(j,k) \in \mathcal{I}$ and again $CPRESS(x) = 0$. Donoho proposes to use the universal threshold $\sigma\sqrt{2\log n}$, [7]. For good MSE results this threshold is too large, though. Differently from $SURE$ and GCV values, $CPRESS$ is no measure for good approximations, even though in all cases one may consider the threshold value λ to be a weight to control sparsity. I.e., for large thresholds it is less desirable to keep coefficients than for small ones. Hence, I claim that thresholds produced by GCV or $SURE$ are better candidates than the universal

thresholds in terms of risk minimization. Indeed, experiments show (see table 8.1 and chapter 11) that these thresholds are not only better than the universal threshold but come very close to the optimal thresholds in terms of MSE reduction for tree structured thresholding. Since tree structured thresholding is a keep or kill method and therefore close to hard thresholding, thresholds generated for sophisticated thresholding (see next chapter) provide better quality than soft thresholds. The optimal threshold has been obtained performing several denois-

Threshold Finder	λ	SNR	MSE
VISU	0.1769	15.819	4.848e-4
Minimax	0.1024	17.078	3.627e-4
SURE Soft	0.0841	15.261	5.512e-4
GCV Soph	0.1204	17.191	3.534e-4
SURE Soph	0.1131	17.224	3.508e-4
Optimal	0.1095	17.256	3.482e-4

Table 8.1: Optimal threshold for $CPRESS$ and speech example 4 and Gaussian white noise, $\sigma = 0.05$, $MSE = 2.5e-3$, $SNR = 8.696$, transform used Daubechies wavelets $db20$ and $J = 9$

ing procedures using different values of λ. However, it is only optimal for this choice of wavelets and this speech example and does not provide any information about optimal threshold for other examples. One can see, though, that using $CPRESS$ for this example, one can not achieve better MSE than $3.482e-4$.

Chapter 9

Sophisticated Thresholding

All previous methods try to find a single global threshold that is then applied on all coefficients. In this chapter I will present some arguments that validate the assumption that using different thresholds depending on the coefficient magnitude lead to better results in MSE minimization. Finally, I will develop an efficient method for the detection of such thresholds and call it sophisticated thresholding. It will turn out that good approximations can be achieved minimizing with respect of only one parameter using revised forms of $SURE$ or GCV.

9.1 Optimal Thresholds

Let's reconsider figures 7.2 and 7.3 where risk and optimal thresholds $\lambda^{opt}(S)$ for soft thresholding are plotted. The optimal threshold clearly depends not only on the noise standard deviation σ but as well on the uncorrupted signal wavelet coefficient. Small values of S require large thresholds that approach infinity as S comes close zero, whereas for large coefficients S, one expects small thresholds to be better, approaching now zero as S becomes very large. Unfortunately, we can not apply $\lambda^{opt}(S)$ directly to the data since S is of course unknown. However, let's do some further analysis of the optimal threshold, the corresponding risk and their dependence on σ.

Lemma 9.1.1. *Let $Y = S + E$ be a noisy signal coefficients and $E \sim N(0, \sigma^2)$. Furthermore, let $\lambda_\sigma^{opt}(S)$ denote its optimal soft threshold depending on the underlying uncorrupted signal wavelet coefficients S. Then, it holds that*

$$\lambda_\sigma^{opt}(\sigma S) \;=\; \sigma \lambda_1^{opt}(S) \tag{9.1}$$

Proof. Let $risk_\sigma(\lambda, S)$ denote the risk of soft thresholding some noisy Y, given

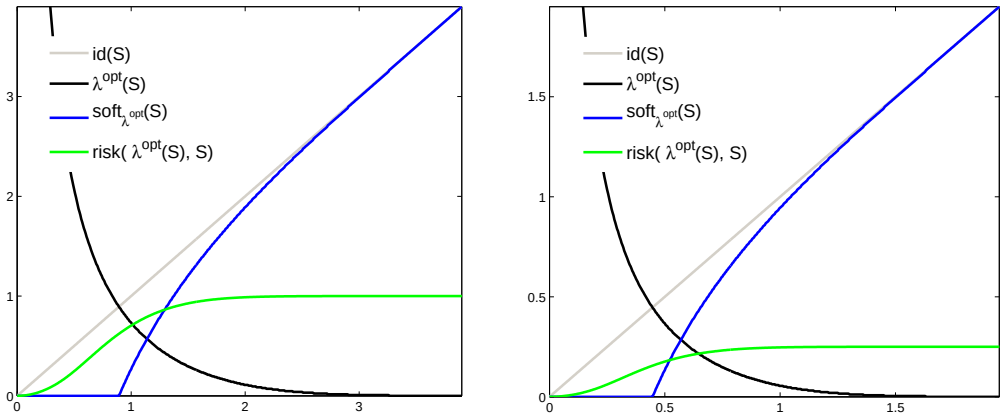

(a) $\sigma = 1.0$ (b) $\sigma = 0.5$

Figure 9.1: $\lambda^{opt}(S)$ with corresponding $risk$ and $soft_{\lambda^{opt}(S)}(S)$

the noise level σ and the underlying signal coefficient S. Using equation (7.17), one obtains

$$risk_\sigma(\sigma\lambda, \sigma S) \quad = \quad \sigma^2 risk_1(\lambda, S) \tag{9.2}$$

Hence, if λ_1^{opt} minimizes $risk_1(\lambda, S)$, then $\sigma\lambda_1^{opt}$ minimizes $risk_\sigma(\lambda, \sigma S)$. □

This result is visualized in figure 9.1. The optimal threshold $\lambda^{opt}(S)$ and the corresponding risk are provided for two different values of σ and plotted as a function of $S \in [0, 4\sigma]$, respectively. Lemma 9.1.1 says that the knowledge of λ^{opt} for a certain noise level σ is equivalent to the knowledge of the optimal threshold for any noise level. Hence, in the following we can assume σ to be equal to one without loss of generality.

Additionally, figure 9.1 shows the result of soft thresholding coefficients S (blue line) using threshold $\lambda^{opt}(S)$. This is is in fact the best approximation of S we can expect using soft thresholding. However, using a single threshold for all coefficients this is not attainable. In order to find good thresholds, two values of $\lambda^{opt}(S)$ seem to be important: the largest value of S such that $soft_{\lambda^{opt}}(S) = 0$, and secondly, the value of S such that $soft_{\lambda^{opt}}(S) \approx S$. Since $\lambda^{opt}(S)$ is never exactly zero and therefore $soft_{\lambda^{opt}}(S) \neq S$ for alls S, I define the second value to be chosen such that $\lambda^{opt}(S)$ is arbitrarily small. Let's denote these two values by α and β, respectively, precisely

$$\alpha \quad = \quad \sup\{S \in \mathbb{R} | \lambda^{opt}(S) \geq S\} \tag{9.3}$$

$$\beta \quad = \quad \inf\{S \in \mathbb{R} | \lambda^{opt}(S) < \varepsilon\}. \tag{9.4}$$

In fact, α can be obtained by the intersection of S and $\lambda^{opt}(S)$. It turns out that $\alpha \approx 0.893\sigma$ and, for $\varepsilon = 2^{-5}\sigma$, one obtains $\beta \approx 2.867\alpha$.

9.2 Sophisticated Thresholding

The idea of sophisticated thresholding is use find a thresholding function that is easy to compute and approximates $soft_{\lambda^{opt}}(S)$, i.e. a functions, let's call it $soph_{\alpha,\beta}$, such that the following restrictions hold:

(i) $soph_{\alpha,\beta}(S) = 0 \quad \forall S \in [0, \alpha]$

(ii) $soph_{\alpha,\beta}(S) = S \quad \forall S \geq [\beta, \infty)$

(iii) $soph_{\alpha,\beta}(S) \approx soft_{\lambda^{opt}}(S) \quad \forall S \in [\alpha, \beta]$,
i.e. a concave easy computable function with rather large slope at α and

(iv) the slope one at β, i.e. $\frac{\partial}{\partial S} soph_{\alpha,\beta}(\beta) = 1$.

(v) $soph_{\alpha,\beta}(-S) = -soph_{\alpha,\beta}(S)$

The last condition allows to consider only positive values of S for further analysis, where condition (iv) ensures differentiability at $S = \beta$. No differentiability condition is set at $S = \alpha$ since obviously even $soft_{\lambda^{opt}}$ is not smooth at this point. However, continuity is demanded and covered by overlapping intervals for S in the first and third condition. Some experiments with different concave functions resulted in

$$soph_{\alpha,\beta}(x) = \begin{cases} 0 & \text{, if } x \in [0, \alpha] \\ \frac{a_1}{a_2 - x} + a_3 & \text{, if } x \in (\alpha, \beta) \\ x & \text{, if } x \in [\beta, \infty) \end{cases} \tag{9.5}$$

where, for $\beta = 2.867\alpha$,

$$\begin{aligned} a_1 = &\quad (\beta - \beta^2/\alpha)^2 &&= 28.651\alpha^2 \\ a_2 = &\quad 2\beta - \beta^2/\alpha &&= -2.486\alpha \\ a_3 = &\quad \beta^2/\alpha &&= 8.220\alpha. \end{aligned}$$

The approximation is surprisingly good, as shown in figure 9.2. The mean square error $\frac{1}{m}||soph_{\alpha,\beta} - soft_{\lambda^{opt}}||^2$ for $S \in [\alpha, \beta]$ is less than $10^{-3}\sigma^2$, where $m >> 1$ denotes the number of grid points in $[\alpha, \beta]$. There still is the problem of the unknown S, though, and so far we do not know how to apply the soph threshold

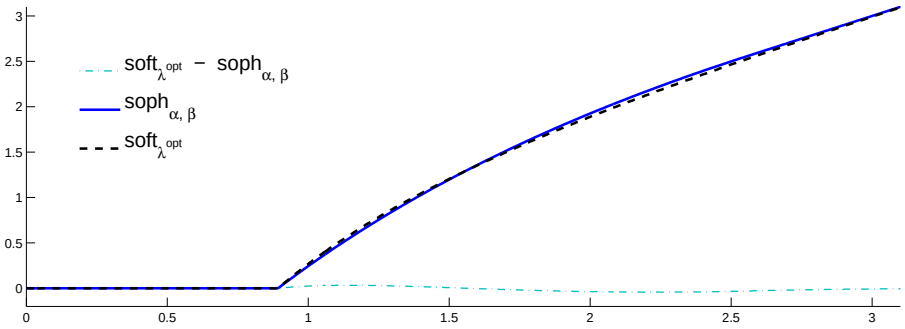

Figure 9.2: $soft_{\lambda^{opt}}(S)$ and $soph_{\alpha,\beta}(S)$ with $\alpha = 0.893$ and $\beta = 2.867\alpha$

function on noisy coefficients Y. Of course one could consider to apply the *soph* function directly on Y instead S, but I will show that it is possible to achieve much better results, using other values α than before.

9.3 Sophisticated Thresholding, SURE and GCV

Let's consider $soph_\alpha := soph_{\alpha,2.867\alpha}$ as a threshold function of a single parameter α, similar to hard and soft thresholding in section 7.1. Figure 9.3 compares these methods using $\lambda = \alpha = 1$. One can see that sophisticated thresholding can bee considered as a kind of compromise between soft and hard thresholding. For $\alpha = \beta$ one would obtain hard thresholding while for $\alpha \to \infty$ it rather approximates soft thresholding. Hence, one could try to use similar methods than before to find optimal threshold values for sophisticated thresholding. We will see that $SURE$ and GCV, introduced in section 7.6 and 7.7, respectively, originally based on soft thresholding, can be modified in order to use the MSE minimization for sophisticated thresholding as well.

SURE: In section 7.6 we derived

$$risk(S, soft_\lambda(Y)) = \mathbb{E}\left[F(\lambda)\right] - \sigma^2 + \frac{2}{n}\mathbb{E}\left[(E, E^\lambda)\right]$$

where

$$\begin{aligned} F(\lambda) &= \frac{1}{n}||soft_\lambda(Y) - Y||^2 \\ E^\lambda &= soft_\lambda(Y) - S \end{aligned}$$

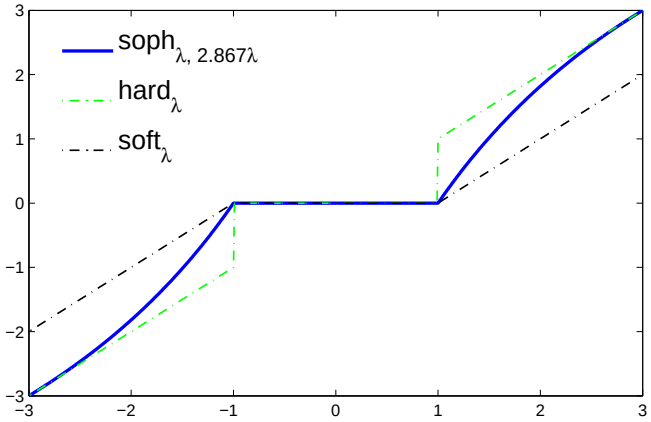

Figure 9.3: $soft_\lambda$, $hard_\lambda$ and $soph_{\lambda,\beta}$ for $\beta = 2.867\alpha$

and derived that the last term can be approximated by $2\sigma^2 n_1/n$. In the same way we now derive a version of $SURE$ adapted to sophisticated thresholding. We therefore need to find a new approximation for the last term. For $E^\alpha = soph_\alpha(Y) - S$ and $E = Y - S$, we have

$$\mathbb{E}\left[(E, E^\alpha)\right] = \sum_{(j,k)\in\mathcal{I}} \mathbb{E}[E_{jk}E^\alpha_{jk}]$$

and like in the proof of lemma 7.6.2, substituting $E = Y + S$ and using (9.5), we obtain

$$\begin{aligned}
\mathbb{E}[E_{jk}E^\alpha_{jk}] &= \sigma^2 \int_{-\infty}^{\infty} \frac{\partial E^\alpha_{jk}}{\partial E_{jk}} \phi(E_{jk}) dE_{jk} \\
&= \sigma^2 \left(\int_{Y:\alpha<|Y|<\beta} \frac{a_1}{(a_2 - |Y|)^2} \phi(Y) dY + \int_{Y:|Y|\geq\beta} 1 \cdot \phi(Y) dY \right) \\
&= \sigma^2 \int_{Y:\alpha<|Y|<\beta} \frac{a_1}{(a_2 - |Y|)^2} \phi(Y) dY + \sigma^2 P(|Y| \geq \beta).
\end{aligned}$$

The approximation is now a little more complicated than for soft thresholding. Nevertheless, it can be easily computed by

$$\begin{aligned}
\mathbb{E}\left[(E, E^\alpha)\right] &= \sum_{(j,k)\in\mathcal{I}} \mathbb{E}[E_{jk}E^\alpha_{jk}] \\
&\approx \sigma^2 \sum_{Y:\alpha<|Y|<\beta} \frac{a_1}{(a_2 - |Y|)^2} + \sigma^2 n_2
\end{aligned}$$

where n_2 denotes the number of coefficients Y such that $|Y| \geq \beta$ which leads to the approximation $P(|Y| \geq \beta) \approx n_2/n$. Eventually the new $SURE$ function is given by

$$SURE(\alpha) \;=\; F(\alpha) - \sigma^2 + \frac{2\sigma^2}{n}\left(n_2 + \sum_{Y:\alpha<|Y|<\beta} \frac{a_1}{(a_2 - |Y|)^2}\right). \qquad (9.6)$$

The complexity is not much worse than for $SURE$ based on soft thresholding. For each Y such that $\alpha < |Y| < \beta$, two extra divisions and additions have to be performed and the total complexity is still $\mathcal{O}(n)$.

GCV: We use again the results of section 7.7.1 and 7.7.2. In formula (7.31) we had

$$GCV(\lambda) \;=\; \frac{1}{(1-D)^2} F(\lambda) \qquad (9.7)$$

where D denoted the average over all derivatives $\partial \hat{S}^{\lambda}_{jk}/\partial Y_{jk}$, i.e

$$D = \frac{1}{n} \sum_{(j,k)\in\mathcal{I}} \frac{\partial \hat{S}^{\lambda}_{jk}}{\partial Y_{jk}}$$

We can use exactly the same Formula for sophisticated thresholding, only the computation of the derivatives is different and $F(\alpha)$ is of course obtained using the *soph* function. The derivative is given by

$$soph'_{\alpha,\beta}(Y) = \begin{cases} 0 & \text{, if } |Y| \in [0,\alpha] \\ \frac{a_1}{(a_2-|Y|)^2} & \text{, if } |Y| \in (\alpha,\beta) \\ 1 & \text{, if } |Y| \in [\beta,\infty) \end{cases} \qquad (9.8)$$

and therefore have

$$D \approx \frac{1}{n}\left(0 \cdot n_0 + \sum_{Y:\alpha<|Y|<\beta} \frac{a_1}{(a_2 - |Y|)^2} + 1 \cdot n_2\right) \qquad (9.9)$$

where $n_0 = |\{Y :\ |Y| \leq \alpha\}|$ and $n_2 = |\{Y :\ |Y| \geq \beta\}|$. As before, there is not much more computational effort than for soft thresholding.

9.4 Comparison

The thresholding method introduced in the previous section is assumed to produce less MSE. In this section I will verify this, comparing the risk contribution of a single coefficient for soft, hard and sophisticated thresholding. The next lemma provides the risk contribution for sophisticated and hard thresholding.

Lemma 9.4.1. *The risk contribution of a single coefficient using sophisticated thresholding is given by*

$$\begin{aligned}
\rho^{soph}(\alpha,\beta,S) &= \mathbb{E}\left[(soph_{\alpha,\beta}(Y)-S)^2\right] \\
&= s2\sigma^2 - S^2 \\
&\quad + \Phi(\beta-S)(-\sigma^2+S^2) \;+\; \Phi(\beta+S)(-\sigma^2+S^2) \\
&\quad + \phi(\beta-S)(\sigma^2(\beta-S)) \;+\; \phi(\beta+S)(\sigma^2(\beta+S)) \\
&\quad + \int_{\alpha}^{\beta} \left(soph^2_{\alpha,\beta}(x) - 2S soph_{\alpha,\beta}(x)\right)\phi(x-S)dx \\
&\quad + \int_{-\beta}^{-\alpha} \left(soph^2_{\alpha,\beta}(x) - 2S soph_{\alpha,\beta}(x)\right)\phi(x-S)dx \qquad (9.10)
\end{aligned}$$

For hard thresholding we have

$$\begin{aligned}
\rho^{hard}(\lambda,S) &= \mathbb{E}\left[(hard_{\lambda}(Y)-S)^2\right] \\
&= 2\sigma^2 - S^2 \\
&\quad + \Phi(\lambda-S)(-\sigma^2+S^2) \;+\; \Phi(\lambda+S)(-\sigma^2+S^2) \\
&\quad + \phi(\lambda-S)(\sigma^2(\lambda-S)) \;+\; \phi(\lambda+S)(\sigma^2(\lambda+S)) \qquad (9.11)
\end{aligned}$$

Proof. Simple calculation similar to lemma 7.5.1 and lemma 7.5.2 lead to (9.10). The second part of the proof is obtained using the fact that hard thresholding can be seen as a special case of sophisticated thresholding with $\lambda = \alpha = \beta$, i.e. $\rho^{hard}(\lambda,S) = \rho^{soph}(\lambda,\lambda,S)$. Hence, hard thresholding is obtained by omitting the integrals in equation (9.10). □

There is no known analytic solution for the two integrals of (9.10). However, for the subsequent analysis it is sufficient to leave them this way. With lemma

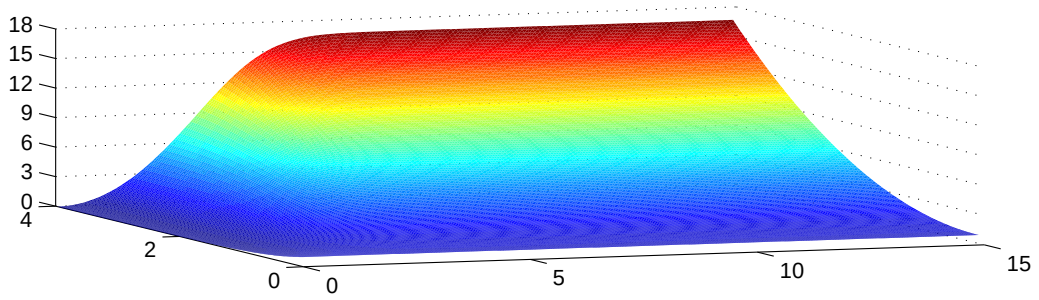

(a) $\rho^{soft}(\lambda, S)$, $\lambda \in (0, 4)$, $S \in (0, 15)$

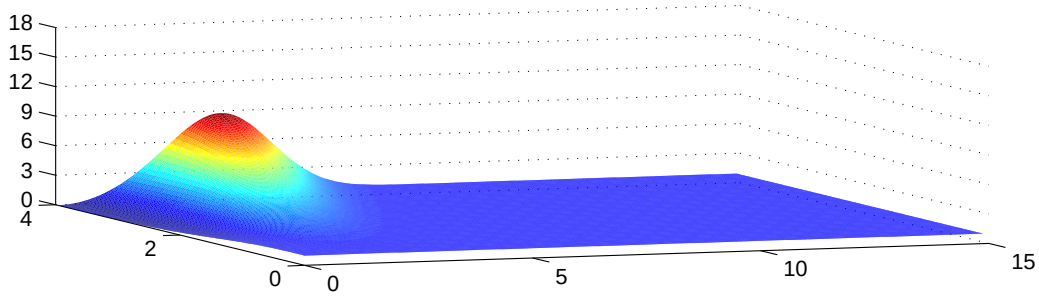

(b) $\rho^{hard}(\lambda, S)$, $\lambda \in (0, 4)$, $S \in (0, 15)$

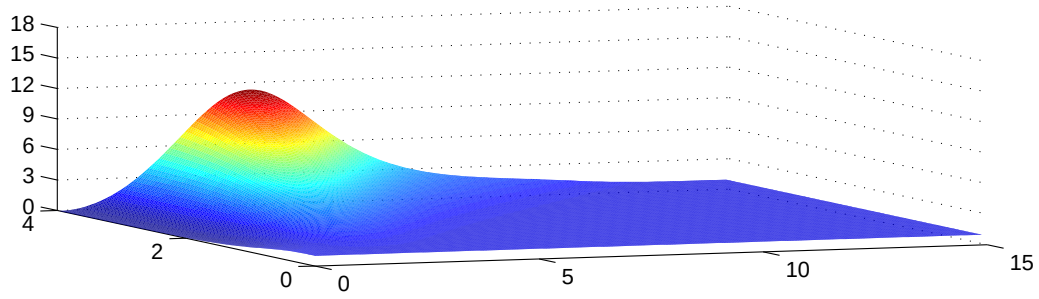

(c) $\rho^{soph}(\alpha, \beta, S)$, $\alpha \in (0, 4)$, $\beta = 2.867\alpha$, $S \in (0, 15)$

Figure 9.4: risk contribution of (a) soft, (b) hard and (c) sophisticated thresholding with $\sigma = 1$

7.5.2 and lemma 9.4.1, it is clear that for large S and fixed thresholds,

$$\begin{aligned} \rho^{soph}(\alpha, \beta, S) &\rightarrow \sigma^2 \\ \rho^{hard}(\lambda, S) &\rightarrow \sigma^2 \\ \rho^{soft}(\lambda, S) &\rightarrow \sigma^2 + \lambda^2 \end{aligned}$$

since $\phi(x - S)$, $\phi(x + S)$, $\Phi(x - S)$ approach zero and $\Phi(x + S)$ approaches one where x denotes any fixed value independent of S. The two integrals of (9.10) approach zero, too, since $soph_{\alpha,\beta}$ is bounded for fixed α and β. Hence, large coefficients contribute much more risk for soft thresholding than for sophisticated

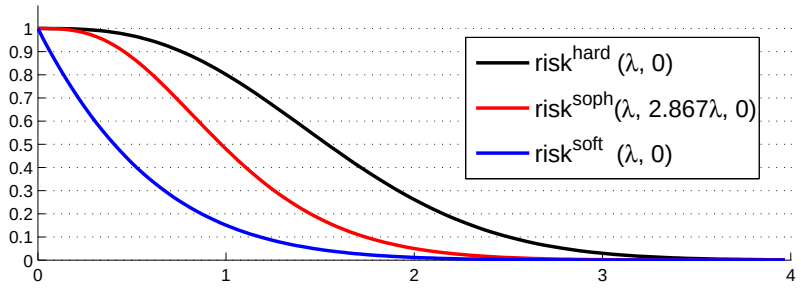

Figure 9.5: risk contribution for $S = 0$ and $\sigma^2 = 1$ as a function of λ

or hard thresholding. Additionally, since risk contribution for large coefficients is almost independent of the threshold, hard and sophisticated thresholding enable the choice of larger thresholds. Larger thresholds however lead to less risk for small values S, as seen in figure 9.1. Small S requires very large thresholds. Therefore, one might expect a smaller MSE.

Figure 9.4 displays the risk contributions of all three thresholding methods for $\sigma^2 = 1$ and $S \in [0, 15]$. Indeed, it seems like hard and sophisticated thresholding are to favor. Surprisingly, hard thresholding seems to be of superior quality since sophisticated thresholding converges slower to σ^2. However, it might be useful to take a closer look on small coefficients S, since one expect most uncorrupted signal wavelet coefficients to be zero or almost zero for piecewise smooth functions. Hence, risk contribution for small S might be much more important than the risk contribution of larger S.

$$\begin{aligned}
\rho^{soft}(\lambda, 0) &= 2\sigma^2 + 2\lambda^2 - 2\Phi(\lambda)(\sigma^2 + \lambda^2) - 2\phi(\lambda)(\sigma^2\lambda) \\
\rho^{hard}(\lambda, 0) &= 2\sigma^2 - 2\Phi(\lambda)(\sigma^2) + 2\phi(\lambda)(\sigma^2\lambda) \\
\rho^{soph}(\lambda, 2.867\lambda, 0) &= \rho^{hard}(2.867\lambda, 0) + 2\int_{\lambda}^{2.867\lambda} soph_{\lambda}^2(x)\phi(x)dx
\end{aligned}$$

Indeed, figure 9.5 indicates that

$$\rho^{soft}(\lambda, 0) \leq \rho^{soph}(\lambda, 2.867\lambda, 0) \leq \rho^{hard}(\lambda, 0).$$

Following the horizontal lines in figure 9.5, one can see that hard and sophisticated thresholding require larger thresholds to attain the same risk as soft thresholding. Indeed experiments confirm this assumption. For figure 9.6, the threshold value has been fixed and the risk contribution is plotted as a function of S. The graphs on the left side show the risk evolution for $S \in [0, 10\sigma]$, the graphs on the right side show only risk for very small S. For the construction of figures 9.6(a) and 9.6(b),

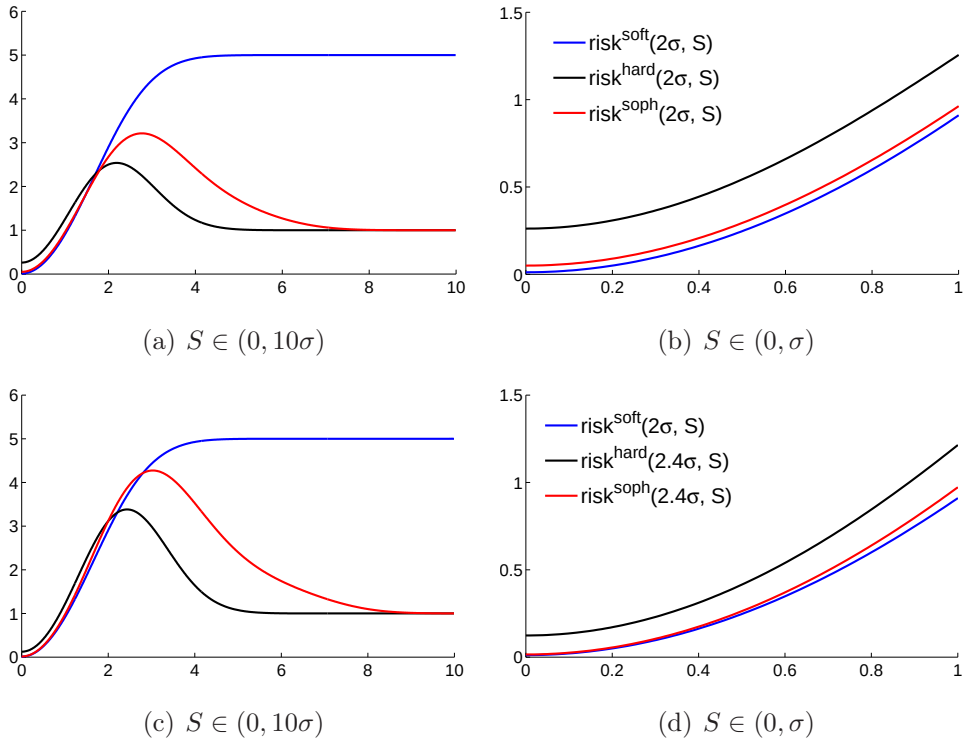

(a) $S \in (0, 10\sigma)$ (b) $S \in (0, \sigma)$

(c) $S \in (0, 10\sigma)$ (d) $S \in (0, \sigma)$

Figure 9.6: risk contribution for fixed λ, where $\sigma = 1$, $\lambda = \alpha = 2\sigma$ in (a) and (b), $\lambda = \alpha = 2.4\sigma$ for hard and soph, $\lambda = 2\sigma$ for soft in (c) and (d)

the same threshold $\lambda = 2\sigma$ has been used for all methods, whereas in figures 9.6(c) and 9.6(c) a 20% larger threshold has been used for hard and sophisticated thresholding. One can see that for small values of S (which is expected to be the case for most signal coefficients) the risk contribution is much smaller for soft thresholding. Especially hard thresholding performs bad. However, in the second case the difference between soft and soph risk contribution became much smaller, at the expense of a larger risk in the interval approximately $[\sigma, 8\sigma]$ (compare red lines). Hence, the optimal threshold clearly depends on the "distribution" of S, i.e. the number (or percentage) of uncorrupted signal wavelet coefficients that are very small versus the number of rather large ones and so on. One could use histograms for an analysis.

Under the assumption that the majority of coefficients S is small, it might be useful to try to shrink the risk for small coefficients even more without loosing too much at larger coefficients. Sophisticated thresholding provides a second parameter that can be modified, i.e. one increases β instead of α. An example is provided by figure 9.7, where $\rho^{soph}(\alpha, \beta, S)$, using $\alpha = 2\sigma$ and $\beta = 6\alpha$ is compared with all previous versions of sophisticated thresholding and soft thresholding. For very small S, it is still worse than the soph version with 20% larger α and

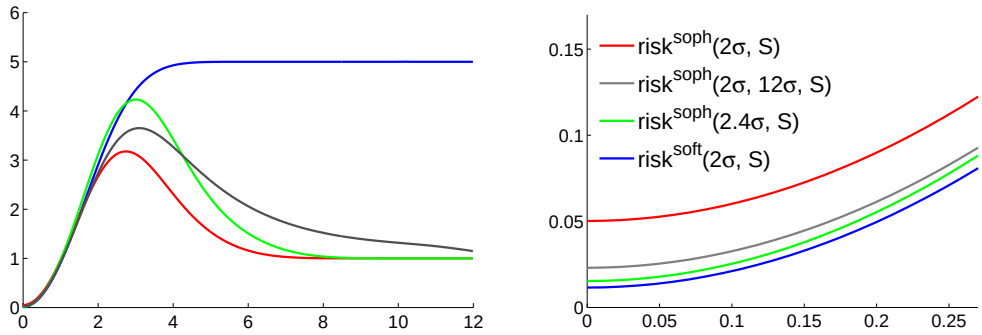

(a) $S \in (0, 12\sigma)$ (b) $S \in (0, 0.27\sigma)$

Figure 9.7: risk contribution with $\alpha = 2\sigma$ and $\beta = 6\alpha$, $\sigma = 1$

$\beta = 2.867\alpha$, but it became better for S in an interval of about $[0.5\sigma, 4.5\sigma]$, then it is again worse, so we don't win much. Still, for small uncorrupted signal wavelet coefficients soft thresholding remains the best choice. This leads to a further generalization of sophisticated thresholding that also includes characteristics of soft thresholding and is discussed in the next section.

9.5 Generalization and Improvement

The objective is to embed soft thresholding in sophisticated thresholding. For the creation of this new thresholding function, I therefore change some of the restrictions introduced in section 9.2. Now, we are looking for a concave function $soph_{\alpha,\beta,\gamma}$ such that

(i) $soph_{\alpha,\beta,0} = soph_{\alpha,\beta}$

(ii) $soph_{\alpha,\alpha,0} = hard_{\alpha}$

(iii) $soph_{\alpha,\alpha,\alpha} = soft_{\alpha}$

Similar to section 9.2, a good choice for $soph_{\alpha,\beta,\gamma}$ seems to be

$$soph_{\alpha,\beta,\gamma}(x) = \begin{cases} 0 & , \text{if } x \in [0, \alpha] \\ \frac{a_1}{a_2 - x} + a_3 & , \text{if } x \in (\alpha, \beta) \\ x - \gamma & , \text{if } x \in [\beta, \infty) \end{cases} \tag{9.12}$$

where $0 \leq \gamma \leq \alpha \leq \beta$, and for continuity and differentiability reasons, coefficients a_1, a_2 and a_3 have to be adjusted such that

(iv) $soph_{\alpha,\beta,\gamma}(\alpha) = 0$

(v) $soph_{\alpha,\beta,\gamma}(\beta) = \beta - \gamma$

(vi) $soph'_{\alpha,\beta,\gamma}(\beta) = 1$.

This leads to coefficients

$$\begin{aligned} a_1 &= (a_2 - \beta)^2 \\ a_2 &= (\beta^2 - 2\alpha\beta + \alpha\gamma)/(\gamma - \alpha) \\ a_3 &= -(a_2 - \beta)^2/(a_2 - \alpha). \end{aligned}$$

Two cases seem to need special treatment. First assume $a_2 = \alpha$, then a_3 is not computable. However, one can easily show that this occurs if and only if $\alpha = \beta$. Now, a computation of a_3 is no more necessary since the second case $x \in (\alpha, \beta)$ of equation (9.12) is impossible. For $\alpha = \gamma$ the value a_2 does not exist. One could of course restrict on cases where $\alpha \neq \gamma$ but this would not allow to embed soft thresholding any more. Hence, another condition has to be introduced,

(vii) allow $\alpha = \gamma$ only if $\alpha = \beta$.

As before, for $\alpha = \beta = \gamma$, we have $x \notin (\alpha, \beta)$ and one obtains soft thresholding. Knowing the distribution of S, i.e. the amount of coefficients S_{jk} of a certain value and for a fixed σ, one could minimize the risk in α, β, and γ that is given by formula 9.13 below. However, the $SURE$ and GCV formulas introduced in section 9.3 and given by (9.6) and (9.7),(9.9), respectively, can be applied in exactly the same way, just using the coefficients a_1, a_2 and a_3 provided in this section.

Table 9.1 compares soft with sophisticated thresholding. For β I used in all cases $\beta = 2.867\alpha$ and tried 4 different values of γ, also dependent on α to enable minimization with respect of only one parameter, α. GCV has been used for both, soft and sophisticated thresholding, to attain the best threshold value. Gaussian white noise with $\sigma = 0.05$ has been added to a speech signal with 2^{17} samples an a sampling rate of 44100 samples per second. Hence, MSE before thresholding has been about $2.5e{-}3$ and SNR has been $6.340dB$. I used Daubechies wavelets with 8 vanishing moments, periodic boundary conditions, and resolution up to level $J = 8$. One can see that sophisticated thresholding outperforms soft thresholding. Here, $\gamma = 0.18\alpha$ seemed to be optimal, MSE obtained by soft thresholding is about 26% larger in this case. As in the sections before, one can find a direct formula for the risk contribution. In fact, it embeds again risk contribution formulas for soft, hard and the previous version of sophisticated thresholding. It

	α	$\beta = 2.867\alpha$	$\gamma = c * \alpha$	MSE	SNR
$soph$	0.133	0.381	$0.00\alpha = 0.000$	3.45e-4	14.919
	0.124	0.356	$0.18\alpha = 0.022$	3.42e-4	14.963
	0.120	0.344	$0.36\alpha = 0.043$	3.54e-4	14.817
	0.107	0.307	$0.54\alpha = 0.058$	3.64e-4	14.687
$soft$	0.091			4.32e-4	14.063

Table 9.1: $n = 2^{17}$, $\sigma = 0.05$, $SNR = 6.340$

is given by

$$\begin{aligned}
\rho^{soph}(\alpha,\beta,\gamma,S) &= \mathbb{E}\left[(soph_{\alpha,\beta,\gamma}(Y)-S)^2\right] \\
&= 2\sigma^2 + 2\gamma^2 - S^2 \\
&+ \Phi(\beta - S)(-\sigma^2 - \gamma^2 + S^2) \\
&+ \Phi(\beta + S)(-\sigma^2 - \gamma^2 + S^2) \\
&+ \phi(\beta - S)(\sigma^2(\beta - S - 2\gamma)) \\
&+ \phi(\beta + S)(\sigma^2(\beta + S - 2\gamma)) \\
&+ \int_{\alpha}^{\beta} \left(soph^2_{\alpha,\beta,\gamma}(x) - 2S\,soph_{\alpha,\beta,\gamma}(x)\right)\phi(x-S)dx \\
&+ \int_{-\beta}^{-\alpha} \left(soph^2_{\alpha,\beta,\gamma}(x) - 2S\,soph_{\alpha,\beta,\gamma}(x)\right)\phi(x-S)dx \qquad (9.13)
\end{aligned}$$

Using the knowledge of the distribution of S (in fact some kind of histogram) and applying these values on the risk distribution formula above, one obtains optimal values $\alpha = 0.118$, $\beta = 3.208\alpha$ and $\gamma = 0.0582\alpha$ that, for this example, represent the optimal compromise between reducing risk for different values of S. One can see that α is a little smaller than in the optimal case above while β became larger. The value of γ is very small, only about 0.1σ.

Figure 9.8 compares the different risk contributions of soft (blue) and sophisticated thresholding with thresholds given by GCV (red) and the optimal ones (black). The optimal threshold choice leads to larger risk for small values, but outperforms thresholds generated by GCV with fixed $\beta = 2.867\alpha$ and $\gamma = 0.18\alpha$. The total risk of the optimal thresholds, regarding the given coefficients S_{jk}, i.e. the ideal risk for this specific example, is now given by

$$\begin{aligned}
risk^{soph}(\alpha,\beta,\gamma) &= \sum_{(j,k)\in\mathcal{I}} \rho^{soph}(\alpha,\beta,\gamma,S_{jk}) \\
&= 2.96e-4. \qquad (9.14)
\end{aligned}$$

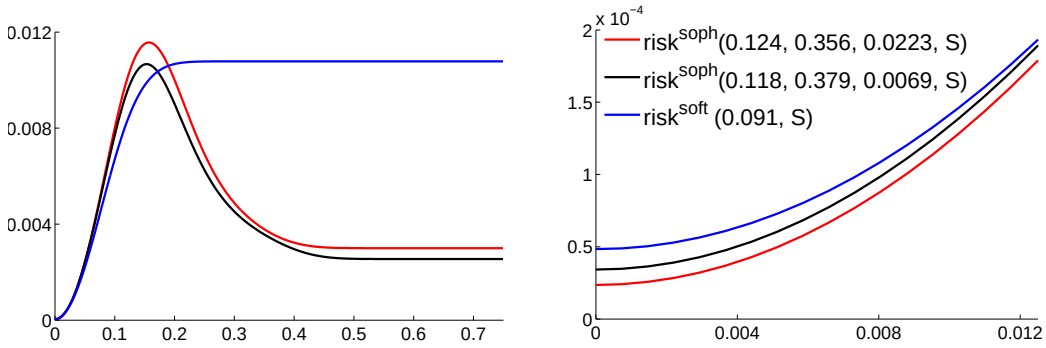

(a) $S \in (0, 15\sigma)$ (b) $S \in (0, 0.25\sigma)$

Figure 9.8: optimal risk contribution for example of table 9.1, $\sigma = 0.05$

This is only the expected MSE, though. Applying these values directly to this particular noisy signal, we obtain a MSE value of only $3.36e-4$ and $SNR = 15.033$ which is not so much better than the result produced by GCV. So we already came very close to the optimal MSE achievable by this thresholding method under the knowledge of the distribution of S. Since sophisticated thresholding embeds hard and soft thresholding, no better MSE can be expected for these methods. Table 9.2 summarizes the results for hard, soft and sophisticated thresholding. For sophisticated thresholding, we used again $\beta = 2.867\alpha$ and $\gamma = 0.18\alpha$ to make $SURE$ and GCV applicable. Risk is obtained using formula (9.13) and the knowledge of the distribution of S. In all cases, the achieved MSE is worse than $risk = \mathbb{E}[MSE]$, even for optimal thresholds. This might be due to approximations of the distribution of S that has been used, or noise that is worse than expected. However, one can again see that sophisticated thresholding outperforms even best possible thresholds for soft and hard thresholding. $SURE$ and GCV are very close to be optimal even though β and γ were given by a fixed dependency on α. For more comparisons see chapter 11.

		thresholds	risk	MSE	SNR
soph	gcv	$\alpha = 0.124$, $\beta = 0.356$, $\gamma = 0.0223$	3.01e-4	3.42e-4	15.003
	sure	$\alpha = 0.115$, $\beta = 0.329$, $\gamma = 0.0207$	2.99e-4	3.38e-4	15.008
	best	$\alpha = 0.118$, $\beta = 0.379$, $\gamma = 0.0069$	2.96e-4	3.36e-4	15.033
soft	gcv	$\lambda = 0.0914$	3.84e-4	4.21e-4	14.063
	sure	$\lambda = 0.0794$	3.76e-4	4.10e-4	14.178
	best	$\lambda = 0.0824$	3.75e-4	4.10e-4	14.177
hard	best	$\lambda = 0.1681$	3.38e-4	3.88e-4	14.411

Table 9.2: $n = 2^{17}$, $\sigma = 0.05$, $SNR = 6.340$

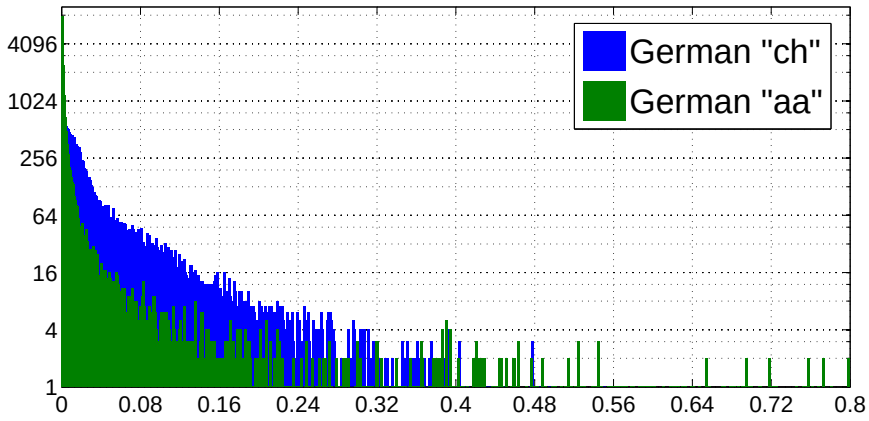

Figure 9.9: Histogram of transformed German "ch" and "aa", Daubechies 16, $J = 8$

9.6 Perspectives

The examples provided in table 9.2 indicate that sophisticated thresholding produces better results than soft and hard thresholding, even for values β and γ dependent on α. These results are supported by several additional tests provided in chapter 11. Sophisticated thresholding has been used in combinations with different threshold finders — GCV, $SURE$ and different level dependent GCV methods — almost always leading to better results than the corresponding finder in combination with soft thresholding. It is however not clear if the chosen values $\beta = 2.867\alpha$ and $\gamma = 0.18\alpha$ are appropriate for all signals. Especially if one would try to use sophisticated thresholding for other denoising applications than speech.

As mentioned before and supported by risk analysis, optimal thresholds depend on the distribution of the uncorrupted signal wavelet coefficients. Two such distributions in wavelet domain, represented by histograms and plotted in logarithmic scale, are provided in figure 9.9. For both examples, 2^{15} samples at a rate of 44100 samples per second have been used. One can see that the sibilant "*ch*" and the vowel "*aa*" lead to completely different numbers of zero coefficients which have been proven to have crucial influence on the optimal threshold values. Vowel "*aa*" concentrates most energy in a small number of large coefficients whereas "*ch*" produces many rather small coefficients.

In previous section, considering equation (9.14) and table 9.2, we have seen that sophisticated thresholding comes very close to the optimal MSE that could be obtained assuming free choice of α, β and γ. However, figure 9.9 indicates that using constant thresholds for the whole signal might not be sufficient. Hence, further research should concentrate on methods to adjust the threshold values in signal time, always being optimal for the current speech part. $SURE$ and GCV

are not appropriate, though. First of all, they both need too many coefficients to obtain good results. Common sampling rates of 22050 or 44100 samples per second do not provide enough data to enable separate treatment of each voice tones like different vowels and consonants. Furthermore, the length of such sounds vary and it is not clear how many samples should be used. A solution might be to use larger intervals, putting in some way more weight on current coefficients. However, after all it would be desirable to adjust β and γ, too, to obtain much better results. Therefore, it will be necessary to find new methods to approximate the distribution of uncorrupted signal wavelet coefficients.

Chapter 10

Biased Risk Based Sound Improvement

In chapter 7 and 9 the main objective was to minimize the risk function that has been introduced in chapter 3. However, the reconstructed signals carry a lot of disturbing noise artifacts, sounding in some way like slight rain on a roof. Before, we studied the universal threshold that produces smooth functions, completely removing noise with high probability, on the expense of very large bias which produces some kind of blurred signals. I will now try to find another approach to obtain a good compromise of both, small risk and smooth signals. The risk contribution of a signal wavelet coefficient can be expressed similarly to (3.9) by

$$\begin{aligned}
\rho(\alpha,\beta,\gamma,S) &= E\left[S-\hat{S}^{soph}\right]^2 \\
&= \left(\mathbb{E}\hat{S}^{soph}-S\right)^2+\mathbb{E}\left[\mathbb{E}\hat{S}^{soph}-\hat{S}^{soph}\right]^2 \\
&= \left(\mathbb{E}\hat{S}^{soph}-S\right)^2+\left(\mathbb{E}(\hat{S}^{soph})^2-(\mathbb{E}\hat{S}^{soph})^2\right) \qquad (10.1)\\
&= bias^2+variance. \qquad (10.2)
\end{aligned}$$

Hence, risk minimizing can be understood as finding a best compromise between bias and variance [19]. So far, both have been weighted the same. The idea is now to put more weight on the variance to achieve better noise removal quality (at the expense of bias). In fact, shrinking the variance directly leads to smoother signals.

10.1 Biased Risk Contribution

Let's first introduce the definition of biased risk.

Definition 10.1.1. For $t \in (0,1)$, we call

$$\begin{aligned}\rho_t(S,\hat{S}) &= t \cdot bias^2 + (2-t) \cdot variance \\ &= t\left((\mathbb{E}\hat{S})^2 - 2S\mathbb{E}\hat{S} + S^2\right) + (2-t)\left(\mathbb{E}\hat{S}^2 - (\mathbb{E}\hat{S})^2\right) \\ &= (2-t)\mathbb{E}\hat{S}^2 + 2(t-1)(\mathbb{E}\hat{S})^2 - 2tS\mathbb{E}\hat{S} + tS^2 \qquad (10.3)\end{aligned}$$

biased risk contribution function.

For $t = 1$, one would obtain the original risk contribution function, whereas values $t > 1$ lead to overweighted bias and hence the risk minimization results in less biased but also less smooth estimated signal functions.

For the computation of biased risk we need the first and second moment of the random variable $\hat{S}^{soph} = soph_{\alpha,\beta,\gamma}(S+E)$. Simple calculations similar to those done for the proofs of lemma 7.5.1 and lemma 7.5.2 lead to

$$\begin{aligned}\mathbb{E}\hat{S}^{soph} &= 2S \\ &- \Phi(\beta - S)(S - \gamma) + \phi(\beta - S)(\sigma^2) \\ &- \Phi(\beta + S)(S + \gamma) + \phi(\beta + S)(-\sigma^2) \\ &+ \int_{\alpha}^{\beta} soph_{\alpha,\beta,\gamma}(x)\phi(x-S)dx + \int_{-\beta}^{-\alpha} soph_{\alpha,\beta,\gamma}(x)\phi(x-S)dx \qquad (10.4)\end{aligned}$$

and

$$\begin{aligned}\mathbb{E}(\hat{S}^{soph})^2 &= 2\sigma^2 + 2\gamma^2 + 2S^2 \\ &- \Phi(\beta - S)(\sigma^2 + (S-\gamma)^2) + \phi(\beta - S)(\sigma^2(\beta + S - 2\gamma)) \\ &- \Phi(\beta + S)(\sigma^2 + (S+\gamma)^2) + \phi(\beta + S)(\sigma^2(\beta - S - 2\gamma)) \\ &+ \int_{\alpha}^{\beta} soph^2_{\alpha,\beta,\gamma}(x)\phi(x-S)dx + \int_{-\beta}^{-\alpha} soph^2_{\alpha,\beta,\gamma}(x)\phi(x-S)dx \qquad (10.5)\end{aligned}$$

Let's now take a separated look at the squared bias and the variance, respectively. Using equations (10.2), (10.4) and (10.5), with $\beta = c\alpha$, $\gamma = d\alpha$ for some constants $c \geq 1$, $d \geq 0$, one obtains

$$\begin{aligned}\lim_{\alpha\to\infty} bias^2(\hat{S}^{soph}) &= |S|^2 \\ \lim_{\alpha\to 0} bias^2(\hat{S}^{soph}) &= 0 \\ \lim_{\alpha\to\infty} var(\hat{S}^{soph}) &= 0 \\ \lim_{\alpha\to 0} var(\hat{S}^{soph}) &= \sigma^2.\end{aligned}$$

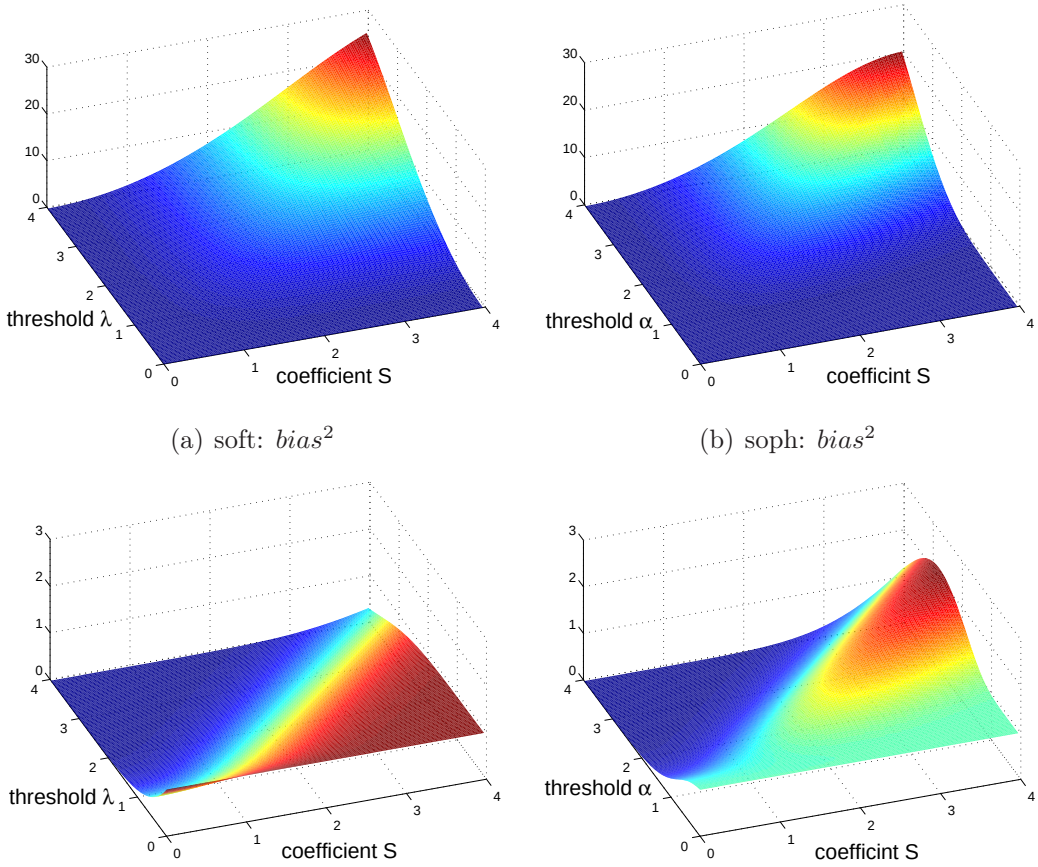

(a) soft: $bias^2$

(b) soph: $bias^2$

(c) soft: *variance*

(d) soph: *variance*

Figure 10.1: $bias^2$ and *variance* for soft and sophisticated thresholding, $\sigma = 1$, $\beta = 2.867\alpha$, $\gamma = 0.18\alpha$

This is also clear using equation (10.1), since for $\alpha \to \infty$ we have $soph(Y) \to 0$ and for $\alpha = 0$ it follows that $\mathbb{E}soph(Y) = S$ and $\mathbb{E}(\hat{S}^{soph})^2 = S^2 + \sigma^2$. Since the best compromise between $bias^2$ and *variance* is now shifted towards the *variance* one expects the threshold value to become larger than before. Figure 10.1 shows both, squared bias and variance, for soft and sophisticated thresholding. One can see that sophisticated thresholding produces less bias but more variance. Hence, for biased risk minimization we will have to adjust especially β and γ.

10.2 Minimization Problem

Table 10.1 shows optimal threshold values for a noisy speech example and different values of t. The optimal threshold values have been obtained using the knowledge of the uncorrupted signal wavelet coefficients and the "Nelder and Mead" minimization method. Orthogonal Daubechies wavelets with 8 vanishing

moments have been used and, the corresponding detail coefficients have been evaluated at $J = 8$ levels. One can see that small t leads to, as expected, larger thresholds α and γ, whereas β does not change much. While α increases approximately 28% from $t = 1$ to $t = 0.2$, the corresponding factor to obtain β decreases about 25%. In fact, for $t = 0.2$, the threshold α is already very close to the universal threshold $\lambda^{univ} = \sigma\sqrt{2\log(2^J)} = 0.1665$. Table 10.2 provides

t	α	β	γ	$risk_t$
1.00	0.1181	3.208α	0.0582α	2.961e-4
0.66	0.1317	2.987α	0.1628α	2.721e-4
0.50	0.1383	2.951α	0.2471α	2.489e-4
0.36	0.1457	2.810α	0.3916α	2.181e-4
0.20	0.1516	2.413α	0.6669α	1.791e-4

Table 10.1: Optimal thresholds for biased risk, $n = 2^{17}$, $\sigma = 0.05$, $MSE = 3.5e-3$, $SNR = 6.340$

the corresponding risk, bias and variance for the thresholds given in table 10.1. For $t = 0.2$, one can indeed see that the actual risk is almost only influenced by bias, leading however to much worse MSE values. Hence, a good compromise might be a choice of $t \approx 0.5$, where variance is already shrunken much more than bias, leading however to risk and MSE not much worse than optimal. So far, I

t	$risk$	$bias^2$	$variance$	MSE	SNR
1.00	2.961e-4	1.687e-4	1.274e-4	3.364e-4	15.033
0.66	3.088e-4	2.132e-4	9.562e-5	3.514e-4	14.844
0.50	3.279e-4	2.455e-4	8.240e-5	3.712e-4	14.606
0.36	3.661e-4	2.969e-4	6.921e-5	4.104e-4	14.170
0.20	4.564e-4	4.021e-4	5.418e-5	5.024e-4	13.291

Table 10.2: Bias and variance for biased risk, $n = 2^{17}$, $\sigma = 0.05$, $MSE = 3.5e-3$, $SNR = 6.340$

used the knowledge of the uncorrupted signal to find good threshold values. The main problem is now to find good $risk_t$ minimization methods for $t \neq 1$. I tried to develop generalizations of $SURE$ and GCV, without success, though. Hence, at the moment the best approximation of $risk_t$ minimization methods is to evaluate good thresholds using a known risk minimization method and adjusting the results due to previous experiments. For the examples provided in chapter 11, I performed a $SURE$ minimizations, adjusting the results in the following way: $\alpha_t = 1.2\alpha$, $\beta_t = \beta$, $\gamma_t = 2\gamma$. However, much more research need to be done to improve biased risk minimization and replace the mentioned heuristic approach.

Chapter 11

Comparisons, Conclusions and Outlook

Explanations: All speech examples of tables 11.2 to 11.7 are specified in appendix A and can be found on the attached CD. Table 11.1 provides the names of the denoised speech files, where "example" stands for the corresponding speech name, specified in appendix A. The first column provides the used denoising

Original		example.wav
Noisy, $\sigma = 0.0x$		example0x.wav
Diffusion	FWT	example0x diff fwt 4 6 1.0 80.wav
Soft VISU	FWT	example0x visu soft FWT 7 8
Soft MiMa	FWT	example0x minimax soft FWT 7 8
Soft SURE	FWT	example0x sure soft FWT 9 10.wav
Soph SURE	FWT	example0x sure soph FWT 9 10.wav
Soft GCV	FWT	example0x gcv soft FWT 9 10.wav
Soph GCV	FWT	example0x gcv soph FWT 9 10.wav
Soft LGCV	FWT	example0x lgcv soft FWT 9 10.wav
Soph LGCV	FWT	example0x lgcv soph FWT 9 10.wav
Cart VISU	FWT	example0x visu cart FWT 9 10.wav
Cart MiMa	FWT	example0x minimax cart FWT 9 10.wav
Cart SURE	FWT	example0x sure cart FWT 9 10.wav
Biased	FWT	example0x sure biased soph FWT 9 10.wav
Soft LGCV	SWT	example0x gcv soft SWT 5 8.wav
Soph LGCV	SWT	example0x gcv soph SWT 5 8.wav
Soft IGCV	SWT	example0x gcv inter SWT 6 6 l1.wav
Lipschitz	SWT	example0x lip 4 7.wav
Wiener	FFT	example0x sdd wf 1024.wav
PSF	FFT	example0x sdd psf 1024.wav
EMF	FFT	example0x sdd emf 1024.wav

Table 11.1: Explanations: $\sigma = 0.0x$

method. For all thresholding methods, the first word describes the thresholding method, the second word for the threshold or threshold finder, respectively. "VISU" refers to the universal threshold, "MiMa" to the miinimax threshold. An "L" at the threshold finder indicates level dependent thresholding, i.e. at each level, a threshold has been evaluated separately. "Cart" refers to the algorithm for tree structured thresholding, CPRESS. Furthermore, for "Cart SURE", I used a threshold obtained using SURE for sophisticated thresholding. "ICGV" refers to inter scale GCV, as described in section 7.10, using coefficients of two subsequent levels, i.e. $l = 1$. Diffusion denoising performes 80 iterations with diffusion step size $\tau = 1$, starting with a threshold 50% larger than universal. At each iteration, the threshold has been shrunken by a factor of 0.99. Thresholds for biased risk thresholding are obtained using "Soph SURE" thresholds, increasing α by a factor of 1.2 and doubling γ. For all methods, I used orthogonal Daubechies wavelets. The number of vanishing moments is provided in the fourth column of tables 11.2 to 11.7. For Fourier based methods, windows with a sub-frame length of 1024 samples are used, 75% overlapping.

On each speech example, Gaussian white noise with standard deviation $\sigma = 0.01$, $\sigma = 0.03$ and $\sigma = 0.05$ has been added. Tables 11.2 to 11.7 list MSE and SNR before and after denoising. For each example, the best FWT based method — in terms of MSE and SNR minimization — is marked blue. If any SWT based procedure produces better results it is additionally marked green. There is no case where FFT based methods are better than the best wavelet based method.

In the following, I will first compare the methods based only on MSE and SNR, and try to provide some conclusions about favorable methods. Then, I will compare the methods based on auditory behavior. However, clear and indisputable results are not possible here, since each method produces its own characteristic noise artifacts and signal deformations, diversely evaluated by different persons. Hence, I recommend to listen to some of the speech examples on the attached CD to form an own view, too. However, I will also try to provide an evaluation which methods might be best for which speech sound, i.e. different preferences for vocals, sibilants and other consonants.

MSE and SNR Comparison: First, I will compare the methods in general, i.e. I try to find results that are true for all speech examples. Later I will consider some special examples an analyze the best method. Diffusion denoising, Lipschitz denoising and VISU shrink are for almost all examples the worst methods. Only Lipschitz denoising outperforms in few cases some of the other

methods. This is however not surprising since all these methods are not based on MSE minimization but rather on smoothing. Only for large noise magnitudes, i.e. large σ, Lipschitz denoising yields some good results. In fact, compared to other methods, the obtained SNR does not change much for decreasing noise magnitude, i.e. the absolute result is less dependent on noise. Although CPRESS is not based on risk minimization, either, for a given threshold, the idea and the actual outcome is not so much different to thresholding. Hence, using risk minimization thresholds also leads to good results. Another remark should be done on biased risk thresholding. Even though it is not directly based on risk minimization, in fact we explicitly adjust thresholds to obtain more bias, it yields good results, not much worse than others. Let's now take a closer look on sophisticated thresholding. We can see that for most cases, sophisticated thresholding produces better results than corresponding threshold finders based on soft thresholding. Especially for level dependent GCV and FWT, there are some examples with very large differences to soft thresholding. E.g. for speech 2 and $\sigma = 0.01$, the difference is over 3dB, i.e. MSE doubles from soph to soft. Furthermore, as mentioned in chapter 9, it would be possible to obtain even better results if we were not restricted on in some way fixed β and γ. Considering inter scale dependencies, I cannot support the assumption, postulated by Maarten Jansen [19], that inter-scale GCV thresholding yields better results than ordinary GCV. In fact, only for few examples better SNR is obtained.

Let's now consider speech example 1 and 2. In contrast to the other examples, both consist of only 2^{16} samples. It is remarkable that, independent of the noise magnitude, CPRESS produces the best results. Especially for $\sigma = 0.03$, no other method comes close to the MSE of CPRESS. The differences between SURE and Minimax threshold is however small. In most cases, Minimax is a little better. For all other examples, the optimal method depends on the noise magnitude. For $\sigma = 0.01$, sophisticated thresholding linked with SURE seems to be the best choice. Whenever it is not optimal, it is at least very close to optimal. If SURE is not applicable because σ is not known, sophisticated GCV is second-best, either ordinary or level dependent based on SWT. FWT based level dependent GCV yields to much worse results for $\sigma = 0.01$. However, for larger noise magnitudes the tide turns and for $\sigma = 0.03$ it is already the best method for some of the speech examples, whereas others still prefer sophisticated SURE or Cart. Finally, for $\sigma = 0.05$, it clearly is the optimal choice. Besides speech example 1 and 2, there is only one other speech example that would prefer Cart. However, the SNR difference to LGCV is rather small. LGCV is only outdone by "itself", based on SWT though. It is remarkable that for SWT, no clear preference between

sophisticated and soft thresholding can bee determined. Finally, the used FFT based methods are outperformed by almost all wavelet based methods!

In summary, for small n, Cart seems to be appropriate. Otherwise, we need a rough noise estimation to find good methods. For large noise magnitude, the best choice is LGCV, based on SWT or FWT. For small noise amplitudes however, LGCV performs much worse than SURE and GCV. For medial noise magnitudes, the differences are small, and furthermore, Cart might be a good choice, too.

Sound Quality Comparison: Let's now take a look at (or rather a listen to) sound quality. The following conclusions are mainly based on my personal perception of noise, i.e. on the evaluation which noise artifact is most disturbing. Other readers may come to different conclusions. Additionally, I've been listening to so much noise recently, such that I've got the feeling to become more and more noise resistant.

However, let's start with reconstructed signals for $\sigma = 0.01$. My clear favorite is the universal threshold, i.e. Soft VISU. We have seen in chapter 7 that with high probability, all noise is removed. Indeed, I can not hear much noisy disturbances. At the same time, since σ and therefore λ is relatively small compared to uncorrupted signal coefficients, the signal deformation is still small. If σ can't be approximated, Lipschitz denoising provides relatively good quality, too. For my perceptual experience, the constant low frequency background noise, characteristic for Lipschitz denoising and described in chapter 5, is less distracting than permanently changing small disturbances. For larger σ, VISU shrink yields much more signal deformation and other methods are preferable.

For $\sigma = 0.03$ it is very hard to state a preference. For some examples, VISU shrink still sounds good. For most examples I prefer Lipschitz denoising, though. Even though many important signal features are kept by Diffusion denoising, noise is not really removed but in some way smoothed to a constant high tone background beeping, as already mentioned in chapter 6. However, also LGCV and biased risk denoising yield to good results for some examples. Especially biased risk seems to become much better than SURE or GCV methods for increasing σ.

Finally, for large σ, I would prefer biased risk thresholding and in some cases Lispchitz denoising. Similar to VISU shrink, almost all noise is removed (besides the mentioned low frequency background, sounding in some way like a far away highway), but there is less signal distortion. However, Lipschitz denoising produces now some additional disturbing swishing sounds, occuring at "s" and similar sounds.

For all noise magnitudes, sophisticated and soft thresholding risk minimization

methods lead to different characteristic chirping and twittering. In my opinion, the residual noise of sophisticated thresholding is a little less disturbing. However, for large noise magnitude these methods are outperformed by biased risk denoising, leading indeed as desired to less "chirping" and about the same signal quality. Cart methods produce typical keep or kill problems. Soft or soph thresholding leads to an additional smoothing by shrinking even large coefficients by a certain amount. Hard thresholding, or in this case a tree structured keep or kill method, yields to abrupt changes of the signal, sounding indeed in some way "hard". Furthermore, cart processes coefficients in blocks. Each tree of coefficients is treated separately, i.e. for one tree most coefficients might be kept, in the following one most might be killed, enhancing the effect of abrupt changes.

Finally, some additional remarks about the optimal method for some different speech sounds. As mentioned in chapter 1, one expects reconstruction problems for sibilant sounds like "*s*", "*ch*" or "*z*", since they sound and look similar to noise. One can see in figure 1.1 that smoothness assumptions do not apply. Hence, it is not surprising that especially smoothness based methods produce bad results. Diffusion and Lipschitz denoising produce additional swishing or soughing artifacts whenever such sounds occur. Similar artifacts can also be observed for Visu Shrink, but not as strong. Indeed, thresholding often produces much better quality, i.e. less signal deformation, on the expense of more audible residual noise. The best result is obtained using level dependent thresholds. Also hard consonants like "*t*" or "*k*" are, similar to sibilants, better preserved by thresholding methods, again especially level dependent ones. The difference is much less conspicuous, though. However, other sounds, especially vowels, or sounds like "*m*", "*l*" and "*r*" that produce smooth curves are much better preserved using Lipschitz denoising or Visu Shrink. Smooth signals produce sparser wavelet representations of the original signal, and therefore, only few important but very large coefficients remain. Hence, Visu Shrink, using very large thresholds to remove all pure noise coefficients, does not kill or deform many important coefficients. For Lipschitz denoising, the same fact facilitates the detection of noise coefficients that need to be removed. For all other thresholding methods there is not much signal deformation either, but much more residual noise since the selected thresholds are too small. In fact, these results also support the statement made in chapter 9 that large original signal coefficients prefer larger thresholds, i.e. global thresholds can not be optimal.

However, as mentioned, I recommend to listen to some examples and decide for yourself. For a very quick overview and comparison of the different residual

noise artifacts and denoising results, I recommend to select only Lipschitz, VISU, biased, Soph LGCV and Soft SURE. Then, most typical artifacts are covered and the audible differences to other methods are rather small.

Outlook, Perspectives: I have shown that wavelet based denoising methods can outperform some of the existing and commonly used Fourier based methods. However, some further improvements are possible. I will now give a brief overview of possible enhancements. First of all, different wavelets may lead to better results, without even changing a lot of the actual methods. For example, Yu, Bacry and Mallat recently proposed to use complex wavelets in audio signal processing to protect the phase of the signal [38]. Furthermore, I developed two new denoising methods, sophisticated thresholding and biased risk thresholding. However, for both methods the threshold finding procedure should be improved. For sophisticated thresholding, we adjust in fact only one out of three parameters for risk minimization purpose. Biased risk thresholding lacks of any appropriate method to find good thresholds, using a simple heuristic approach so far. Additionally, as mentioned in chapter 9, it will be better not to use constant thresholds for the whole signal but adjust it in accordance to the current signal features. In fact, this bridges to speech recognition methods. In summary, we see that further research is necessary to obtain satisfactorily results.

Method		J	D	Ex. 1	Ex. 2	Ex. 3	Ex. 4	Ex. 5	Ex. 6	Ex.7	Ex. 8	Ex. 9
START	-	-	-	19.866	21.411	22.778	22.672	24.019	24.692	22.720	22.808	24.255
Diffusion	FWT	4	6	18.681	24.442	18.311	22.551	25.015	23.064	18.632	18.539	21.706
Soft VISU	FWT	7	8	19.493	21.289	19.146	22.118	23.369	22.288	18.867	19.819	21.646
Soft MiMa	FWT	7	8	22.735	24.444	22.617	25.304	26.558	25.611	22.239	23.222	25.008
Soft SURE	FWT	9	10	23.621	25.354	24.747	26.311	27.620	27.209	24.423	25.039	26.685
Soph SURE	FWT	9	10	24.242	25.940	24.894	26.746	28.026	27.447	24.400	25.226	26.933
Soft GCV	FWT	9	10	23.569	25.245	24.696	26.186	27.450	26.978	24.091	24.703	26.559
Soph GCV	FWT	9	10	24.117	25.840	24.443	26.682	27.797	27.201	24.042	24.904	26.559
Soft LGCV	FWT	9	10	20.619	20.594	21.666	23.214	25.910	22.730	24.141	20.765	26.557
Soph LGCV	FWT	9	10	22.488	23.647	23.199	25.869	27.605	25.572	23.196	23.483	26.245
Cart VISU	FWT	9	10	22.872	24.788	21.409	25.194	23.955	24.936	21.583	23.090	24.726
Cart MiMa	FWT	9	10	24.328	26.185	22.814	26.863	25.011	26.417	23.443	24.990	26.494
Cart SURE	FWT	9	10	23.960	26.051	22.650	26.787	24.992	26.318	23.222	24.597	26.279
Biased	FWT	9	10	23.946	25.554	24.556	26.273	27.647	27.033	24.137	24.974	26.597
Soft LGCV	SWT	5	8	23.962	25.848	24.677	26.748	27.952	27.261	24.060	24.991	26.659
Soph LGCV	SWT	5	8	24.163	25.892	24.326	26.717	27.994	27.018	23.846	24.933	26.596
Soft IGCV	SWT	6	6	18.443	22.175	23.388	25.167	27.481	26.455	22.490	23.599	25.519
Lipschitz	SWT	4	7	15.190	18.365	12.803	19.380	17.605	15.900	13.542	14.516	14.765
Wiener	FFT	-	-	20.178	20.877	17.472	20.569	21.700	20.109	16.611	17.920	17.569
PSF	FFT	-	-	21.422	22.055	18.652	21.622	22.572	21.243	17.652	19.030	18.703
EMF	FFT			21.303	21.893	18.512	21.513	22.468	21.102	17.509	18.877	18.549

Table 11.2: SNR Comparison: $\sigma = 0.01$, *IGCV = Inter Scale GCV, *LGCV = Level Dependent GCV

Method		J	D	Ex. 1	Ex. 2	Ex. 3	Ex. 4	Ex. 5	Ex. 6	Ex.7	Ex. 8	Ex. 9
START	-	-	-	9.999e-5	1.002e-4	1.001e-4	1.001e-4	1.001e-4	1.001e-4	1.001e-4	1.001e-4	1.002e-4
Diffusion	FWT	4	6	1.314e-4	4.983e-5	2.798e-4	1.029e-4	7.955e-5	1.456e-4	2.565e-4	2.674e-4	1.803e-4
Soft VISU	FWT	7	8	1.090e-4	1.030e-4	2.309e-4	1.137e-4	1.162e-4	1.740e-4	2.430e-4	1.991e-4	1.828e-4
Soft MiMa	FWT	7	8	5.165e-5	4.982e-5	1.038e-4	5.458e-5	5.575e-5	8.097e-5	1.118e-4	9.096e-5	8.427e-5
Soft SURE	FWT	9	10	4.212e-5	4.040e-5	6.358e-5	4.329e-5	4.366e-5	5.605e-5	6.761e-5	5.986e-5	5.728e-5
Soph SURE	FWT	9	10	3.650e-5	3.530e-5	6.146e-5	3.916e-5	3.977e-5	5.305e-5	6.796e-5	5.734e-5	5.410e-5
Soft GCV	FWT	9	10	4.262e-5	4.142e-5	6.432e-5	4.454e-5	4.541e-5	5.911e-5	7.298e-5	6.468e-5	5.896e-5
Soph GCV	FWT	9	10	3.757e-5	3.612e-5	6.818e-5	3.974e-5	4.192e-5	5.615e-5	7.381e-5	6.176e-5	5.896e-5
Soft LGCV	FWT	9	10	8.407e-5	1.209e-4	1.292e-4	8.832e-5	6.474e-5	1.572e-4	7.215e-5	1.602e-4	5.899e-5
Soph LGCV	FWT	9	10	5.467e-5	5.985e-5	9.081e-5	4.792e-5	4.382e-5	8.171e-5	8.968e-5	8.565e-5	6.339e-5
Cart VISU	FWT	9	10	5.005e-5	4.602e-5	1.371e-4	5.598e-5	1.015e-4	9.460e-5	1.300e-4	9.378e-5	8.993e-5
Cart MiMa	FWT	9	10	3.580e-5	3.337e-5	9.922e-5	3.811e-5	7.962e-5	6.725e-5	8.472e-5	6.054e-5	5.985e-5
Cart SURE	FWT	9	10	3.895e-5	3.441e-5	1.030e-4	3.879e-5	7.996e-5	6.881e-5	8.913e-5	6.628e-5	6.290e-5
Biased	FWT	9	10	3.908e-5	3.858e-5	6.644e-5	4.366e-5	4.340e-5	5.836e-5	7.221e-5	6.076e-5	5.845e-5
Soft LGCV	SWT	5	8	3.894e-5	3.605e-5	6.461e-5	3.914e-5	4.045e-5	5.538e-5	7.350e-5	6.053e-5	5.762e-5
Soph LGCV	SWT	5	8	3.717e-5	3.569e-5	7.004e-5	3.942e-5	4.006e-5	5.857e-5	7.721e-5	6.135e-5	5.846e-5
Soft IGCV	SWT	6	6	1.388e-4	8.400e-5	8.695e-5	5.633e-5	4.508e-5	6.667e-5	1.055e-4	8.340e-5	7.492e-5
Lipschitz	SWT	4	7	2.935e-4	2.020e-4	9.948e-4	2.135e-4	4.381e-4	7.576e-4	8.282e-4	6.753e-4	8.913e-4
Wiener	FFT	-	-	1.861e-4	2.265e-4	3.395e-4	1.624e-4	1.707e-4	2.875e-4	4.085e-4	3.083e-4	4.673e-4
PSF	FFT	-	-	1.398e-4	1.727e-4	2.587e-4	1.274e-4	1.396e-4	2.214e-4	3.214e-4	2.388e-4	3.599e-4
EMF	FFT			1.437e-4	1.792e-4	2.672e-4	1.306e-4	1.430e-4	2.287e-4	3.322e-4	2.474e-4	3.729e-4

Table 11.3: MSE Comparison: $\sigma = 0.01$, $MSE = 1.000e-4$

Method		J	D	Ex. 1	Ex. 2	Ex. 3	Ex. 4	Ex. 5	Ex. 6	Ex.7	Ex. 8	Ex. 9
START	-	-	-	10.323	11.870	13.234	13.128	14.475	15.148	13.177	13.265	14.712
Diffusion	FWT	4	6	12.896	17.057	12.840	16.646	19.379	16.916	13.417	13.901	15.603
Soft VISU	FWT	7	8	12.875	15.050	13.092	16.049	17.493	16.243	13.192	13.967	15.543
Soft MiMa	FWT	7	8	15.780	17.696	16.060	18.759	20.150	19.127	15.959	16.756	18.468
Soft SURE	FWT	9	10	16.116	18.037	16.929	19.094	20.415	19.713	16.801	17.439	19.114
Soph SURE	FWT	9	10	16.761	18.695	17.192	19.827	21.148	20.100	16.886	17.618	19.540
Soft GCV	FWT	9	10	16.096	18.010	16.868	19.010	20.423	19.690	16.566	17.364	19.032
Soph GCV	FWT	9	10	16.741	18.676	17.157	19.826	21.128	20.087	16.707	17.547	19.347
Soft LGCV	FWT	9	10	15.693	17.378	16.764	18.959	21.223	19.591	16.092	16.652	18.699
Soph LGCV	FWT	9	10	15.529	18.701	17.005	19.975	21.356	20.205	16.615	17.266	19.188
Cart VISU	FWT	9	10	15.240	17.734	14.948	18.685	19.454	18.506	14.691	15.489	17.846
Cart MiMa	FWT	9	10	17.111	19.329	16.798	19.921	20.470	20.144	16.544	17.618	19.642
Cart SURE	FWT	9	10	17.112	19.291	16.548	19.996	20.541	19.799	16.292	17.449	19.601
Biased	FWT	9	10	16.280	18.476	16.945	19.460	20.765	19.965	16.697	17.382	19.137
Soft LGCV	SWT	5	8	16.801	18.975	17.149	19.957	21.120	20.218	16.892	17.417	19.418
Soph LGCV	SWT	5	8	16.882	18.988	17.021	19.946	21.376	20.193	16.692	17.592	19.475
Soft IGCV	SWT	6	6	15.433	18.361	15.939	18.610	20.150	19.400	15.532	16.662	18.380
Lipschitz	SWT	4	7	13.921	16.461	12.047	17.746	16.306	15.095	12.537	13.772	14.069
Wiener	FFT	-	-	13.120	14.858	11.026	14.154	16.137	13.960	11.112	12.201	17.569
PSF	FFT	-	-	14.160	15.681	11.879	15.077	17.027	14.734	11.775	12.908	18.703
EMF	FFT			14.057	15.603	11.781	15.008	16.943	14.659	11.702	12.837	12.427

Table 11.4: SNR Comparison: $\sigma = 0.03$

Method		J	D	Ex. 1	Ex. 2	Ex. 3	Ex. 4	Ex. 5	Ex. 6	Ex.7	Ex. 8	Ex. 9
START	-	-	-	9.001e-4	9.010e-4	9.007e-4	9.007e-4	9.007e-4	9.007e-4	9.008e-4	9.008e-4	9.022e-4
Diffusion	FWT	4	6	4.977e-4	2.729e-4	9.863e-4	4.007e-4	2.912e-4	5.996e-4	8.522e-4	7.780e-4	7.348e-4
Soft VISU	FWT	7	8	5.001e-4	4.333e-4	9.307e-4	4.597e-4	4.496e-4	7.001e-4	8.976e-4	7.663e-4	7.451e-4
Soft MiMa	FWT	7	8	2.562e-4	2.356e-4	4.699e-4	2.463e-4	2.438e-4	3.604e-4	4.747e-4	4.032e-4	3.800e-4
Soft SURE	FWT	9	10	2.371e-4	2.178e-4	3.846e-4	2.281e-4	2.294e-4	3.149e-4	3.910e-4	3.445e-4	3.274e-4
Soph SURE	FWT	9	10	2.044e-4	1.872e-4	3.620e-4	1.926e-4	1.938e-4	2.880e-4	3.835e-4	3.306e-4	2.968e-4
Soft GCV	FWT	9	10	2.382e-4	2.191e-4	3.901e-4	2.325e-4	2.290e-4	3.166e-4	4.127e-4	3.505e-4	3.336e-4
Soph GCV	FWT	9	10	2.054e-4	1.880e-4	3.650e-4	1.927e-4	1.947e-4	2.889e-4	3.996e-4	3.360e-4	3.103e-4
Soft LGCV	FWT	9	10	2.614e-4	2.535e-4	3.996e-4	2.352e-4	1.905e-4	3.239e-4	4.603e-4	4.130e-4	3.602e-4
Soph LGCV	FWT	9	10	2.714e-4	1.869e-4	3.780e-4	1.862e-4	1.847e-4	2.812e-4	4.081e-4	3.585e-4	3.219e-4
Cart VISU	FWT	9	10	2.901e-4	2.335e-4	6.071e-4	2.506e-4	2.862e-4	4.157e-4	6.356e-4	5.397e-4	4.385e-4
Cart MiMa	FWT	9	10	1.886e-4	1.618e-4	3.964e-4	1.885e-4	2.265e-4	2.851e-4	4.148e-4	3.306e-4	2.899e-4
Cart SURE	FWT	9	10	1.885e-4	1.632e-4	4.200e-4	1.853e-4	2.228e-4	3.087e-4	4.396e-4	3.437e-4	2.927e-4
Biased	FWT	9	10	2.284e-4	1.969e-4	3.833e-4	2.096e-4	2.116e-4	2.971e-4	4.005e-4	3.491e-4	3.256e-4
Soft LGCV	SWT	5	8	2.025e-4	1.755e-4	3.657e-4	1.869e-4	1.950e-4	2.803e-4	3.829e-4	3.463e-4	3.053e-4
Soph LGCV	SWT	5	8	1.988e-4	1.750e-4	3.766e-4	1.874e-4	1.839e-4	2.819e-4	4.009e-4	3.326e-4	3.013e-4
Soft IGCV	SWT	6	6	2.775e-4	2.021e-4	4.832e-4	2.549e-4	2.439e-4	3.384e-4	5.236e-4	4.119e-4	3.877e-4
Lipschitz	SWT	4	7	3.930e-4	3.131e-4	1.184e-3	3.110e-4	5.909e-4	9.120e-4	1.044e-3	8.014e-4	1.046e-3
Wiener	FFT	-	-	9.455e-4	9.056e-4	1.498e-3	7.112e-4	6.144e-4	1.184e-3	1.449e-3	1.151e-3	1.780e-3
PSF	FFT	-	-	7.440e-4	7.493e-4	1.231e-3	5.751e-4	5.005e-4	9.910e-4	1.244e-3	9.778e-4	1.503e-3
EMF	FFT	-	-	7.619e-4	7.628e-4	1.259e-3	5.842e-4	5.103e-4	1.008e-3	1.265e-3	9.939e-4	1.527e-3

Table 11.5: MSE Comparison: $\sigma = 0.03$, $MSE = 9.000e-4$

Method		J	D	Ex. 1	Ex. 2	Ex. 3	Ex. 4	Ex. 5	Ex. 6	Ex.7	Ex. 8	Ex. 9
START	-	-	-	5.922	7.424	8.801	8.696	10.043	10.716	8.744	8.832	10.278
Diffusion	FWT	4	6	10.610	13.672	11.096	14.026	16.178	14.582	11.608	12.185	13.445
Soft VISU	FWT	7	8	10.199	12.299	10.418	13.187	14.704	13.487	10.772	11.526	12.760
Soft MiMa	FWT	7	8	12.771	14.675	13.138	15.738	17.219	16.163	13.260	13.994	15.453
Soft SURE	FWT	9	10	12.896	14.816	13.636	15.837	17.356	16.509	13.712	13.647	15.865
Soph SURE	FWT	9	10	13.632	15.323	13.714	16.882	18.285	17.030	13.843	14.577	16.350
Soft GCV	FWT	9	10	12.812	13.947	13.510	15.807	16.289	16.433	13.647	13.647	15.804
Soph GCV	FWT	9	10	13.596	15.262	13.714	16.845	18.276	16.932	13.829	14.517	16.282
Soft LGCV	FWT	9	10	13.450	15.479	13.687	16.738	17.924	16.331	13.763	14.160	15.665
Soph LGCV	FWT	9	10	13.172	15.917	13.964	17.226	18.714	17.162	14.001	14.589	16.400
Cart VISU	FWT	9	10	12.105	14.575	11.872	15.819	17.229	15.442	12.165	12.715	14.392
Cart MiMa	FWT	9	10	13.938	16.123	13.733	17.078	18.142	17.147	13.653	14.442	16.418
Cart SURE	FWT	9	10	13.916	15.902	13.570	17.224	18.205	17.072	13.645	14.440	16.422
Biased	FWT	9	10	13.183	14.534	12.997	16.459	17.703	16.845	13.320	14.239	15.988
Soft LGCV	SWT	5	8	13.903	15.995	14.041	17.301	18.464	17.232	14.158	14.773	16.309
Soph LGCV	SWT	5	8	13.971	16.030	13.999	17.314	18.667	17.211	13.961	14.608	16.433
Soft IGCV	SWT	6	6	13.206	15.062	13.088	16.593	17.883	16.198	13.192	13.928	15.496
Lipschitz	SWT	4	7	12.554	14.550	11.258	16.149	15.108	14.202	11.567	12.914	13.195
Wiener	FFT	-	-	10.188	12.468	8.656	11.381	13.459	11.738	9.173	10.085	9.559
PSF	FFT	-	-	11.233	13.337	9.467	12.396	14.413	12.539	9.808	10.858	10.332
EMF	FFT	-	-	11.157	13.268	9.398	12.322	14.353	12.494	9.761	10.802	10.274

Table 11.6: SNR Comparison: $\sigma = 0.05$

Method		J	D	Ex. 1	Ex. 2	Ex. 3	Ex. 4	Ex. 5	Ex. 6	Ex.7	Ex. 8	Ex. 9
START	-	-	-	2.480e-3	2.508e-3	2.499e-3	2.499e-3	2.499e-3	2.499e-3	2.500e-3	2.499e-3	2.504e-3
Diffusion	FWT	4	6	8.425e-4	5.951e-4	1.474e-3	7.325e-4	6.086e-4	1.026e-3	1.293e-3	1.155e-3	1.208e-3
Soft VISU	FWT	7	8	9.262e-4	8.164e-4	1.723e-3	8.886e-4	8.546e-4	1.320e-3	1.567e-3	1.344e-3	1.414e-3
Soft MiMa	FWT	7	8	5.122e-4	4.723e-4	9.209e-4	4.939e-4	4.788e-4	7.132e-4	8.836e-4	7.615e-4	7.607e-4
Soft SURE	FWT	9	10	4.978e-4	4.573e-4	8.211e-4	4.828e-4	4.640e-4	6.585e-4	7.962e-4	8.248e-4	6.919e-4
Soph SURE	FWT	9	10	4.202e-4	4.069e-4	8.064e-4	3.795e-4	3.746e-4	5.841e-4	7.727e-4	6.658e-4	6.187e-4
Soft GCV	FWT	9	10	5.075e-4	5.586e-4	8.453e-4	4.861e-4	5.932e-4	6.701e-4	8.083e-4	8.248e-4	7.016e-4
Soph GCV	FWT	9	10	4.237e-4	4.127e-4	8.064e-4	3.828e-4	3.754e-4	5.974e-4	7.751e-4	6.752e-4	6.285e-4
Soft LGCV	FWT	9	10	4.381e-4	3.926e-4	8.115e-4	3.923e-4	4.071e-4	6.860e-4	7.870e-4	7.330e-4	7.244e-4
Soph LGCV	FWT	9	10	4.671e-4	3.549e-4	7.613e-4	3.506e-4	3.394e-4	5.665e-4	7.451e-4	6.639e-4	6.116e-4
Cart VISU	FWT	9	10	5.972e-4	4.833e-4	1.232e-3	4.848e-4	4.778e-4	8.419e-4	1.137e-3	1.022e-3	9.711e-4
Cart MiMa	FWT	9	10	3.915e-4	3.384e-4	8.029e-4	3.627e-4	3.872e-4	5.685e-4	8.072e-4	6.868e-4	6.091e-4
Cart SURE	FWT	9	10	3.935e-4	3.561e-4	8.337e-4	3.508e-4	3.816e-4	5.785e-4	8.087e-4	6.872e-4	6.085e-4
Biased	FWT	9	10	4.659e-4	4.879e-4	9.512e-4	4.183e-4	4.284e-4	6.094e-4	8.716e-4	7.197e-4	6.725e-4
Soft LGCV	SWT	5	8	3.947e-4	3.485e-4	7.480e-4	3.446e-4	3.595e-4	5.576e-4	7.186e-4	6.365e-4	6.245e-4
Soph LGCV	SWT	5	8	3.885e-4	3.457e-4	7.552e-4	3.436e-4	3.431e-4	5.603e-4	7.520e-4	6.611e-4	6.070e-4
Soft IGCV	SWT	6	6	4.634e-4	4.321e-4	9.315e-4	4.056e-4	4.110e-4	7.074e-4	8.977e-4	7.731e-4	7.532e-4
Lipschitz	SWT	4	7	5.385e-4	4.861e-4	1.420e-3	4.493e-4	7.786e-4	1.120e-3	1.305e-3	9.764e-4	1.279e-3
Wiener	FFT	-	-	1.857e-3	1.570e-3	2.585e-3	1.347e-3	1.138e-3	1.975e-3	2.265e-3	1.873e-3	2.955e-3
PSF	FFT	-	-	1.460e-3	1.286e-3	2.144e-3	1.066e-3	9.136e-4	1.643e-3	1.957e-3	1.568e-3	2.473e-3
EMF	FFT	-	-	1.485e-3	1.306e-3	2.179e-3	1.084e-3	9.264e-4	1.660e-3	1.978e-3	1.588e-3	2.507e-3

Table 11.7: MSE Comparison: $\sigma = 0.05$, $MSE = 2.500e-3$

Appendix A

Sound Examples: Specifications

Sound Example 1 arbeit.wav

Speech Text:	"Du versuchst zu arbeiten"
File Name:	arbeit.wav
Samples:	2^16
Samples/sec:	44100
Bits/Sample:	16
Mode:	Stereo

Sound Example 2 bursche.wav

Speech Text:	"Ein hübscher Bursche"
File Name:	bursche.wav
Samples:	2^16
Samples/sec:	44100
Bits/Sample:	16
Mode:	Stereo

Sound Example 3 illustrierte.wav

Speech Text:	"Kölner Illustierte. Jetzt für 2 Euro am Kiosk."
File Name:	illustrierte.wav
Samples:	2^17
Samples/sec:	44100
Bits/Sample:	16
Mode:	Mono

Sound Example 4 ironie.wav

```
Speech Text:      "Nein, irgendeine Ironie war nicht
                   herauszuhören."
File Name:        ironie.wav
Samples:          2^17
Samples/sec:      44100
Bits/Sample:      16
Mode:             Mono
```

Sound Example 5 leer.wav

```
Speech Text:      "Keine Idee. Nichts. Leer."
File Name:        leer.wav
Samples:          2^17
Samples/sec:      44100
Bits/Sample:      16
Mode:             Mono
```

Sound Example 6 lieblingsmusik.wav

```
Speech Text:      "Ihre Lieblingsmusik aus dem integrierten
                   MP3 Player."
File Name:        lieblingsmusik.wav
Samples:          2^17
Samples/sec:      44100
Bits/Sample:      16
Mode:             Mono
```

Sound Example 7 muecken.wav

```
Speech Text:      "Sämtliche Stechmücken Südfrankreichs
                   quälen dich."
File Name:        muecken.wav
Samples:          2^17
Samples/sec:      44100
Bits/Sample:      16
Mode:             Mono
```

Sound Example 8 woche.wav

```
Speech Text:      "Woche für Woche sitzt du auf deiner Terasse."
File Name:        woche.wav
Samples:          2^17
Samples/sec:      44100
Bits/Sample:      16
Mode:             Mono
```

Sound Example 9 worte.wav

```
Speech Text:      "Plötzlich hörst du sie, die Worte, die Reime,
                   die Sprüche, die du so gut kennst"
File Name:        worte.wav
Samples:          2^18
Samples/sec:      44100
Bits/Sample:      16
Mode:             Mono
```

Sound Example 10 musicalnoise.wav

```
Noise:            Musical Noise
File Name:        musicalnoise.wav
Samples:          100 * 2^9
Samples/sec:      22050
Bits/Sample:      16
Mode:             Mono
```

Sound Example 11 diffusionnoise.wav

```
Noise:            Characteristic Diffusion Noise
File Name:        diffusionnoise.wav
Samples:          2^17
Samples/sec:      44100
Bits/Sample:      16
Mode:             Mono
```

Bibliography

[1] Paul Bao and Lei Zhang. Noise reduction for magnetic resonance images via adaptive multiscale products thresholding. *IEEE Transactions on Medical Imaging*, 22(9):1089 – 1099, Sept. 2003.

[2] Ronald R. Coifman and David L. Donoho. Translation-invariant de-noising. Technical report, Stanford University, Department of Statistics, 1995.

[3] Ingrid Daubechies. The wavelet transform, time-frequency localization and signal analysis. *IEEE Trans. Inform. Theory*, 36(5):961–1005, 1990.

[4] Ingrid Daubechies. *Ten lectures on wavelets*, volume 61 of *CBMS-NSF Regional Conference Series in Applied Mathematics*. Society for Industrial and Applied Mathematics (SIAM), Philadelphia, PA, 1992.

[5] David L. Donoho. Cart and best-ortho-basis: A connection. Technical report, Department of Statistics, Stanford University, October 1995.

[6] David L. Donoho. De-noising by soft-thresholding. *IEEE Trans. Inform. Theory*, 41(3):613–627, 1995.

[7] David L. Donoho. CART and best-ortho-basis: a connection. *Ann. Statist.*, 25(5):1870–1911, 1997.

[8] David L. Donoho and Iain M. Johnstone. Ideal spatial adaptation by wavelet shrinkage. *Biometrika*, 81(3):425–455, 1994.

[9] David L. Donoho and Iain M. Johnstone. Adapting to unknown smoothness via wavelet shrinkage. *J. Amer. Statist. Assoc.*, 90(432):1200–1224, 1995.

[10] David L. Donoho and Iain M. Johnstone. Minimax estimation via wavelet shrinkage. *Ann. Statist.*, 26(3):879–921, 1998.

[11] David L. Donoho and Iain M. Johnstone. Asymptotic minimaxity of wavelet estimators with sampled data. *Statist. Sinica*, 9(1):1–32, 1999.

[12] Yariv Ephraim and David Malah. Speech enhancement using a minimum-mean square error short-time spectral amplitude estimator. *Acoustics, Speech and Signal Processing, IEEE Transactions on*, 32(6):1109–1121, Dec 1984.

[13] Ningping Fan, Radu V. Balan, and Justinian Rosca. Comparison of wavelet- and fft-based single-channel speech signal noise reduction techniques. volume 5607, pages 127–138. SPIE, 2004.

[14] Simon J. Godsill and Peter J.W. Rayner. *Digital Audio Restoration - a statistical model based approach*. Springer-Verlag London, September 1998.

[15] Zenton Goh, Kah-Chye Tan, and T.G. Tan. Postprocessing method for suppressing musical noise generated by spectral subtraction. *Speech and Audio Processing, IEEE Transactions on*, 6(3):287–292, May 1998.

[16] A. Grossmann, M. Holschneider, R. Kronland-Martinet, and J. Morlet. Detection of abrupt changes in sound signals with the help of wavelet transforms. In *Inverse problems: an interdisciplinary study (Montpellier, ss1986)*, Adv. Electron. Electron Phys., Suppl. 19, pages 289–306. Academic Press, London, 1987.

[17] M. Holschneider. *Wavelets*. Oxford Mathematical Monographs. The Clarendon Press Oxford University Press, New York, 1995. An analysis tool, Oxford Science Publications.

[18] Matthias Holschneider and Philippe Tchamitchian. Régularite locale de la fonction "non-différentiable" de Riemann. In *Les ondelettes en 1989 (Orsay, 1989)*, volume 1438 of *Lecture Notes in Math.*, pages 102–124, 209–210. Springer, Berlin, 1990.

[19] Maarten Jansen. *Noise reduction by wavelet thresholding*, volume 161 of *Lecture Notes in Statistics*. Springer-Verlag, New York, 2001.

[20] Maarten Jansen and Adhemar Bultheel. Multiple wavelet threshold estimation by generalized cross validation for images with correlated noise. *IEEE Trans. Image Process.*, 8(7):947–953, 1999.

[21] Maarten Jansen, Maurits Malfait, and Adhemar Bultheel. Generalized cross validation for wavelet thresholding. *Signal Processing*, 56(1):33–44, 1997.

[22] Stephane Mallat. *A Wavelet Tour of Signal Processing*. Academic Press, 1998.

[23] Stephane Mallat and Wen Liang Hwang. Singularity detection and processing with wavelets. *IEEE Trans. Inform. Theory*, 38(2, part 2):617–643, 1992.

[24] Stephane Mallat and Sifen Zhong. Characterization of signals from multiscale edges. *IEEE Transactions on Pattern Analysis and Machine Intelligence*, 14(7):710–732, July 1992.

[25] Yves Meyer. *Wavelets: Algorithms & Applications*. SIAM, 1993.

[26] Guy P. Nason. Wavelet shrinkage using cross-validation. *J. Roy. Statist. Soc. Ser. B*, 58(2):463–479, 1996.

[27] Guy P. Nason and Bernard W. Silverman. The stationary wavelet transform and some statistical applications. In Anestis Antoniadis and Georges Oppenheim, editors, *Wavelets and Statistics*, number 103 in Lecture Notes in Statistics, pages 281–300. Springer-Verlag, 1995.

[28] Pietro Perona and Jitendra Malik. Scale-space and edge detection using anisotropic diffusion. *Pattern Analysis and Machine Intelligence, IEEE Transactions on*, 12(7):629–639, Jul 1990.

[29] H. L. Resnikoff and R. O. Wells Jr. *Wavelet Analysis, The Scalable Structure of Information*. Springer-Verlag, New York, 1998.

[30] Charles M. Stein. Estimation of the mean of a multivariate normal distribution. *Ann. Statist.*, 9(6):1135–1151, 1981.

[31] Nathalie Virag. Single channel speech enhancement based on masking properties of the human auditory system. *Speech and Audio Processing, IEEE Transactions on*, 7(2):126–137, March 1999.

[32] Martin Welk, Achim Bergmeister, and Joachim Weickert. Denoising of audio data by nonlinear diffusion. In Ron Kimmel, Nir Sochen, and Joachim Weickert, editors, *Scale Space and PDE Methods in Computer Vision , 5th International Conference, Scale-Space 2005, Hofgeismar, Germany, April 7-9, 2005, Proceedings*, volume 3459 of *Lecture Notes in Computer Science*, pages 598–609. Springer Verlag Berlin / Heidelberg, 2005.

[33] Norman Weyrich and Gregory T. Warhola. Wavelet shrinkage and generalized cross validation for image denoising. *Image Processing, IEEE Transactions on*, 7(1):82–90, Jan 1998.

[34] Mladen V. Wickerhauser. *Adaptive Wavelet-Analysis: Theory and Software*. Vieweg & Sohn, 1993.

[35] Norbert Wiener. *Extrapolation, Interpolation, and Smoothing of Stationary Time Series. With Engineering Applications.* The Technology Press of the Massachusetts Institute of Technology, Cambridge, Mass, 1949.

[36] Y. Xu, J. B. Weaver, D. M. Healy Jr., and J. Lu. Wavelet transform domain filters: A spatially selective noise filtration technique. *IEEE Transactions of Image Processing*, 3(6), November 1994.

[37] Kôsaku Yosida. *Functional analysis.* Second edition. Die Grundlehren der mathematischen Wissenschaften, Band 123. Springer-Verlag New York Inc., New York, 1968.

[38] Guoshen Yu, Emmanuel Bacry, and Stephane Mallat. Audio signal denoising with complex wavelets and adaptive block attenuation. *Acoustics, Speech and Signal Processing, 2007. ICASSP 2007. IEEE International Conference on*, 3:III–869–III–872, April 2007.